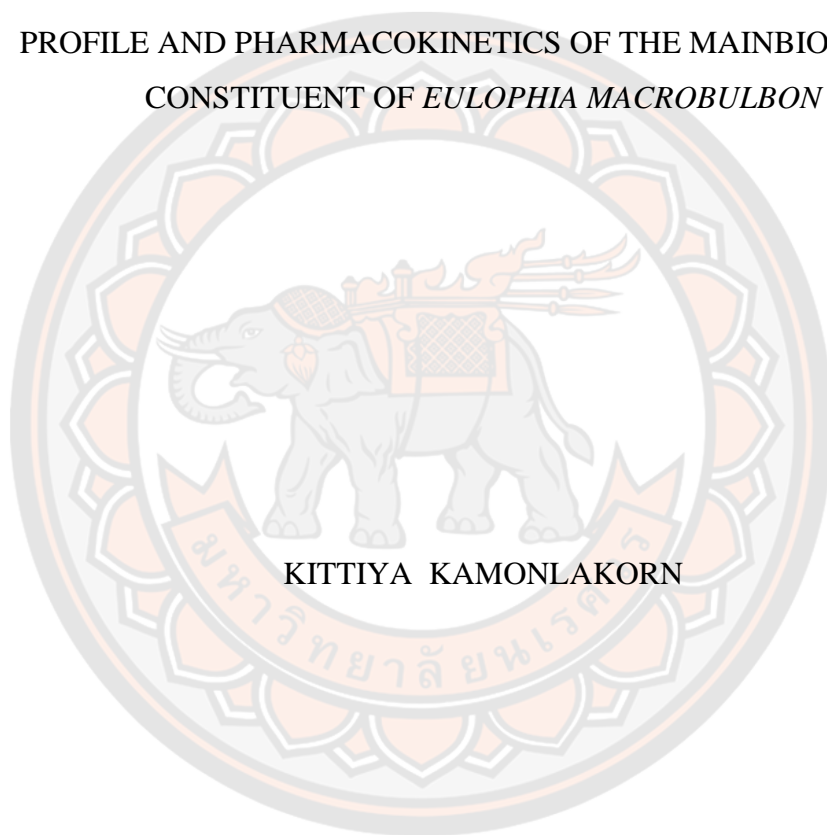# MULTIPLE *IN VITRO* SYSTEMS FOR ASSESSMENT OF METABOLIC PROFILE AND PHARMACOKINETICS OF THE MAINBIOACTIVE CONSTITUENT OF *EULOPHIA MACROBULBON*

KITTIYA KAMONLAKORN

A Thesis Submitted to the Graduate School of Naresuan University
in Partial Fulfillment of the Requirements
for the Master of Science in Pharmaceutical Chemistry and Natural Products
2021

MULTIPLE *IN VITRO* SYSTEMS FOR ASSESSMENT OF METABOLIC
PROFILE AND PHARMACOKINETICS OF THE MAINBIOACTIVE
CONSTITUENT OF *EULOPHIA MACROBULBON*

KITTIYA KAMONLAKORN

A Thesis Submitted to the Graduate School of Naresuan University
in Partial Fulfillment of the Requirements
for the Master of Science in Pharmaceutical Chemistry and Natural Products
2021

Thesis entitled "Multiple *in vitro* systems for assessment of metabolic profile and pharmacokinetics of the mainbioactive constituent of *Eulophia macrobulbon*"

By KITTIYA KAMONLAKORN

has been approved by the Graduate School as partial fulfillment of the requirements

for the Master of Science in Pharmaceutical Chemistry and Natural Products of Naresuan University

Oral Defense Committee

.... Chair
(Wiriyaporn Sumsakul, Ph.D.)

.... Advisor
(Assistant Professor Dumrongsak Pekthong, Ph.D.)

.... Co Advisor
(Associate Professor Kornkanok Ingkaninan, Ph.D.)

.... Internal Examiner
(Assistant Professor Piyarat Srisawang, Ph.D.)

.... Internal Examiner
(Supawadee Parhira, Ph.D.)

Approved

....
(Associate Professor Krongkarn Chootip, Ph.D.)

Dean of the Graduate School

Title	MULTIPLE *IN VITRO* SYSTEMS FOR ASSESSMENT OF METABOLIC PROFILE AND PHARMACOKINETICS OF THE MAINBIOACTIVE CONSTITUENT OF *EULOPHIA MACROBULBON*
Author	KITTIYA KAMONLAKORN
Advisor	Assistant Professor Dumrongsak Pekthong, Ph.D.
Co-Advisor	Associate Professor Kornkanok Ingkaninan, Ph.D.
Academic Paper	M.S. Thesis in Pharmaceutical Chemistry and Natural Products, Naresuan University, 2021
Keywords	Eulophia macrobulbon, phenanthrenes, metabolic profile, pharmacokinetics

ABSTRACT

Eulophia macrobulbon belongs to Orchidaceae family, commonly known as Orchids. It has been used in Thai traditional medicine, especially as an aphrodisiac. The main bioactive compound of *E. macrobulbon* is EM2. There are reports on its chemical composition and pharmaceutical activity but reports about its cytotoxicity and pharmacokinetic parameters are rare. The objectives of this study are to gain new knowledge in the process of structural changes and pharmacokinetic values of EM2 by in vitro methods to predict the pharmacokinetics of EM2 for further safety data for humans. Also, to screen for cytotoxicity of EM2 using Hep G2 cells and Caco-2 cells. The cytotoxicity of EM2 in Hep G2 cells and Caco-2 cells were evaluated by MTT assay. The results showed that EM2 was toxic to 50% of Hep G2 cells at a concentration (IC_{50}) of 30.08 ± 0.62 micromolar compared with the control (the concentration of dimethyl sulfoxide (DMSO) was 0.01%). For the cytotoxicity of EM2 in Caco-2 cells, the result of IC_{50} was 41.64 ± 1.60 micromolar compared with the control. This, the concentrations of EM2 at 1 and 10 µM were chosen and use for further experiment to determine its effectives. Caco-2 monolayers in 12 trans-well insert plate was collected to use in permeability testing of EM2 compound. The TEER values were checked to confirm monolayers formation between apical chamber (AP) and basolateral chamber (BL). The Papp values shows the time dependence of sample

EM2 at initial concentration 1 µM and 10 µM in absorptive and secretory directions across Caco-2 monolayers. The Papp values of EM2 results have shown that absorptive transport (AP-BL) from 30 to 120 minutes has decreased which means that sample EM2 at start concentration 1 µM and 10 µM has the high permeability through the Caco-2 monolayers compared to caffeine and rhodamine123. The absorptive permeability or $P_{app, (AP-BL)}$ values of EM2 at initial concentrations of 1 and 10 µM were ranged 3.48~0.90 and 1.20~0.46 $\times 10^{-4}$ cm/s, respectively (R123 was ranged 1.01~0.50 $\times 10^{-4}$ cm/s and caffeine was ranged 2.25~1.38 $\times 10^{-4}$ cm/s), the secretory permeability or $P_{app, (BL-AP)}$ values were 1.17~0.30 and 0.26~0.14 $\times 10^{-4}$ cm/s, respectively (R123 was ranged 0.90~6.20 $\times 10^{-4}$ cm/s and caffeine was ranged 2.31~0.57 $\times 10^{-4}$ cm/s). EM2 was used to determines the concentration of the drug in dialysis buffer compared to plasma to provides an indication of drug binding protein. The results of EM2 at initial concentration of 1 and 10 µM were obtained %bound with protein in plasma close to 100%. Metabolic study in time dependence of EM2 at initial concentration 10 µM in pooled human liver microsomes, human hepatocytes and Hep G2 cells were half-life ($t_{1/2}$) at 2.71, 15.23 and 67.41 hours, respectively. The conventional clearance (CL) obtained from the comparison of hepatocytes applied to the total number of human hepatocytes were 7.56, 7.12 and 1.75 liters per hour, respectively. However, EM2 also be selected for investigation CYP-phenotyping. The results from exhibited that there were at least 4 metabolites showing in LC-MS chromatogram.
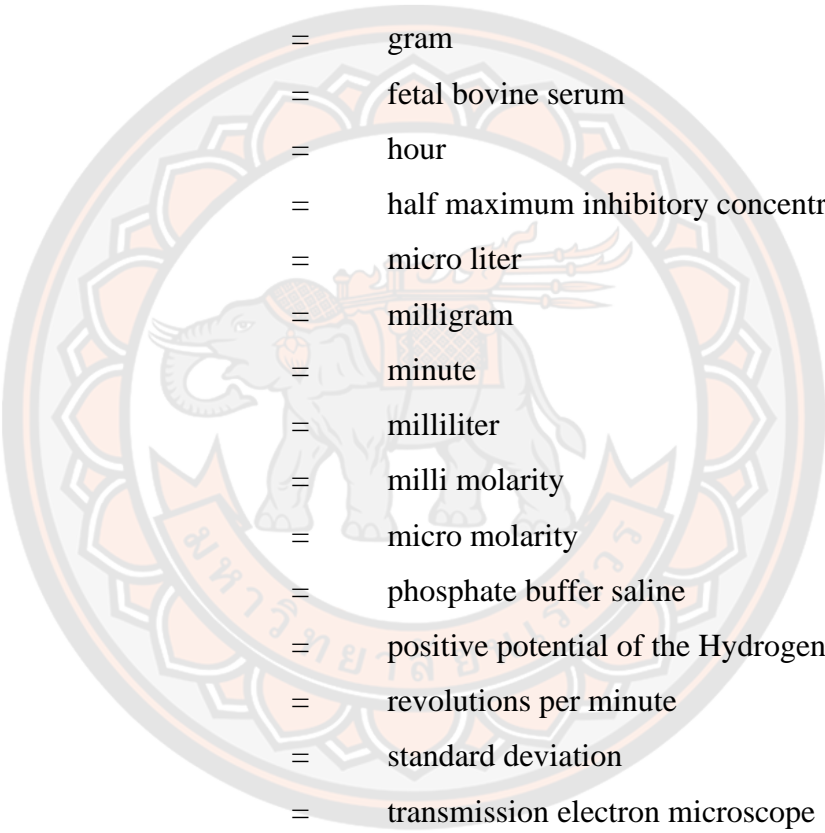
ACKNOWLEDGEMENTS

ABBREVIATIONS

ANOVA	=	analysis of variance
°C	=	degree Celsius
CO2	=	carbon dioxide
DMEM	=	Dulbecco's Modified Eagle Medium
DMSO	=	dimethyl sulfoxide
g	=	gram
FBS	=	fetal bovine serum
h	=	hour
IC50	=	half maximum inhibitory concentration
μl	=	micro liter
Mg	=	milligram
min	=	minute
ml	=	milliliter
mM	=	milli molarity
μM	=	micro molarity
PBS	=	phosphate buffer saline
pH	=	positive potential of the Hydrogen ions
rpm	=	revolutions per minute
SD	=	standard deviation
TEM	=	transmission electron microscope
UV	=	ultraviolet

TABLE OF CONTENTS

LIST OF TABLES

LIST OF FIGURES

CHAPTER I

INTRODUCTION

1.1 Statement of the Problems

      Eulophia macrobulbon (Parish & Rchb.f.) Hook.f., 1890 belongs to Orchidaceae family commonly known as Orchid. The background about investigated the chemical constituents of the tubers of *E. macrobulbon* [1]. There are, a new phenanthrene 9,10-dihydro-4-(4'-hydroxybenzyl)-2,5-dimethoxyphenanthrene-1,7-diol and three known phenanthrenes, such as, 1-(4'-hydroxybenzyl)-4,8-dimethoxyphenanthrene-2,7-diol (a main bioactive compound of *E. macrobulbon,* EM2), (9,10-dihydro-2,5-dimethoxy-phenanthrene-1,7-diol, and 1,5,7-trimethoxyphenanthrene-2,6-diol were isolated. The structures of them were shown in Fig. 2A-D. All of these compounds were evaluated inhibitory action towards PDE5 by the $[^3H]$cGMP radio-assay method. EM2 was the most potent PDE5 inhibitor with IC_{50} at the concentration 1.67±0.54 µM. Moreover, it induced vasorelaxant effects on rat resistance vessels [2]. In conclusion, EM2 is the strongest PDE5 inhibitor in this report. It is a potential compound for future investigation. However, there were rare reports about EM2 in the term of pharmacokinetic studies. This study aimed to study the process of structural changes and pharmacokinetic values by in vitro methods with screening to predict the pharmacokinetics of the main bioactive constituent of the *E. macrobulbon* extracts in humans. Its tubers were shown in Figure 1 and in the Figure 2 were shown the structural of phenanthrene EM2, respectively.

Figure 1 *E. macrobulbon*
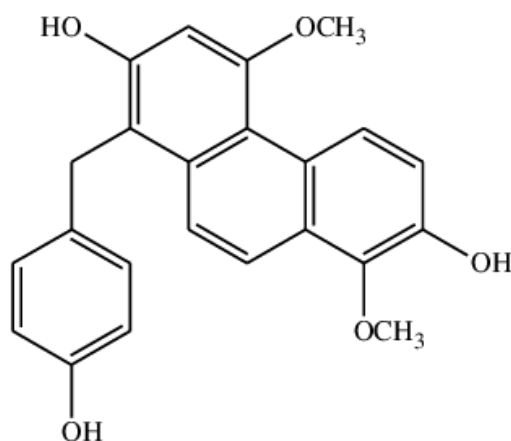
Figure 2 The structural of phenanthrene 1-(4'-hydroxybenzyl)-4,8-dimethoxyphenanthrene-2,7-diol (EM2) [3]

It is well known that natural products are an important source of medicines. This is an advantage of Thailand that has high natural resources with biodiversity and the use of herbs in medicine for a long time. In order to effectively use extracts from *E. macrobulbon* extract in humans, the pharmacokinetics information about the substance is of major importance (EM2), including the active metabolites is necessary to use to more fully evaluate the effectiveness of *E. macrobulbon* extract to obtain safety information and will lead to more complete treatment in the future.

1.2 Purposes of the Study

1. To study the process of structural changes and pharmacokinetic values of main bioactive constituent (EM2) in the *E. macrobulbon* extracts by *in vitro* methods.

2. To predict the pharmacokinetics of main bioactive constituent (EM2) in the *E. macrobulbon* extracts in humans.

1.3. Scope of the Study

This thesis was conducted in a laboratory to study the process of structural changes and the pharmacokinetic values of main bioactive constituent in the *E. macrobulbon* (EM2).
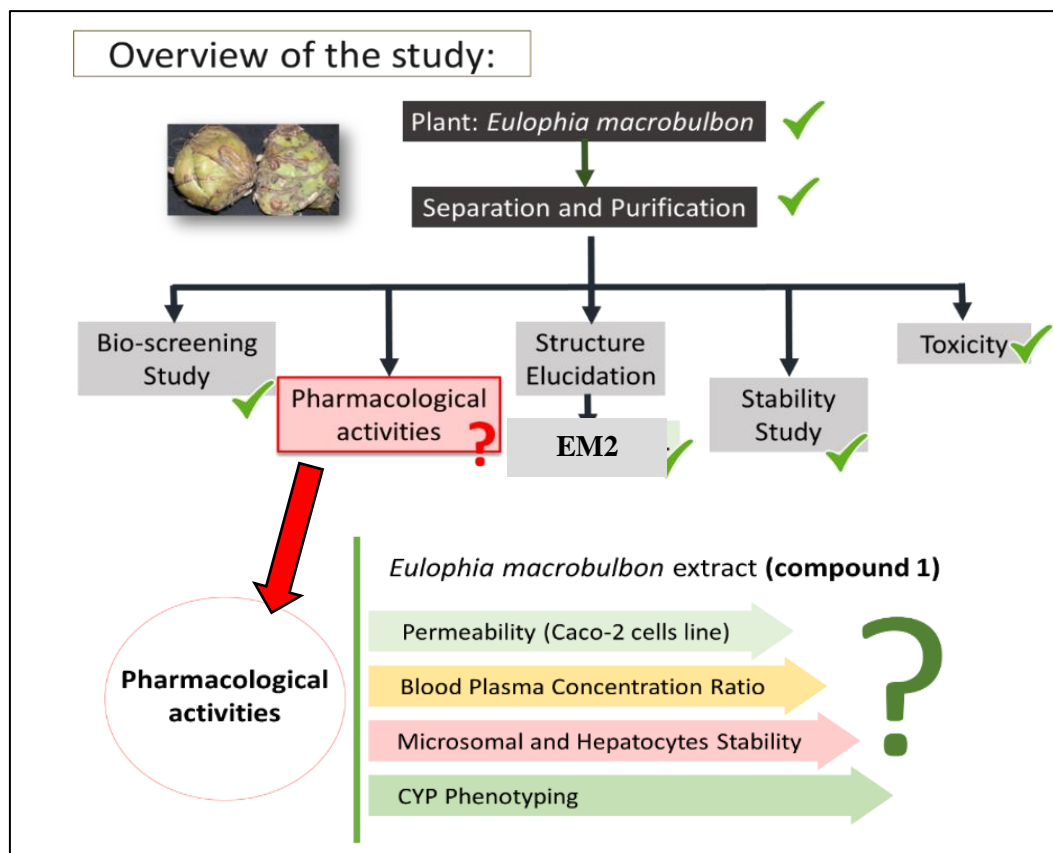
Figure 3 The overview of research study

1.4 Expected or Anticipated Benefit Gain

1. To gain new knowledge in the process of structural changes and pharmacokinetic values of the main bioactive constituent (EM2) in the *E. macrobulbon* extracts by *in vitro* methods.

2. Use of the results from 1.4.1 to predict the pharmacokinetics of the main bioactive constituent (EM2) in the *E. macrobulbon* extracts for further safety data for humans.

1.5 Keywords

Eulophia macrobulbon, phenanthrenes, metabolic profile, pharmacokinetics

1.6 Research Hypothesis

1. EM2 may have the suitable solubility, permeability and stability.

2. EM2 may not cause toxicity to microsomal and hepatocytes.

3. Pharmacokinetic profiles of the selected compound can be estimated to be suitable candidate for future development as potential therapeutics.

CHAPTER II

LITERATURE REVIEWS

2.1 Plant Material: *Eulophia macrobulbon*

2.1.1 General Information of *Eulophia macrobulbon*

Eulophia macrobulbon (Parish & Rchb.f.) Hook.f., 1890 belongs to Orchidaceae family [4] commonly known as Orchid. The Orchidaceae family is one of the largest families with roughly around 28,484 species [5] of flowering the Orchids are widely used for the traditional used in herbal medicine, acting as an aphrodisiac, antiseptic, antimicrobial, and anti-cancer agent [6]. This plant found in eastern Himalayas, Northern Myanmar, Thailand, Laos, Cambodia, and Vietnam at elevations around 700 meters as a medium-sized, warm to cool terrestrial orchid with a large tuber-like pseudobulb carrying oblong to elliptic-lanceolate, acuminate leaves [7]. Its body, tubers and flowers were shown in Figure 4A, 4B and 4C [4, 5], respectively.
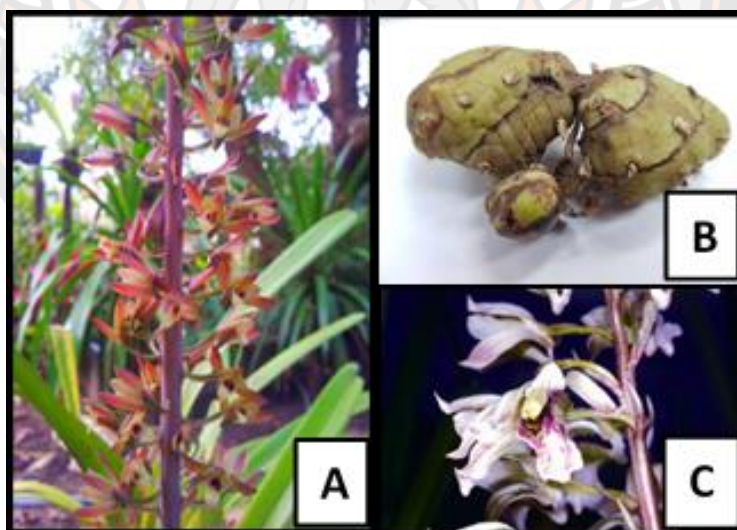
Figure 4 The body (A), tubers (B) and flowers (C) of *E. macrobulbon*

2.1.2 Phytochemicals and Chemical Constituents of *Eulophia macrobulbon*

Phytochemically, orchids have been reported to contain alkaloids, triterpenoids, flavonoids, and stilbenoids [8, 9, 10]. The phytochemical studies reported that *Eulophia* species contain phenolics, saponins, alkaloids, flavonoids, terpenoids, and phenanthrene derivatives [11, 12, 13, 14, 15].

2.1.3 Traditional Used of *Eulophia macrobulbon*

Orchids belong to the plant family Orchidaceae, one of the most diverse groups among the angiosperm with near 25,000 species (Behera *et al.,* 2013). Aside from their ornamental value, orchids are also acknowledged for their use in traditional medicines [13, 14, 16, 17, 18]. Chinese medicine was probably the first to describe orchids for their medicinal use. Other pharmacopeias from India and many countries from SouthAsia such as Taiwan, Singapore, Vietnam, Sri Lanka, Thailand, Myanmar, use orchids in traditional medicine since the ancient time [19, 20, 21]. Likewise, the use of orchids in America also has a long history.

For instance, in India, the word Amarkand is commonly used for 30 plant species from genus Eulophia and for one species from the genus Dioscorea. Since ancient times, Amarkand is believed to be an excellent health-promoting agent. Rhizomes/tubers of Amarkand are routinely consumed by the tribal parts of India as food as well as a therapeutic entity for better health and longevity [14].

2.1.4 Biological Activity of *Eulophia macrobulbon*

Ethnopharmacological studies demonstrated that Eulophia species exhibited anti-inflammatory [22, 23, 6], anti-cancer [24, 6], antioxidant, anti-diabetic and hypolipidemic [25] properties.

2.2 Phenanthrene

2.2.1 General Information of Phenanthrene

Chemical properties

The phenanthrene (Figure 5, molecular formula: $C_{14}H_{10}$ and molecular weight: 178.23 g/mol) is a polycyclic aromatic hydrocarbon composed of three fused benzene rings which take its name from the two terms 'phenyl' and 'anthracene' [26]. It appears as white luster and fluorescent flake crystals, not soluble in water, slightly soluble in

ethanol, soluble in ether, acetic acid, benzene, carbon tetrachloride, and carbon disulfide [27]. The phenanthrene is a leaf-like crystal with a relative density of 1.179 (25/4 °C) and a refractive index of 1.6450, melting point of 101 °C and boiling point of 340 °C.
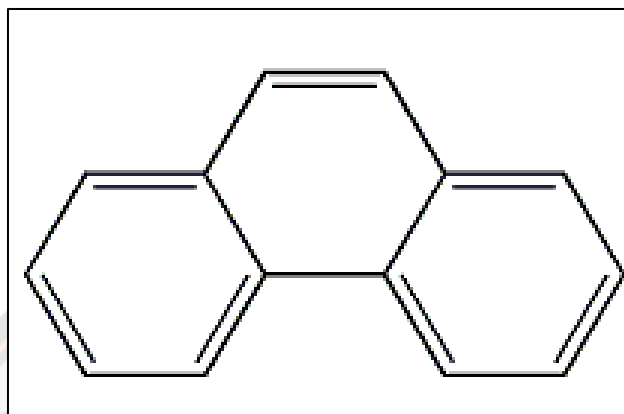
Figure 5 The structural of phenanthrene

In order to effectively use extracts from *E. macrobulbon* extract were isolated to obtain the phenanthrenes compound in humans, the pharmacokinetics information about the substance is of major importance, including the active metabolites is necessary to use to more fully evaluate the effectiveness of *E. macrobulbon* extract to obtain safety information and will lead to more complete treatment in the future.

Biological activities and toxicity

Phenanthrene is ineffective as an initiator. It is not classifiable as to human carcinogenicity [28]. The radioactivity accumulation by coalfish administered 14C-labeled phenanthrene, radioactivity was greater in liver than in gallbladder or muscle following intragastric admin [29]. Following intragastric administration in Norway lobster of 14C-labeled phenanthrene, the highest amount of radioactivity was found in the hepatopancreas system and muscle [30]. The information on the carcinogenicity of phenanthrene in humans following oral exposure was not available.

In animals, Simmon and team [31] reported an oral LD_{50} of 750 mg/kg for mice. Single doses of 100 mg/kg/day of phenanthrene administered by gavage for 4 days suppressed carboxylesterase activity in the intestinal mucosa of rat but did not

produce other signs of gastrointestinal toxicity. Phenanthrene had no effect on hepatic or extrahepatic carboxylesterase activities [32].

2.2.2 General Information of EM2 (Phenanthrene)

The background investigated the chemical constituents of the tubers of *E. macrobulbon* [1]. The isolation and purification from the tubers of *E. macrobulbon* lead to obtain a new phenanthrene is 9,10-dihydro-4-(4'-hydroxybenzyl)-2,5-dimethoxyphenanthrene-1,7-diol and three known phenanthrenes i.e., 1-(4'-hydroxybenzyl)-4,8-dimethoxyphenanthrene-2,7-diol (EM2), (9,10-dihydro-2,5-dimethoxy-phenanthrene-1,7-diol and 1,5,7-trimethoxyphenanthrene-2,6-diol. These compounds were isolated and purified by using various separation procedures, i.e., reverse phase column chromatography (Sephadex LH-20), preparative SiO_2 thin layer chromatography, size exclusion chromatography, and high-performance liquid chromatography. The structures of them were shown in Figure 6 [1].
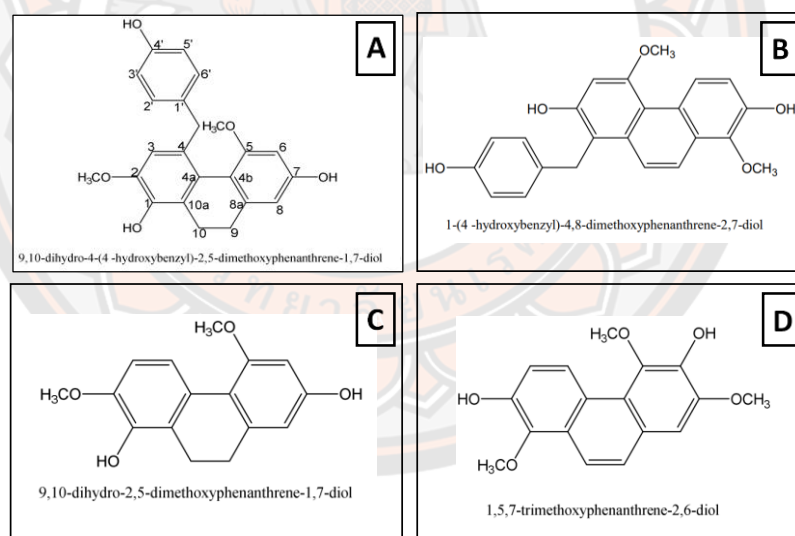
Figure 6 The chemical constituents of the tubers of *E. macrobulbon*; 9,10-dihydro-4-(4'-hydroxybenzyl)-2,5-dimethoxyphenanthrene-1,7-diol (A), 1-(4'-hydroxybenzyl)-4,8-dimethoxyphenanthrene-2,7-diol (EM2, B), (9,10-dihydro-2,5-dimethoxy-phenanthrene-1,7-diol (C), and 1,5,7-trimethoxyphenanthrene-2,6-diol (D)

The separation of *E. macrobulbon* tuber extracts yielded four compounds (Figure 6). The HREIMS data of EM2 exhibited a molecular ion peak at *m/z* 378.1478, which represented [MH]$^+$ for $C_{23}H_{22}O_5$. Finally, a new phenanthrene was unambiguously identified as 9,10-dihydro-4-(4′-hydroxybenzyl)-2,5-dimethoxyphenanthrene-1,7-diol, a new 9,10-dihydrophenanthrene derivative. The structures were identified by spectroscopy and by comparing with published spectroscopic data [11, 33, 34, 35].

9,10-Dihydro-4-(4′-hydroxybenzyl)-2,5-dimethoxyphenanthrene1,7-diol (a new phenanthrene) from Temkitthawon et al., 2017 [1]

Pale yellow amorphous.

$[\alpha]_D^{20}$:0 (*c* 0.1, MeOH).

IR (KBr): ν_{max} 3412, 1612, 1512, 1463 cm^{-1}.

UV (MeOH) λ_{max} (log ε): 273 (5.48).

^{1}H NMR (400 MHz, in methanol-d_4): 2.04 (H, ddd, *J* = 14.5, 14.7, 4.0 Hz, H-10′), 2.38 (H, ddd, *J* = 14.7, 14.0, 4.0 Hz, H-9′), 2.61 (H, ddd, *J* = 14.0, 4.0, 2.4 Hz, H-9″), 3.20 (H, ddd, *J* = 14.5, 4.0, 2.4 Hz, H-10″), 3.62 (3H, s, C-5-OCH$_3$), 3.69 (3H, s, C-2-OCH$_3$), 3.73 (1H, d, *J* = 15.0 Hz, benzylic-CH$_2$), 3.81 (1H, d, *J* = 15.0 Hz, benzylic-CH$_2$), 6.36 (H, d, $J_{6,8}$ = 2.0 Hz, H-6), 6.38 (H, d, $J_{8,6}$ = 2.0 Hz, H-8), 6.47 (H, s, H-3), 6.61 (2H, d, $J_{3',2'}$ or $J_{5',6'}$ = 8.4 Hz, H-3′ and H-5′), 6.81 (2H, d, $J_{2',3'}$ or $J_{6',5'}$ = 8.4 Hz, H-2′ and H-6′) .

^{13}C-NMR (100 MHz, methanol-d_4): 24.4 (CH$_2$, C-10), 32.2 (CH$_2$, C-9), 40.4 (benzylic-CH$_2$), 55.3 (C, C-5-OCH$_3$), 56.2 (C, C-2- OCH$_3$), 98.6 (CH, C-6), 107.7 (CH, C8), 112.1 (CH, C-3), 115.8 (CH, C-3′and C-5′), 117.3 (C, C-4b), 127.0 (C, C-10a), 127.4. (C, C-8a), 131.0 (CH, C-2′ and C-6′), 132.7 (C, C-4a), 135.5 (C, C-1′), 141.0 (C, C-4), 144.4 (C, C-1), 147.1 (C, C-2), 156.0 (C, C-4′), 158.1 (C, C-7), 158.3 (C, C-5). EIMS m/z (relative intensity): 378 [M]$^+$ (100), 363 [M-15]$^+$ (23), 347[M-31$^+$] (22), 335 [M-43$^+$] (11), 272 [M-106$^+$] (11), 107 [M271$^+$] (19).

HREIMS *m/z*: 378.1478 (calcd. for $C_{23}H_{22}O_5$)

2.3 Literature Review or Related Works

2.3.1 Phosphodiesterase-5 (PDE5) Inhibitors Activity

Erectile dysfunction (ED) is an inability to get an erection firm enough to have sexual intercourse and causes low self-esteem [36, 37]. Currently, the most common drugs used to treat ED are phosphodiesterase-5 (PDE5) inhibitors [36]. PDE5-inhibitors are also used in pulmonary artery hypertension treatment [38, 2]. The isolation and purification from the study of Temkitthawon and team [1], were reported the tubers of *E. macrobulbon* lead to obtain 4 phenanthrene compounds constituent. All of these compounds were evaluated inhibitory action towards PDE5 by the [^{3}H]cGMP radio-assay method. EM2 was the most potent PDE5 inhibitor with IC$_{50}$ at the concentration 1.67 ± 0.54 µM.

2.3.2 Vasorelaxant Effects on Rat Resistance Vessels

Following the results studied by Wisutthathum and team, 2018 [39]. EM2, it induced vasorelaxant effects on rat resistance vessels. The vasorelaxant effect of *E. macrobulbon* ethanolic extract or phenanthrene and the underlying mechanism was evaluated in the second mesenteric artery from Sprague Dawley rats. And the acute hemorrhage in anesthetized rats with cumulative concentrations of *E. macrobulbon* extract.

For the results, both extract (10^{-4}–1 mg/ml) and phenanthrene (10^{-7}–10^{-4} M) undamaged endothelium, some reduced results from endothelium removal (p < 0.001). A significant decrease in the relaxation effect of the extract and phenanthrene was detected with L-NAME and apamin/charybdotoxin in the endothelium-intact container and with iberiotoxin in the abandoned container SNP (sodium nitroprusside)-Induced relaxation has been significantly improved by extracting from the extract and phenanthrene. By contrast, ODQ (1H-[1,2,4]oxadiazolo[4,3-a]quinoxaline-1-one), 4- aminopyridine and glibenclamide (endothelium-denuded vessels) and indomethacin (endothelium-intact vessels) had no effect. In a calcium-free solution, both EM and phenanthrene extracts inhibit cell contraction extracellular Ca^{2+}-induced with high contraction of KCl and phenylephrine (PE). They also inhibited the intracellular Ca^{2+} release sensitive to PE. The acute infusion of the

extract (20 and 70 mg/kg) induced an immediate and transient dose-dependent hypotensive effect.

In conclusion, EM2 is the strongest PDE5 inhibitor in this report. It is a potential compound for future investigation.

2.3.3 Pulmonary Vasodilation in Rats

The study on the effect of pulmonary vasodilation in rats from Wisutthathum and team 2018 [2] studied. It was found that extracts and the EM2 or phenanthrene have a good effect on the pulmonary artery on the rats that specific less effective on the aorta blood vessels. The study of the effects of astragalus on the tissue loosening of the corpus cavenosum of those isolated in the study (From the testes of the transsexual men) found that the extract was resulting in the cavernosum tissue that contract was relaxed by phenylephrine.

The study of the stimulant effect of *E. macrobulbon* in stress-inducing rats from the study of Preedapirom and team [40, 41]. It was found that the extracts 15, 150 and 450 mg/kg of body weight has a strong stimulant effect after receiving the extract 1 time which works to reduce the amount of time that male rats start straddling female rats (mount latency) and reduce the amount of time that the male rats have penetrating the penis into female's rats (intromission latency). When given the extract that astragalus for 7 consecutive days, it was found that it reduced the duration of the insertion of the testes into the female vagina and with ejaculation for the first time until the male rats have penetrated the penis into female's rats next time (post-ejaculatory interval (PEI)) and inter-intermission interval.

In addition, the research team also studied the effects of extracts of *E. macrobulbon* on reproductive behavior and the change in pressure within the lingam core caused by electrical stimulation of natural old rats. The behavioral testing found that after receiving the extract once a day for 3 weeks consecutively, the older rat had better sexual behavior than rats in the control group that received only solvent. And when the unconscious of the rats to measure the pressure inside the testes, it was found that older rats receiving the extract at 450 mg/kg had increased sensitivity to electrical stimulation more than rats in the control group. Importantly, it was found

that the older rats that received the extract from *E. macrobulbon* had significantly higher sperm count than the older rats in the control group.

From all the results of the study, it may be concluded that *E. macrobulbon* extract helps to increase sexual performance in older rats. That may cause a result of an increase in dopamine neurotransmitter levels in the brain and a result of the anti-enzyme PDE5 in the testes. Later, the research team studied the effects of *E. macrobulbon* extract on the amount of Dopamine1 (D1) and Dopamine2 (D2) receptor in the hypothalamus brain region in rats that were induced to be impaired with sexual stress (immobilization stress) It was found that the number of D1 and D2 receptors were significantly decreased ($p < 0.05$ when compared to normal rats). However, it was found that rats were induced to be impaired with sexual stress and receiving 150 and 450 mg of/bodyweight could increase D1 and D2 receptor significantly ($p < 0.05$). This studied confirms *E. macrobulbon* has anti-PDE5 effects and increases the density of D1 and D2 receptors in the hypothalamus.

2.3.4 The Toxicity Testing

The acute toxicity tested of the *E. macrobulbon* extracts according to the OECD Guideline No. 420 (limit test) [42], by using 2 types of experimental animals in rats and mouses. Entering the extract in the size of 2 g/kg of body weight and see results within 2 weeks after. Testing results showed no rat death or abnormal symptoms, and after murder, the blood tests showed no abnormalities and enzyme levels that were an index of liver and kidney function were not different from the control group. Results of the histology study of each internal organ tissue showed no abnormal characteristics.

In addition, the chronic toxicity test according to the OECD Guideline No. 452 [43] found that when the extract was given to 3 doses to rats are 5, 50 and 500 mg/kg of body weight once a day, every day for 6 months, no abnormal growth rate was observed in the body. blood value liver enzyme level, and histology of internal organs tissue. From the results of all studies, it may be concluded that the extract of that *E. macrobulbon* is safe and has an LD50 value greater than 2 g/kg of body weight, which indicates the safety of consumption of *E. macrobulbon* extract.

2.3.5 The Study of Plant Propagation

The *E. macrobulbon* it's a rare orchid. The research team therefore studied the development of tissue culture method, including the development of cultured parts for new origin. By discovering a formula that has effect on stimulating eye cracking and forming a sub head with good new rhizome and found that the sub-head developed from tissue culture can be planted out in the nursery. In the study of planting tubers in the nursery, compared with planting in the ground, it was found that tubers of different sizes that are resulting in the growth and development of new births and the creation of different heads as well. And when planted into a plot that is maintained under cultural control, the *E. macrobulbon* can create a new tuber, so the head creation in the next season is as good as the normal growth cycle in nature [44].

2.3.6 The Study of Products Development and Penetration Study

The developed of a spray solution of *E. macrobulbon* extract [44] at a concentration of 20 mg/mL in water: PEG-400 or propylene glycol:ethyl alcohol (10:40:50) with 2% of tween®80. And studies about the stability of EM2 and products, the solubility in solvent, evaporation rate, and viscosity. It was found that extract had good stability at 45 degrees Celsius, and the spray solution that stabilize at 4 degrees Celsius and room temperature but decomposes at a temperature of 45 degrees Celsius. The recipe should be improved to be more stable, determining the permeability of EM2 and *in vivo* studies to study the diffusion through the skin to the corpus cavenesum, and the efficacy of the spray solution formulation or may develop in the form of medical devices such as condoms coating for use in cases of premature ejaculation (Premature ejaculation).

In addition, the researchers have studied the relationship between the structure of EM2 and its action, the derivatives of EM2 are synthesized by adding the methyl group or the acetate group into the structure. The results that the inhibitory effect of PDE-5 and PDE-6 are decreases and the decrease in effect is due to the number and the size of displacement hydroxyl groups, which clearly shows the importance of the hydroxyl group for its action at PDE-5. From the previous project, the research team has studied that the chemical, pharmacology, toxicology, pharmaceuticals and agriculture [45]. It was found that the extract that has the potential to develop further

is a product that is used to solve the problem of erectile dysfunction. Currently, the research team has submitted 2 patent applications, there are "The process of preparation of extracts with high phenanthrene content from the *Eulophia* orchids", and "The elements that enhance male sexual performance and control high blood pressure". In order to expand the knowledge of product development. And to prepare to convey technology to private sectors interested in developing products for use in treating erectile dysfunction from *E. macrobulbon* extracts. The aim is to be able to replace imported drugs from abroad is expensive and the competitive advantage of Thailand's herbal products market will be further improved.

2.4 *In Vitro* Experimentation

In vitro (Latin: *in glass*; often not italicized in English) studies are conducted using components of an organism that have been isolated from their usual biological surroundings, such as microorganisms, cells, or biological molecules. For example, microorganisms or cells can be studied in artificial culture media, and proteins can be examined in solutions.

2.4.1 Solubility

The solubility is a property referring to the ability for a given substance, the solute, to dissolve in a solvent. It is measured in terms of the maximum amount of solute dissolved in a solvent at equilibrium. This property is known as miscibility. The solubility of a solute in a particular solvent is the maximum concentration that may be achieved under given conditions when the dissolution process is at equilibrium. When a solute's concentration is equal to its solubility, the solution is said to be saturated with that solute. If the solute's concentration is less than its solubility, the solution is said to be unsaturated. A solution that contains a relatively low concentration of solute is called dilute, and one with a relatively high concentration is called concentrated. Solutions may be prepared in which a solute concentration exceeds its solubility. Such solutions are said to be supersaturated, and they are interesting examples of nonequilibrium states. Phenanthrene ($C_{14}H_{10}$) is nearly insoluble in water (1.6 mg/L) but is soluble in most low polarity organic solvents such as toluene, carbon tetrachloride, ether, chloroform, acetic acid and benzene.

2.4.2 Cytotoxicity (MTT assay)

Cytotoxicity assays were among the first in vitro bioassay methods used to predict toxicity of substances to various tissues (OECD GUIDELINE, 2001) [42, 43]. In vitro cytotoxicity testing provides a crucial means for safety assessment and screening, and for ranking compounds. The choice of using a particular cytotoxicity assay technology may be influenced by specific research goals. As such, four main classes of assays are used to monitor the response of cultured cells after treatment with potential toxicants [46]. These methods measure viability, cell membrane integrity, cell proliferation, and metabolic activity. In this chapter, we focus on the 3-(4,5-dimethylthiazol-2-yl)-2,5-diphenyltetrazolium bromide tetrazolium reduction colorimetric assay to evaluate detrimental intracellular effects on metabolic activity. This assay is well-characterized, simple to use and remains popular in several laboratories worldwide.

MTT Assay for Cell Viability and Proliferation

The MTT assay is used to measure cellular metabolic activity as an indicator of cell viability, proliferation and cytotoxicity [47, 48, 49]. This colorimetric assay is based on the reduction of a yellow tetrazolium salt (3-(4,5-dimethylthiazol-2-yl)-2,5-diphenyltetrazolium bromide or MTT) to purple formazan crystals by metabolically active cells (Figure 7A to 7B) [50]. The viable cells contain NAD(P)H-dependent oxidoreductase enzymes which reduce the MTT to formazan [51]. The insoluble formazan crystals are dissolved using a solubilization solution and the resulting-colored solution is quantified by measuring absorbance at 500-600 nanometers using a multi-well spectrophotometer. The darker the solution, the greater the number of viable, metabolically active cells [52, 53].

$$\text{Relative cell viability} = \frac{\left(\text{OD}_{550,\text{sample}} - \text{OD}_{550,\text{blank}}\right) \times 100}{\left(\text{OD}_{550,\text{control}} - \text{OD}_{550,\text{blank}}\right)} \quad ....(1)$$

This non-radioactive, colorimetric assay system using MTT was first described by Mosmann, 1983 [54] and improved in subsequent years by several other investigators. The Cell Proliferation Kit I (MTT) is an optimized MTT assay kit containing ready to use reagents, does not need washing steps or additional reagents. It is a quantitative assay that allows rapid and convenient handling of a high number of samples.
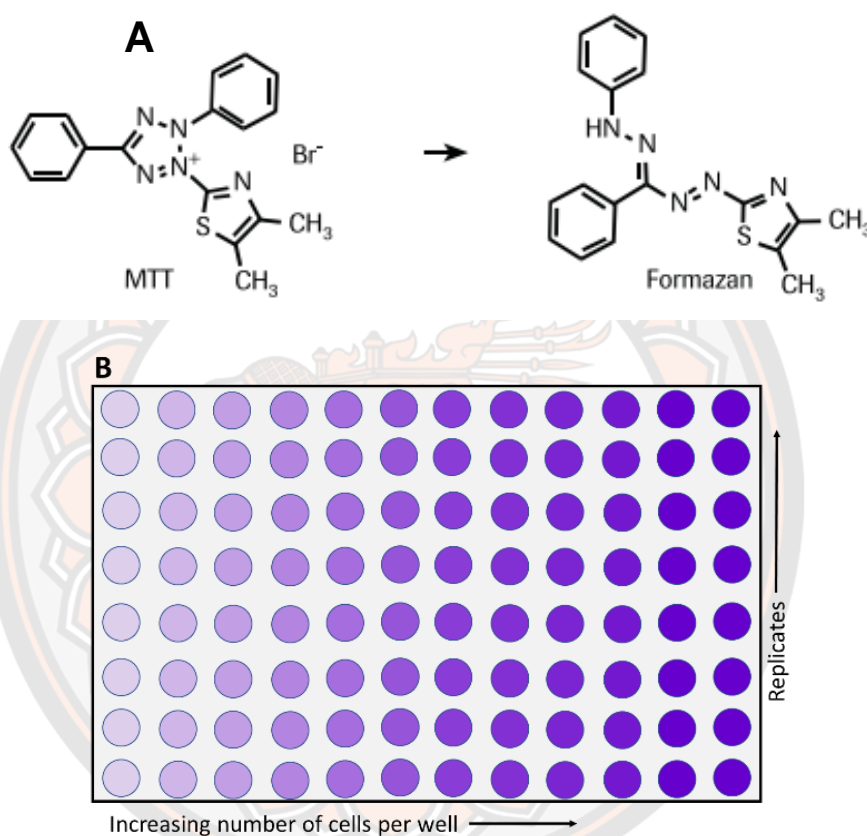
Figure 7 Metabolism of MTT to a formazan salt by viable cells as shown in a chemical reaction (A) and in a 96-well plate (B)

Tetrazolium dye reduction is generally assumed to be dependent on NAD(P)H-dependent oxidoreductase enzymes largely in the cytosolic compartment of the cell [55]. Therefore, reduction of MTT and other tetrazolium dyes depends on the cellular metabolic activity due to NAD(P)H flux. Cells with a low metabolism such as thymocytes and splenocytes reduce very little MTT. In contrast, rapidly dividing cells exhibit high rates of MTT reduction. It is important to keep in mind that assay conditions can alter metabolic activity and thus tetrazolium dye reduction without

affecting cell viability. In addition, the mechanism of reduction of tetrazolium dyes, intracellular (MTT, MTS) vs. extracellular (WST-1), will also determine the amount of product. Additionally, proof has been provided as to the spontaneous MTT reduction in lipidic cellular compartments/structures, without enzymatic catalysis involved. Nevertheless, even under this alternative paradigm, MTT assay still assesses the reduction potential of a cell (availability of reducing compounds to drive cellular energetics). As such, the final cell viability interpretation remains unchanged.

2.5 Pharmacokinetic Profile

2.5.1 Pharmacokinetic Values

The determining of pharmacokinetic parameters during drug development and optimization is now a primary focus for drug discovery. Prediction of bioavailability, half-life, distribution etc. are the pharmacokinetic parameters [56] of great interest as far as a new chemical entity must be developed as a drug for human use. In-vitro systems utilized to accurately predict this pharmacokinetics appears to be a very challenging task [57]. Optimization of absorption, distribution, metabolism and excretion (ADME) via incorporation of pharmacokinetic profile is the ultimate goal of drug discovery. The desired potential candidate carrying desirable efficacy and safety evidence obtained via concentration- time profile aims at identification of newer and potent leads. However, it is still necessary to incorporate the data obtained from pharmacokinetic parameters to be included for its pharmacological activity by drug delivery into in vivo animals [58].

2.5.2 Permeability (Caco-2 cells line)

Caco-2 cells are a human colon epithelial cancer cell line used as a model of human intestinal absorption of drugs and other compounds. When cultured as a monolayer, Caco-2 cells differentiate to form tight junctions between cells to serve as a model of paracellular movement of compounds across the monolayer. In addition, Caco-2 cells express transporter proteins, efflux proteins, and Phase II conjugation enzymes to model a variety of transcellular pathways as well as metabolic transformation of test substances. In many respects, the Caco-2 cell monolayer mimics the human intestinal epithelium. One of the functional differences between

normal cells and Caco-2 cells is the lack of expression of the cytochrome P450 isozymes and in particular, CYP3A4, which is normally expressed at high levels in the intestine. However, Caco-2 cells may be induced to express higher levels of CYP3A4 by treatment with vitamin D3. Caco-2 cell monolayers are usually cultured on semipermeable plastic supports that may be fitted into the wells of multi-well culture plates. Test compounds are then added to either the apical or basolateral sides of the monolayer. After incubation for various lengths of time, aliquots of the buffer in opposite chambers are removed for the determination of the concentration of test compounds and the computation of the rates of permeability for each compound (called the apparent permeability coefficients). Although radiolabeled compounds were used in the original Caco-2 cells monolayer assays, radiolabeled compounds have been replaced in most laboratories using liquid chromatography-mass spectrometry (LC-MS) and LC-tandem mass spectrometry (LC-MS-MS). Mass spectrometry not only eliminates the need for radiolabeled compounds but permits the simultaneous measurement of multiple compounds. The measurement of multiple compounds per assay reduces the number of incubations that need to be carried out, thereby increasing the throughput of the experiments. Furthermore, LC-MS and LC-MS-MS add another dimension to Caco-2 assays by facilitating the investigation of the metabolism of compounds by Caco-2 cells.

Cell Cultures

Caco-2 cells were maintained in DMEM at pH 7.4, supplemented with 20% fetal bovine serum, 2 mM L-glutamine, 1% non-essential amino acid solution and 1% penicillin-streptomycin solution in a humidified atmosphere (5% CO_2, 95% air, 37°C) [64]. The cells were grown under standard conditions until 60–70% confluency. Cells were used for all the experiments [59]. The cells were seeded on tissue culture polycarbonate membrane filters (pore size 3.0 µm) in 12-well Transwell® plates at a seeding density of 2×10^4 cells/cm^2 (following the recommendation from CORNING; Transwell® Permeable Supports) [60].

Table 1 Recommended transwell permeable support medium volumes

Transwell Insert Diameter	Insert Membrane Growth Area	Multiple Well Plate or Dish Type	Volume Added per Plate Well	Volume Added to Inside of Transwell Insert
4.26 mm	0.143 cm^2	96 well	0.235 mL	0.075 mL
6.5 mm	0.33 cm^2	24 well	0.6 mL	0.1 mL
12 mm	1.12 cm^2	12 well	1.5 mL	0.5 mL
24 mm	4.67 cm^2	6 well	2.6 mL	1.5 mL
75 mm	44 cm^2	100 mm dish	13 mL	9.0 mL

The culture medium was added to both the donor and the acceptor compartment. Medium was changed every second day. The cells were left to differentiate for 14–21 days after seeding with monitoring of TEER values were more than 300 Ω cm^2 using a Millicell® ERS meter (Millipore, Bedford, MA, USA).

2.5.3 Blood to Plasma Concentration ratio

The blood to plasma ratio determines the concentration of the drug in whole blood compared to plasma and provides an indication of drug binding to erythrocytes. The significance of blood to plasma concentration ratio, the pharmacokinetic parameters are usually determined by analysis of drug concentrations in plasma rather than whole blood. The blood to plasma ratio determines the concentration of the drug in whole blood compared to plasma and provides an indication of drug binding to erythrocytes. At blood to plasma ratios of greater than 1 (usually as a consequence of the drug distributing into the erythrocyte), the plasma clearance significantly overestimates blood clearance and could exceed hepatic blood flow [61].

The blood to plasma ratio protocol is adapted from a method by Yu *et al.,* 2005. Test compound is spiked into fresh heparinized whole blood, reference red blood cells and reference plasma. Following the incubation period, the whole blood is centrifuged. Both fractions of the whole blood (plasma and red blood cells) are analyzed by LC-MS/MS alongside the reference samples.

$$K_{RBC/PL} = \frac{C_{RBC}}{C_{PL}}$$

….(2)

As shown in Equation (2), the partition coefficient of a given drug in red blood cells, $K_{RBC/PL}$, is determined by the ratio of the concentration of the compound in RBC (C_{RBC}) over that in the equilibrating plasma (C_{PL}).

2.5.4 Microsomal and Hepatocyte Stability

Microsomal stability assay is the method with measurement of in vitro intrinsic clearance using microsomes. The liver is the most important site of drug metabolism in the body. Approximately 60 % of marketed compounds are cleared by hepatic CYP-mediated metabolism. Use of species-specific microsomes can be used to enable an understanding of interspecies differences in drug metabolism.

Hepatocyte stability assay is the method with measurement of in vitro intrinsic clearance using hepatocytes. The liver is the most important site of drug metabolism in the body. Approximately 60% of marketed compounds are cleared by hepatic CYP-mediated metabolism. Use of species-specific cryopreserved hepatocytes can be used to enable an understanding of interspecies differences Hepatocytes contain the full complement of hepatic drug metabolizing enzymes (both phase I and phase II) maintained within the intact cell.

2.5.5 CYP Phenotyping

For the human CYPs, reagents are readily available and in vitro reaction-phenotyping data are now routinely included in most regulatory documents. Ideally, the various metabolites have been definitively identified, incubation conditions have afforded robust kinetic analyses, and well characterized reagents and human tissues have been employed. It is also important that the various in vitro data are consistent and enable an integrated in vitro CYP reaction-phenotype. If the NCE receives market approval, information on key routes of clearance and their associated potential for drug-drug interactions are included in the product label. The present review focuses on in vitro CYP reaction-phenotyping and the integration of data. Relatively simple strategies enabling the design and prioritization of follow up clinical studies are also discussed.

CHAPTER III

RESEARCH METHODOLOGY

3.1 Materials and Equipment

3.1.1 Chemicals and reagents

- Acetone (Analytical grade, Batch No. 08021002, RCI Labscan Limited, Thailand)

- Caffeine (Analytical standard, Thailand)

- Calcium chloride dehydrated (Ultra-pure grade, EC No. 2331408, Lot No. 1123415, Fluka, Sigma-Aldrich, Germany)

- Digoxin (Analytical standard, Lot No. 100M1327V, Fluka Analytical, Sigma-Aldrich, USA)

- D-Glucose anhydrous (Certified AR for Analysis, Batch No. 0196879, Fisher Scientific, Thailand)

- DMEM, Dulbecco's Modified Eagle Minimum (Cell culture medium, Ref No. 11965-092, Lot No. 2052709, Gibco^{TM}, Thermo Fisher Scientific, Thailand Co., Ltd.)

- HEPES (Ultra-pure grade, Cas No. 7365-45-9, Lot No. 113151, Sigma-Aldrich, Thailand)

- Hexane (HPLC grade, Lot No. 16 04 0092, RCI Labscan Limited, Thailand)

- Hydrochloric acid 37% (Analytical grade, Batch No. 06060130, RCI Labscan Limited, Thailand)

- Magnesium sulfate (Laboratory reagent grade, Batch No. 0438519, Fisher Scientific, Thailand)

- Methanol (Analytical grade, Lot No. CL539, Burdick&Jackson Reagent Plus, USA)

- Methanol (HPLC grade, Lot No. 11 11 0384, RCI Labscan Limited, Thailand)

- Potassium chloride (Ultra-pure grade, EC No. 2312118, Fluka, Sigma-Aldrich, Germany)

- Potassium dihydrogen orthophosphate (Analytical reagent, Lot No. 0911208, UNIVAR®, Ajax Finechem Pty Ltd., New Zeland)

- Sodium acetate (Cell culture tested, S5636, Cas No. 127-09-3, Batch No. 064K0014, SIGMA®, Sigma Chemical, Japan)

- Sodium bicarbonate (Analytical reagent, Lot No. 1704100134, UNIVAR®, Ajax Finechem Pty Ltd., New Zeland)

- Sodium chloride (Analytical reagent, Batch No. 1506196155, UNIVAR®, Ajax Finechem Pty Ltd., New Zeland)

- Sterile water for injection (Lot NO. 591331, A.N.B. Laboratories CO., LTD., Thailand)

- Theophylline (Reference standard, Lot No. 53H59521, SIGMA, Sigma Chemical, USA)

- Thiazolyl blue tetrazolium bromide (MTT, Ultra-pure grade, Lot No. 0880C145, Amresco®, Ohio, USA)

- Trypan blue (Cell culture tested, T6146, Cas No. 72-57-1, Lot No. 123K53301, Sigma-Aldrich, Germany)

- Trypsin-EDTA (0.25% Trypsin-EDTA, Ref No. 25200-072, Lot No. 2063861, Gibco^{TM}, Thermo Fisher Scientific, Thailand Co., Ltd.)

3.1.2 Instruments and equipment

- Autoclave (HA-300P, Hirayama Manufacturing Corporation, Saitama, Japan)

- Epithelial Volt-Ohm Meter (Millicell® ERS-2, MERSSTX04, Lot No. CP8SA0234, MERCK Millipore®, France)

- Freezer -20 °C (SANYO, Thailand)

- Incubator CO_2 (Forma series II, Thermo Fisher Scientific Inc., MA, USA)

- Inverted microscope (Model TS100, Nikon Eclipse, Tokyo, Japan)

- Lamina flow hood (Heal force®, HF safe 1200/c+, Shanghai, China)

- Microplate Spectrophotometer (Multimode detector DTX 880, Beckmann, Switzerland)

- Micro refrigerated centrifuge (Kubota 3740, Japan)

- pH meter (Mettler Toledo Model S20-K, GmbH Schwerzenbach, Switzerland)

- Transwell® Permeable Supports (12 mm Diameter Insert, 12 well, Ref No. 3041, Lot No. 35418016, Costar®, Kennebunk ME, USA)

- Vertical laminar flow cabinet (Model BHG2004S, Faster SRL., Ferrara, Itary)

3.1.3 Preparation of EM2

Following the methods of Temkitthawon and team, 2017 [1]. Cut the tubers of *E. macrobulbon* into small pieces and then dry at 55 degrees Celsius, grind to a fine powder (2 kilograms), macerate in 95% ethanol (14 litters) for 3 days, then filter and evaporate dry by using a rotary evaporator to get a crude extract (ethanolic extract). Measure the quantities of phenanthrene or EM2 (1-(4′-hydroxybenzyl)-4,8-dimethoxyphenanthrene-2,7-diol)

3.2 Methods

3.2.1 Cell culture

Cell culture was concerned technically by aseptically decantation. Human epithelial cell line Caco-2 were purchased from American Type Culture Collection (ATCC, HTB-37) and cells were used at passage number 30-35 throughout. The Caco-2 grown in DMEM-F12, supplemented with 20% (v/v) FBS and 1% (v/v) penicillin-streptomycin. Caco-2 cells were maintained at 37° C, 95% air and 5% CO_2. The cells were grown under maintain condition until 70-80% cell confluency and were split 1:4 or 1:6 before afterward cultivation.

3.2.2 Cell viability

The effect of EM-2 on the Caco-2 Cell was assessed using MTT method. Briefly, the cells were seeded in a 96 well plate at 20,000 cells per well [62] and cultured for 24 hr. EM-2 at different concentrations of 0.5 to 50 µM was treated in a culture medium without FBS and incubate for 20 hr. MTT solution (5 mg/ml in water) 10 µl was added to each well and the mixture was incubated for another 4 hr. Then the solution was removed and 50% DMSO in ethanol was added to each well. The absorbance was detected at 570 nm using microplate reader. Cell viability was expressed as a percentage of the control [63, 64].

3.2.3 Caco-2 Permeability

Caco-2 cells were resuspended in medium to culture on the apical chamber of 12-well Transwell® polycarbonate membrane filters (pore size 0.4 µm and diameter 12 mm). The resuspended Caco-2 cells 0.5 ml were seeded at a density of $2x10^4$ cells•cm^{-2} [65]. Meanwhile, only medium 1.5 ml were added to the basolateral compartment. The cells were incubated in standard condition, the medium was changed every couple of days. The cells would be fully monolayers for 14-21 days post-seeding to authorize full of the cell's maturation, especialy *P-gp* expression and suitable tight junctions [66]. The Caco-2 monolayers with TEER values ≥ 300 Ω•cm^2 were used in transport experiments.

Determination of the Caco-2 permeability of EM2 at the concentrations of 1 µM and 10 µM by using apical to basolateral (AP-BL) and basolateral to apical (BL-AP) directions. The Caco-2 monolayers grown in12-well Transwell® inserts was used in experiment to prophesy the permeability. Pre-warm HBSS-HEPES buffer solutions (pH 7.4) was used to pre-incubate after removing the DMEM/F-12 medium. The insert plates were incubated on the orbital shaker (300 rpm) at 37 degrees Celsius for 30 minutes to equilibrium both compartments. Measurement of the TEER values of monolayers that higher than 300 Ω•cm2 were considered to use in the assay.

The efflux of the test sample was measured in both transport directions with time dependence. Doner solution of EM2 with 0.1% (v/v) DMSO in HBSS-HEPES buffer was replaced in the doner compartment for absorptive (AP to BL) transport when doner is AP compartment. Likewise, for secretory (BL to AP) transport, the doner was BL compartment. For the receiver compartment, it was replaced by the blank HBSS-HEPES buffer with 0.1% (v/v) DMSO as well. Samples (200 µl) were taken 0, 30, 60, 120, and 240 minutes from both AP and BL sides under the condition [62]. Both compartments were replaced back with an equal concentration and volume. The TEER values were measured again to ensure monolayers after the experiment. The solution in AP compartment was removed out and washed the cells by cold buffer. Then, monolayers on the insert filter were lysed with 200 µl acetonitrile. Rhodamine 123 (*P-gp* substrate, 5 µM) [64] was run as a negative control in the study. The concentrations of sample were determined the concentration for expressing as cumulative transport as a function of time. The apparent permeability coefficients

(P_{app}, unit: cm•s^{-1}) was calculated by following the equation, where A is the area of filter (1.12 cm^2), $V_{reciever}$ is total volume in mililters and Time is total transport time in seconds.

$$P_{app} = [V_{reciever} / (A \bullet Time)] \bullet (C_{reciever} / C_{donor})$$

The uptake ratio ($P_{app(AP-BL)} / P_{app(BL-AP)}$), efflux ratio ($P_{app(BL-AP)} / P_{app(AP-BL)}$, cell accumulation (concentration in buffer and acetonitrile wash) and recovery value (total amount recovered/initial amount added) were calculated [67].

Sample analysis

The amount of EM2 was determined by High-performance liquid chromatography using UV-detector (HPLC-UV) with a 150 x 4.6 mm C18(2) LC column (00F-4252-E0, Luna® 5 µm; Phenomenex, USA) as a stationary phase. The separation was achieved by using 40: 60, acetonitrile: water (v/v) mixture as a mobile phase under isocratic conditions. The system was operated at temperature 25 °C, flow rate for 1.0 ml/min, injection volume for 20 µl, and detection wavelength at 265 nm. Pure compound of EM2 was used as a standard, calibration curve. The within- and between-day precision is determined for both retention times and peak area. The data suggests that the proposed HPLC method can be used for routine quality control of food, drinks, and herbal products. Rhodamine123 was quantified by measuring fluorescence with a microplate reader. The condition to determine was set to the excitation wavelength of 500 nm and emission wavelength of 525 nm [67] at 25 °C.

3.2.4 Stability in Hepatocytes

Thawing protocol

Cryopreserved primary hepatocyte cells suspension (Human liver cells, Lot# S1242T, KaLy-Cell) was used in the study. Two vials of the cell suspension were thawed with thawing medium (DMEM-F12 medium containing 1 µM dexamethasone, 4 µg/ml insulin (Adtrapid®HM), 1% penicillin-streptomycin, and 10% FBS) and isotonic 90% percoll (100 ml of percoll with 10 ml of PBS 10X). Cells in the vials were thawed and centrifuged at 170 g for 20 min at 25 °C. Then the cells were gently resuspended with a seeding medium (the mixture was the same as the thawing medium but use 5% FBS).

Stability in Hepatocytes assay

A cocktail mixture (100 µl) containing hepatocyte cells suspension with EM2 (final concentrations was 10 µM) in a seeding medium was seeded to a deep 96-well plate at a density of 20,000 cells per well. The plate was closed with a sealing film and incubated at 37 °C with constant stirring at 900 rpm on an orbital shaker. The samples 75 µl were taken at 0, 15, 30, 60, 120, and 180 min. The taken samples were quenched with 75 µl of cold acetonitrile and centrifuged at 9,000 rpm for 10 min. The supernatant was kept at -20 °C before measuring sample concentration by HPLC method.

3.2.5 Microsomal Stability

The reactions (0.5 ml) consisted of 50 µM EM2 (10 µl), 1 M potassium phosphate buffer (pH 7.4, 25 µl), 100 mM $MgCl_2$ (15 µl), 100 mM EDTA (5 µl), distilled water (345 µl), and pooled liver microsomes 1 mg/ml in 250 mM sucrose (50 µl). Following pre-incubation (at 37 °C for 10 min), the reactions were initiated by adding 10 mM β-NADPH (50 µl). Samples (75 µl) were withdrawn at 0, 30, 60, 90, and 120 min and stopped reaction with cold acetonitrile (75 µl). Centrifugation at 9,000 rpm for 10 min was used to separate sample solution (the supernatant) from microsome (the residue).

3.2.6 Single-Use RED Plate with Inserts study

This study was designed to determine the percent bound of the sample compound concentrations in whole blood or plasma or buffer chamber after reach equilibrium. The Single-Use RED Plate with Inserts (Thermo Scientific, cutoffs 8 K MWCO, Number; 90006) compose of 48 equilibrium dialysis membrane and dispersible high-density polyethylene was used in the study. EM2 was designed and widely validated for plasma protein binding. Dialysis buffer (pH 7.4) using phosphate-buffered saline (PBS) containing 100 mM sodium phosphate and 150 mM sodium chloride was used in the study.

Blood collection and serum preparation

Whole blood was obtained from the donors (healthy women; 24-25-year-old), contained in an anticoagulant tune. The blood tube was centrifuged at 1200 rpm to collect plasma for 30 min (เยาวลักษณ์ พิมายนอก และคณะ, 2545). Whole blood and plasma were stored at 4 °C until used (Should not storage more than 1 week).

Plasma to buffer concentration ratio study

Plasma was mixed with EM2 at final concentrations of 1 and 10 µM (0.01 % DMSO). The plasma mixture was placed into the sample chamber for 300 µl (red retainer ring chamber) and the buffer chamber was added by 550 µl of PBS buffer saline (containing 100mM sodium phosphate and 150mM sodium chloride). The RED Plate was covered with a sealing tape and incubated at 37 °C on an orbital shaker (300 rpm) for 4 hr sufficient to achieve equilibrium.

After gentle inversion, 200 µl of collected plasma sample was mixed with 200 µl of distilled water and vortexed to hemolysis. The protein was precipitated by adding 800 µl of 0.17 M $ZnSO_4$ in 90% methanol (Mbughuni MM et al, 2020). After precipitation, the sample was then vortexed, incubated on ice (30 min) and centrifuged at 3,500 rpm (10 min). The supernatant was recovered for analysis by HPLC. The study was performed tests in triplicate.

3.3 Statistical Analysis

The statistical analysis showing the experimental results with mean values and standard variance ranges (mean ± SD). Which the results were statistically significant of variance (ANOVA) and followed by post hoc test (Turkey) by the Prism program (GraphPad Software Inc.). When * that is a p-value less than 0.05 ($p<0.05$) to *** that is a p-value less than 0.001 ($p<0.001$) levels.

CHAPTER IV

RESULTS AND DISCUSSION

This chapter shows the outcomes and results that were obtained from the study, which mainly focuses on the EM2's results. After the experiment of EM2 in the field of pharmacology in terms of pharmacokinetic parameters. The results were promised and analyzed.

4.1 Cytotoxicity

4.1.1 Cytotoxicity of Caco-2 cells

Before evaluating of Caco-2 permeability of EM2 through the monolayer cells using 12-Transwell inserts plate in both directions (absorptive and secretory transportation), its direct effects on this type of cells were evaluated in order to assess EM2's cytotoxic effect. This information results would be helpful to decide the appropriate concentrations of EM2 for further studies in this thesis. For this study, Caco-2 cells were seeded in 96-well plate for 24 hours and treated with various concentrations of EM2 (0.5-50.0 µM, 0.01% DMSO). The viability of Caco-2 cells was determined by MTT reagent.

%Cell viability of Caco-2

Table 2 Viability of Caco-2 cells treated with various concentrations of EM2 (0.5-50 µM) by MTT assay (n=3)

EM2 (µM)	%Cell viability of Caco-2 c ells			AVG ± SD
	N 1	N2	N3	
0 (Control)	100.00	100.00	100.00	100.00 ± 0.00
0.5	99.93	99.32	101.72	100.33 ± 1.25
1	100.23	98.08	101.49	99.93 ± 1.72
2.5	101.43	100.91	98.17	100.17 ± 1.75
5	99.48	104.75	98.92	101.05 ± 3.21
7.5	99.24	100.22	98.87	99.44 ± 0.70
10	100.23	98.49	98.92	99.21 ± 0.90
12.5	99.80	97.94	98.14	98.63 ± 1.02
15	99.91	99.12	98.69	99.24 ± 0.62
17.5	99.42	95.49	97.08	97.33 ± 1.98
20	99.16	96.46	98.20	97.94 ± 1.37
22.5	99.13	93.35	96.77	96.42 ± 2.91
25	98.35	91.00	96.82	95.39 ± 3.88
27.5	98.41	88.76	94.93	94.03 ± 4.89
30	96.74	87.96	89.02	91.24 ± 4.79
32.5	94.89	85.23	77.13	85.75 ± 8.89
35	91.17	76.25	67.62	78.35 ± 11.91
40	72.32	61.13	57.61	63.69 ± 7.68
50	16.73	17.37	15.76	16.62 ± 0.81
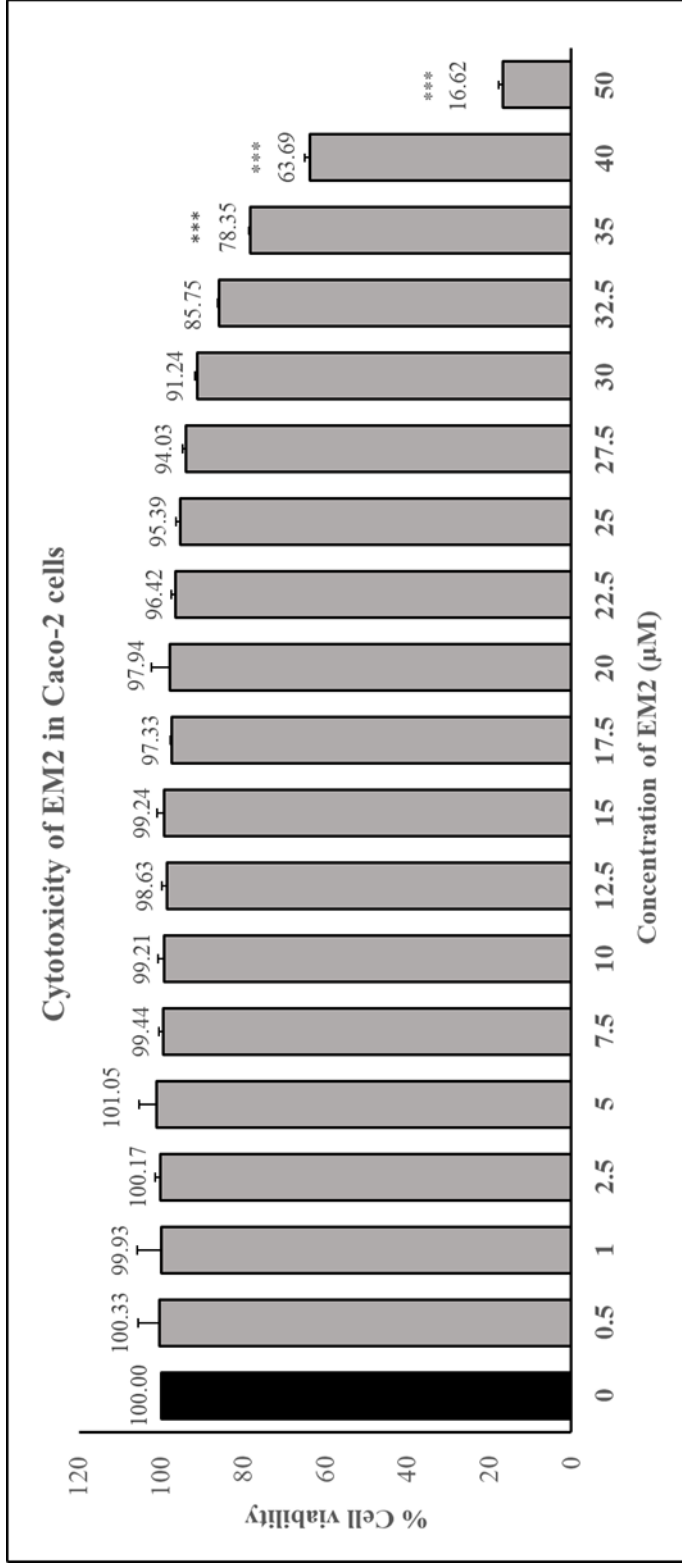
Figure 8 Viability of Caco-2 cells treated with various concentrations of EM2 by MTT assay. The data are the means ± SD of three seperate experiment. Statistical analysis was done using one way ANOVA (Turkey post hoc test). Significantly different from control.

(* = p-value<0.001)**

The results showed high effect of EM2 on Caco-2 cell viability (Table 2 and Figure 8). At low concentration of EM2 (0.5 to 15.0 µM) showed no effect on cell several. As EM2 concentrations increase up to 17.5-32.5 µM, percentage of Caco-2 cells viability gradually decreased. From concentration of EM2 35.0 to 50.0 µM, cells viability was strongly decreased from lower than 80% to 20%. This, the concentrations of EM2 at 1 and 10 µM were chosen and use for further experiment to determine its effectives.

IC$_{50}$ of EM2 in Caco-2 cells
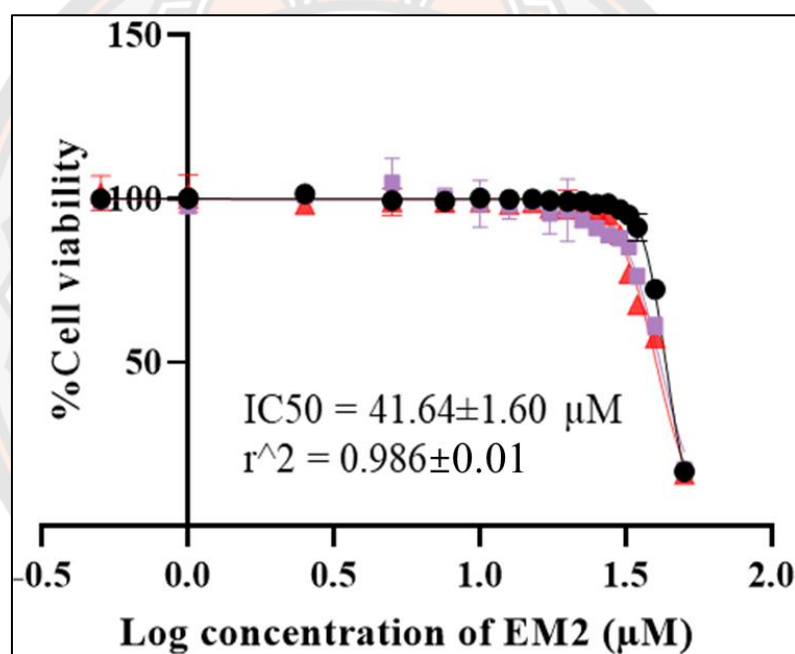
Figure 9 IC50 of EM2 from Caco-2 cells treated with various concentrations (0.5-50 µM) by MTT assay (n=3)

These data from the Table 2 demonstrated that EM2 had an IC50 value was 41.64 ± 1.60 µM (Figure 9) from viability of Caco-2 cells treated with various concentrations of EM2 by MTT assay.

4.1.2 Cytotoxicity of Hep G2 cells

Before evaluating of stability of EM2 (Hep G2 stability stesting) with Hep G2 cells, its direct effects on this type of cells were evaluated in order to assess EM2's cytotoxic effect. This information results would be helpful to decide the appropriate concentrations of EM2 for further studies in this thesis. For this study, Hep G2 cells were seeded in 96-well plate for 24 hours and treated with various concentrations of EM2 (0.5-50.0 µM, 0.01% DMSO). The viability of Hep G2 cells was determined by MTT reagent.

%Cell viability of Hep G2

Table 3 Viability of Hep G2 cells treated with various concentrations of EM2 (0.5-50 µM) by MTT assay (n=3)

EM2 (µM)	%Cell viability of Hep G2 cells			AVG ± SD
	N 1	N2	N3	
0 (Control)	100.00	100.00	100.00	100.00 ± 0.00
0.5	92.36	96.63	96.54	95.18 ± 2.44
1	93.57	97.28	92.78	94.54 ± 2.41
2.5	91.99	95.56	94.68	94.08 ± 1.86
5	93.70	89.80	83.48	89.00 ± 5.16
7.5	91.20	95.56	96.31	94.35 ± 2.76
10	87.76	96.54	91.61	91.97 ± 4.40
15	92.45	85.62	96.77	91.61 ± 5.62
17.5	90.45	91.71	89.06	90.41 ± 1.32
20	90.31	87.94	89.76	89.34 ± 1.24
22.5	83.07	86.04	84.27	84.46 ± 1.49
25	72.06	75.45	78.65	75.38 ± 1.30
27.5	74.52	64.48	72.61	70.54 ± 5.33
30	70.10	57.93	61.42	63.15 ± 6.27
32.5	52.78	46.78	44.79	48.11 ± 4.16
35	30.10	28.99	30.75	29.95 ± 0.89
40	25.13	23.65	28.15	25.64 ± 2.30
50	26.85	19.56	22.49	22.97 ± 3.67
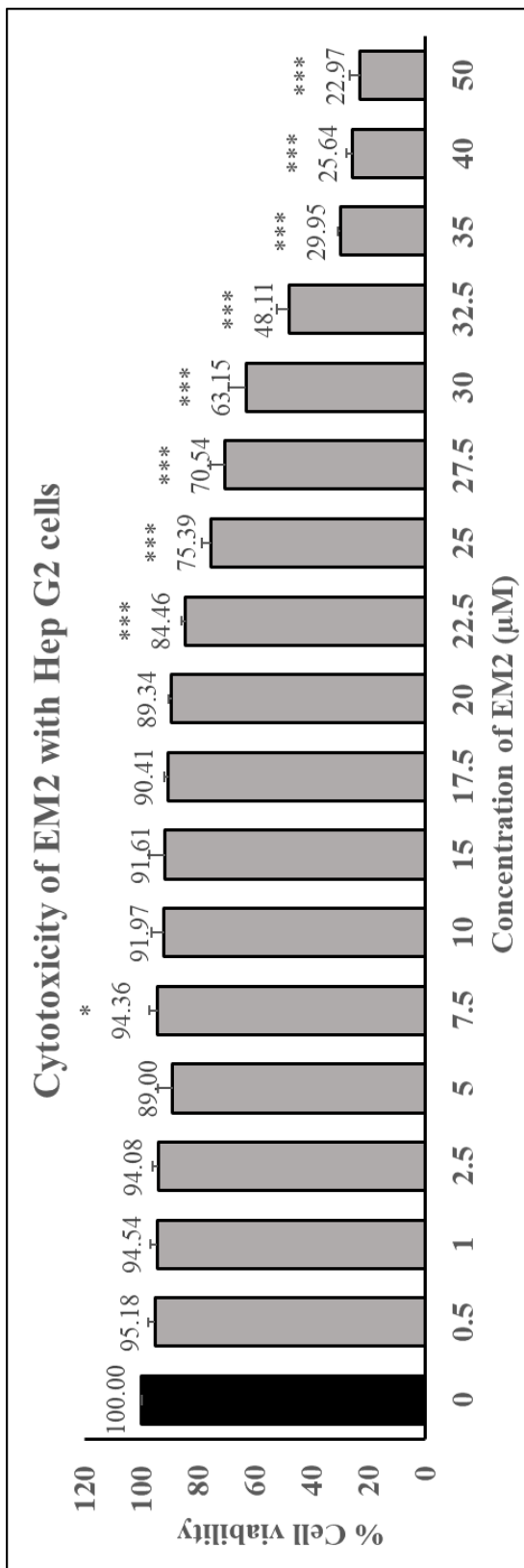
Figure 10. Viablility of Hep G2 cells treated with various concentrations of EM2 by MTT assay. The data are the means ± SD of three seperate experiment. Statistical analysis was done using one way ANOVA (Turkey post hoc test). Significantly different from control.

(* = p-value<0.05 and *** = p-value<0.001)

The results showed high effect of EM2 on Hep G2 cells viability (Table 3 and Figure 10). At low concentration of EM2 (0.5 to 17.5 µM) showed percentage of Hep G2 cells viability gradually decreased. From concentration of EM2 20.0 to 50.0 µM, cells viability was strongly decreased from lower than 90% to 20%. This, the concentrations of EM2 at 1 and 10 µM were chosen and use for further experiment to determine its effectives.

IC_{50} of EM2 in EM2 cells
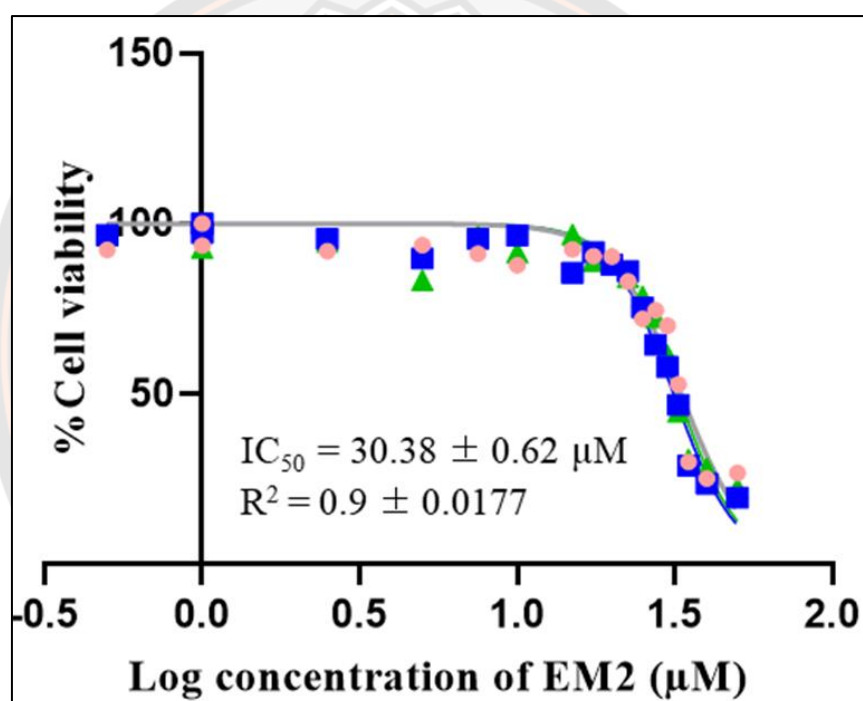
Figure 11 IC_{50} of EM2 from Hep G2 cells treated with various concentrations (0.5-50 µM) by MTT assay (n=3)

These data from the Table 3 demonstrated that EM2 had an IC50 value was 30.08 ± 0.62 µM (Figure 11) from viability of Hep G2 cells treated with various concentrations of EM2 by MTT assay.

4.2 Evaluation of Caco-2 permeability

Caco-2 cells (P38) were seeded in 48-well plate which is area 1.12 mm as the same with 12-Transwell insert plate that would be used in the experiment. Cells were cultured in DMEM/F12 containing 20% FBS and 1% penicillin-streptomycin and maintained at 37 degrees Celsius in CO2 incubator with a saturated humidity atmosphere containing 95% air and 5% of CO. New medium was replaced in each well every 2 days. Pictures were taken at time of seeding at 1, 14 and 21 days after seeding by using Light Microscope.

4.2.1 Cell culture

Caco-2 cells P38 (day 1) in 48-well plate
Light microscope; 4x, Ph0
Light microscope; 10x, Ph1
Light microscope; 20x, Ph2
Light microscope; 40x, Ph2
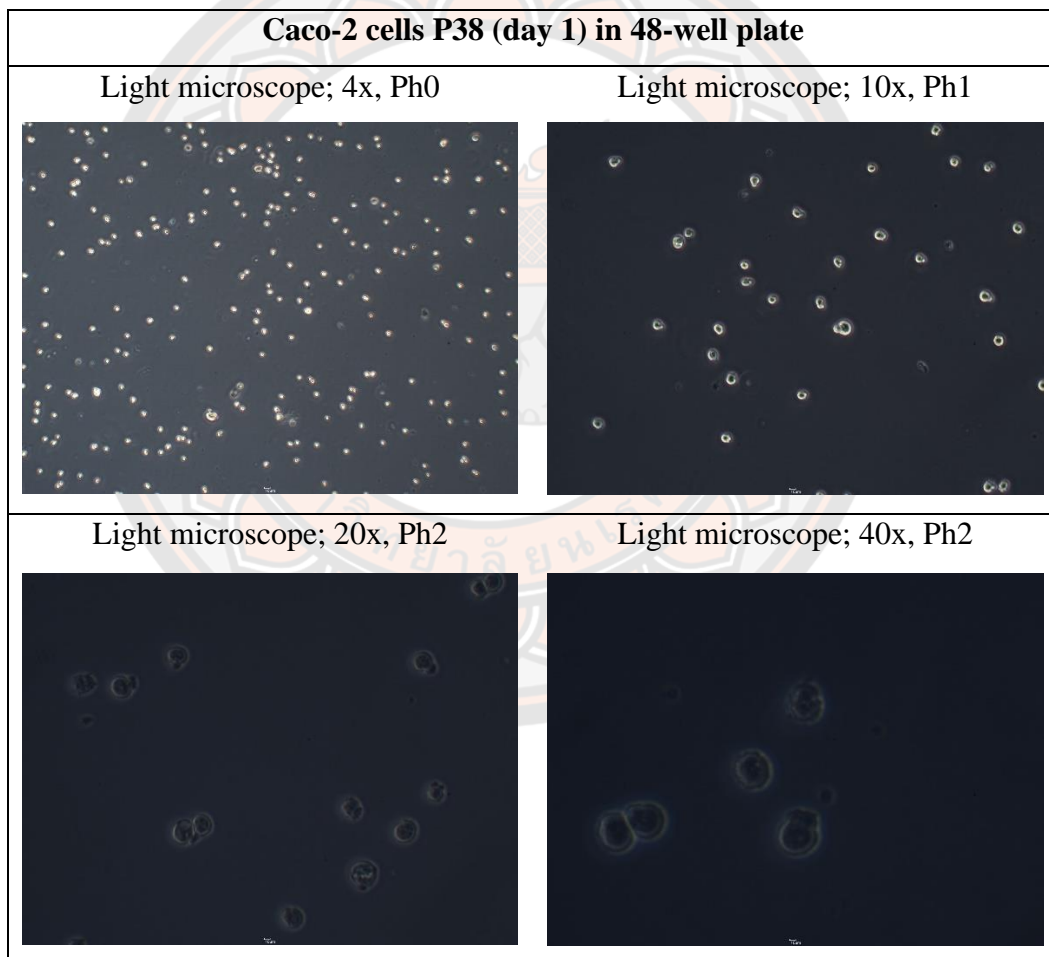
Figure 12 Microscopic photographic of Caco-2 cells in 48-well plate (day 1)

Caco-2 cells P38 (day 14) in 48-well plate	
Light microscope; 4x, Ph0	Light microscope; 10x, Ph1
Light microscope; 20x, Ph2	Light microscope; 40x, Ph2
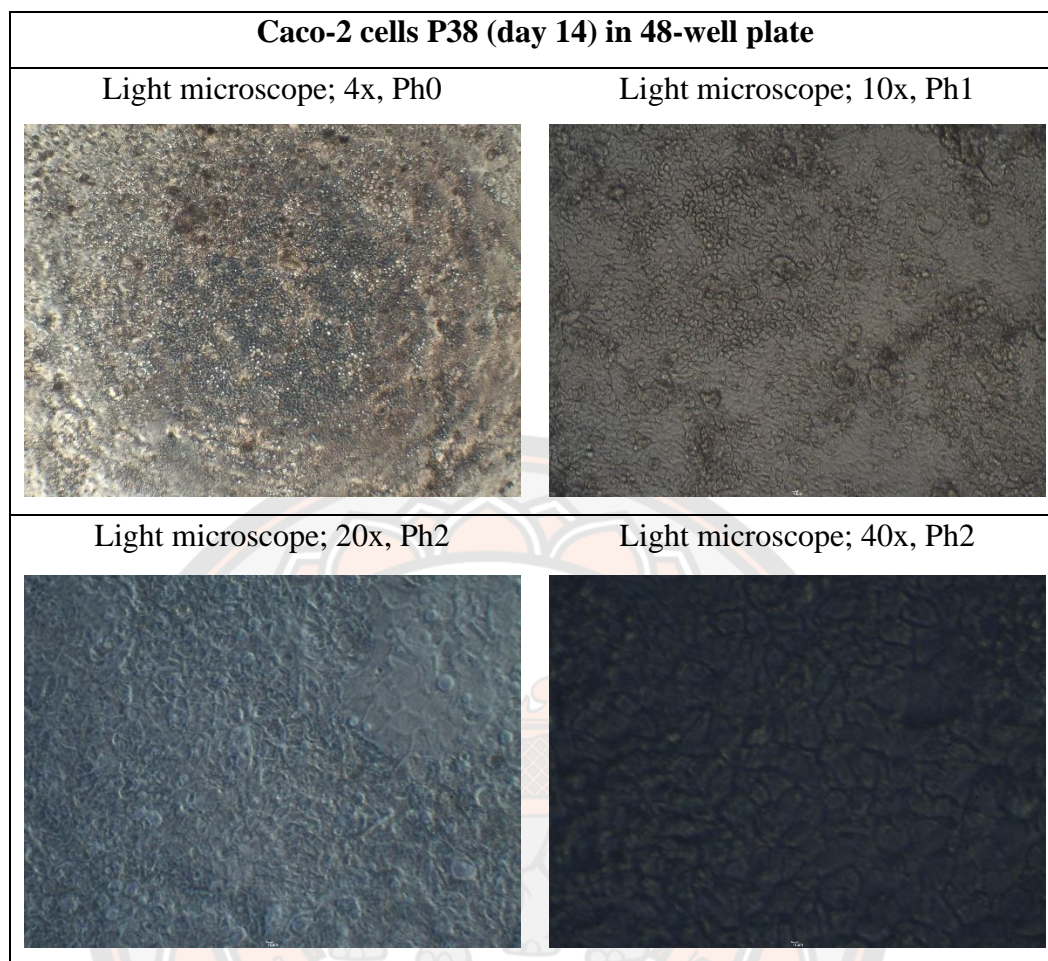
Figure 13 Microscopic photographic of Caco-2 cells in 48-well plate (day 14)

Caco-2 cells P38 (day 21) in 48-well plate	
Light microscope; 4x, Ph0	Light microscope; 10x, Ph1
Light microscope; 20x, Ph2	Light microscope; 40x, Ph2
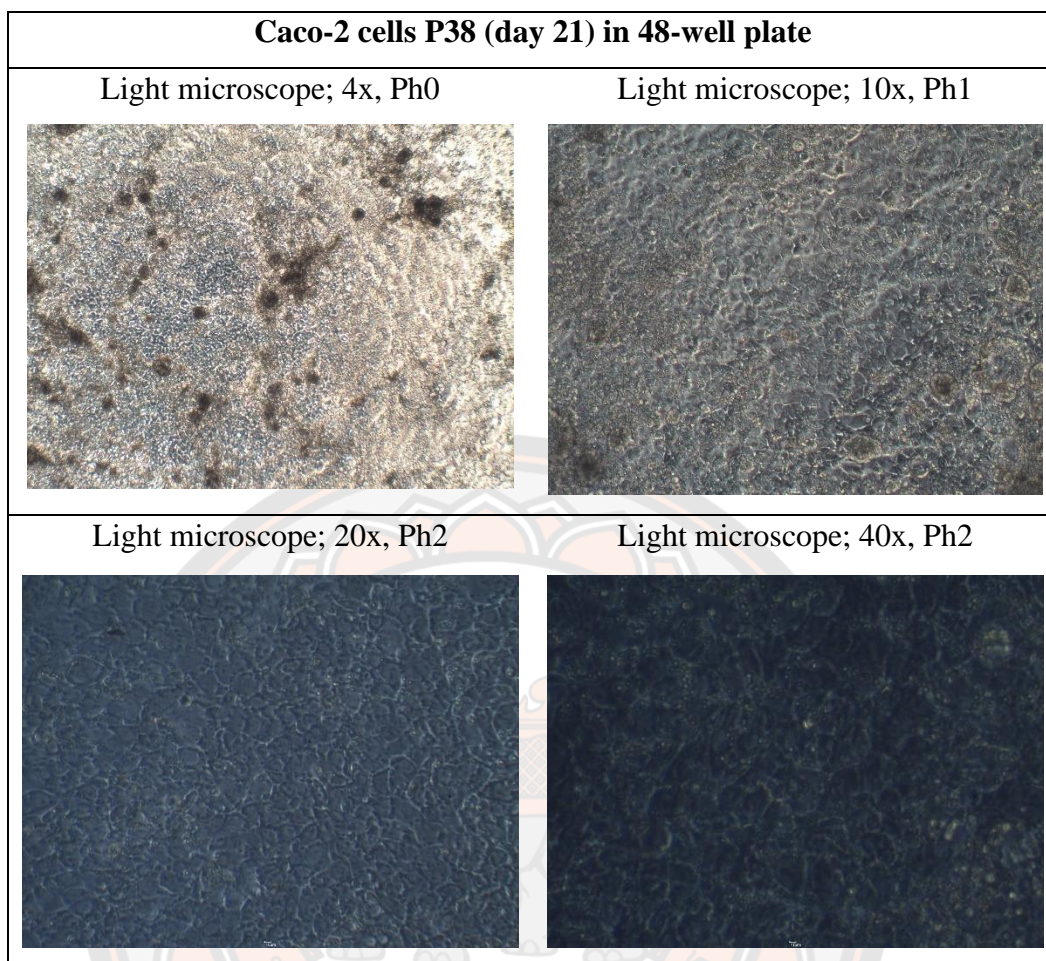
Figure 14 Microscopic photographic of Caco-2 cells in 48-well plate (day 21)

Caco-2 cells P38 in 12-Transwell plate	
Day 14	**Day 21**
Light microscope; 4x, Ph0	Light microscope; 10x, Ph1
Light microscope; 10x, Ph1	Light microscope; 10x, Ph1
Light microscope; 20x, Ph2	Light microscope; 20x, Ph2
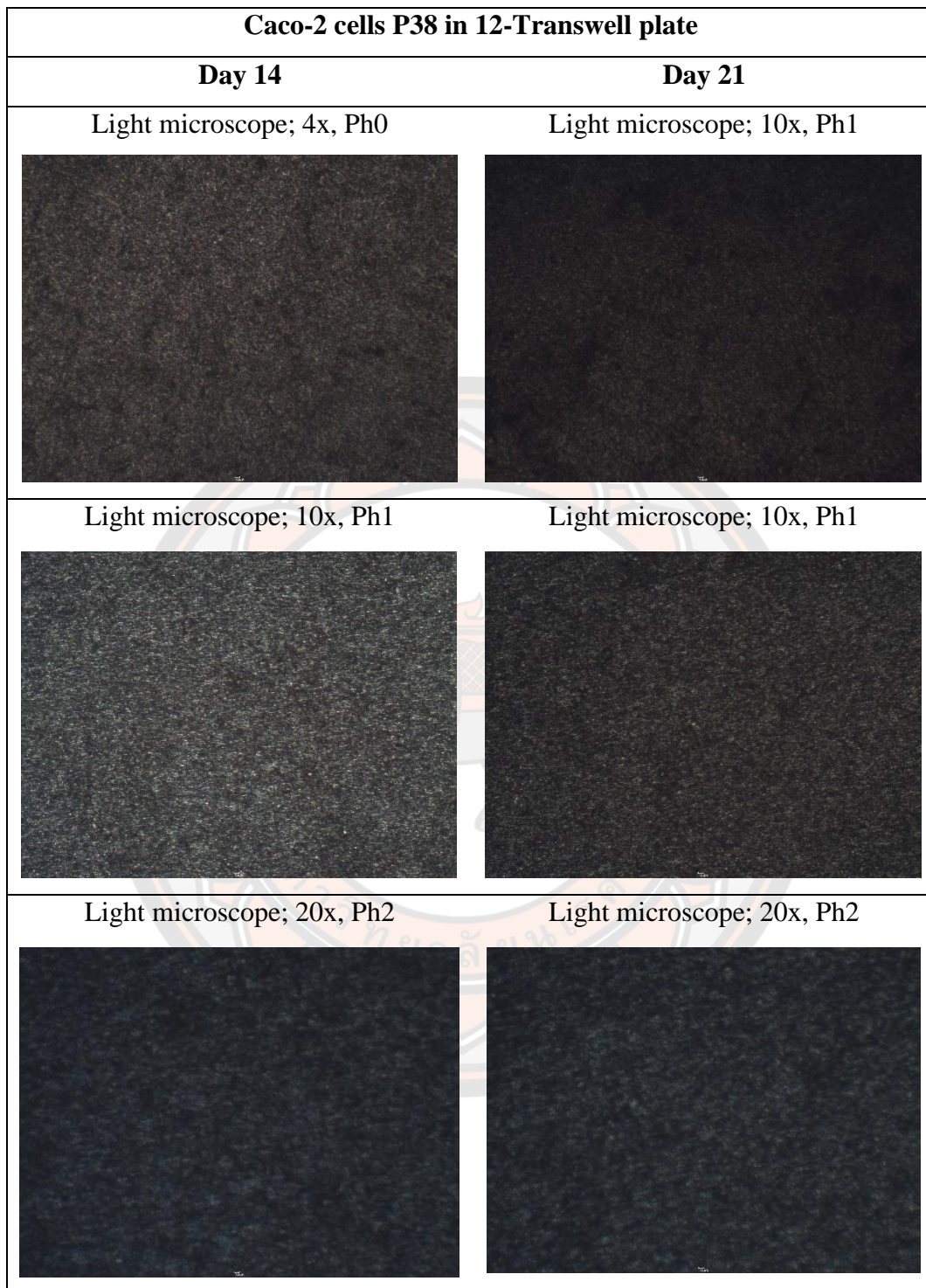
Figure 15 Microscopic photographic of Caco-2 cells in 12-well plate

4.2.2 Evaluation of Monolayer Integrity

The TEER values in the acceptable of ≥300 $\Omega \cdot cm^2$ were applied for further experiments. The TEER determinations for all experiments consumption in this section were in the range of 200 to 350 ohms x cm^2 (table 4-1). This range is indicative of the successful formation of integral monolayers after 14-21 days of culture. The differentiation monolayers with tight junctions were corresponding confirm from TEER values.

Table 4 TEER values in the each 12-Transwell insert

Doner compartment		TEER values		
		Before replacing by HBSS-HEPES buffer	**After replacing by HBSS-HEPES buffer**	**After incubation in HBSS-HEPES buffer for 2/4 hrs.***
EM2 (1 µM) *AP chamber	1	350.33±2.89	344.00±1.73	341.33±1.53
	2	336.67±3.06	331.33±2.89	331.33±2.31
	3	585.67±0.58	399.67±1.15	374.00±0.00
	4	562.33±4.04	376.67±4.04	351.67±0.58
EM2 (1 µM) *BL chamber	1	346.00±15.87	364.67±1.15	359.00±1.73
	2	356.33±1.53	355.33±0.58	354.33±2.52
	3	552.33±3.79	383.67±2.31	356.00±0.00
	4	544.67±4.04	376.00±0.00	351.67±1.15
EM2 (10 µM) *AP chamber	1	957.00±1.73	621.00±1.73	428.33±0.58
	2	977.67±0.58	686.00±1.73	495.67±0.58
	3	962.00±1.73	616.00±0.00	464.33±1.15
EM2 (10 µM) *BL chamber	1	967.00±1.73	672.33±1.53	406.67±2.31
	2	977.33±1.15	640.67±0.58	387.33±1.53
	3	1005.33±0.58	724.67±0.58	435.67±0.58

Doner compartment		TEER values		
		Before replacing by HBSS-HEPES buffer	After replacing by HBSS-HEPES buffer	After incubation in HBSS-HEPES buffer for 2/4 hrs.*
R123	1	1046.67±1.15	772.33±1.15	443.67±2.31
(5 µM)	2	1052.67±1.15	759.00±1.00	413.00±1.00
*AP chamber	3	1044.67±1.15	782.33±2.31	455.67±0.58
R123	1	941.33±0.58	665.67±0.58	400.67±3.79
(5 µM)	2	960.67±1.15	759.00±1.00	425.67±0.58
*BL chamber	3	962.00±1.53	602.67±2.08	417.33±0.58
*AP chamber	3	1044.67±1.15	782.33±2.31	455.67±0.58
R123	1	941.33±0.58	665.67±0.58	400.67±3.79
(5 µM)	2	960.67±1.15	759.00±1.00	425.67±0.58
*BL chamber	3	962.00±1.53	602.67±2.08	417.33±0.58

4.2.4 Evaluation of Caco-2 permeability

Bidirectional transport (AP-BL and BL-AP)

Caco-2 cells were cultured (14-21 days) in the 12-well Transwell® polycarbonate membrane filters for the formation of monolayer cells. The TEER values were checked to confirm monolayers formation. The Caco-2 monolayers were treated with EM2 and were incubated on an orbital shaker (300 rpm) at 37 degrees Celsius. Sample solutions were taken at the time 0, 60, 120, and 240 minutes. By this method, each sample solution was brought to measure the concentration of samples in the apical chamber and basolateral chamber. The sample EM2 has experimented in two concentrations (1 µM and 10 µM) along with caffeine (high permeability compound) and rhodamine 123 (low permeability compound, P-glycol protein substrate) comparison. Table 4 shows the time independence of EM2 in absorptive and secretory directions across Caco-2 monolayers and shows the efflux ratios and uptake ratios.
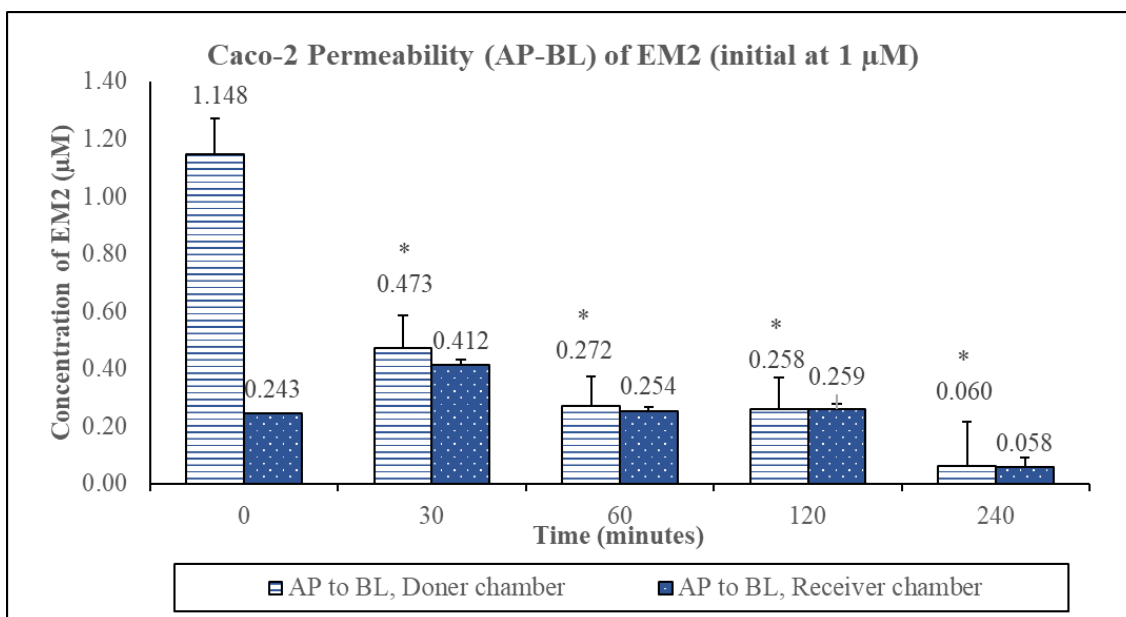
Figure 16 Bidirectional transport of EM2 (initial concentration at 1 µM). EM2 1 µM was added into donor chamber (AP) of Caco2 cell monolayers

Note: Samples were taken from both doner and receiver chambers at different time points (30, 60, 120 and 240 min) with replaced back by same concentration and volume and measured with HPLC. Results are expressed as concentration of EM2 dose (n = 4). Statistical analysis was done using one way ANOVA (Turkey post hoc test). Significantly different from concentration of EM2 at 0 minute. (* = p-value < 0.05)
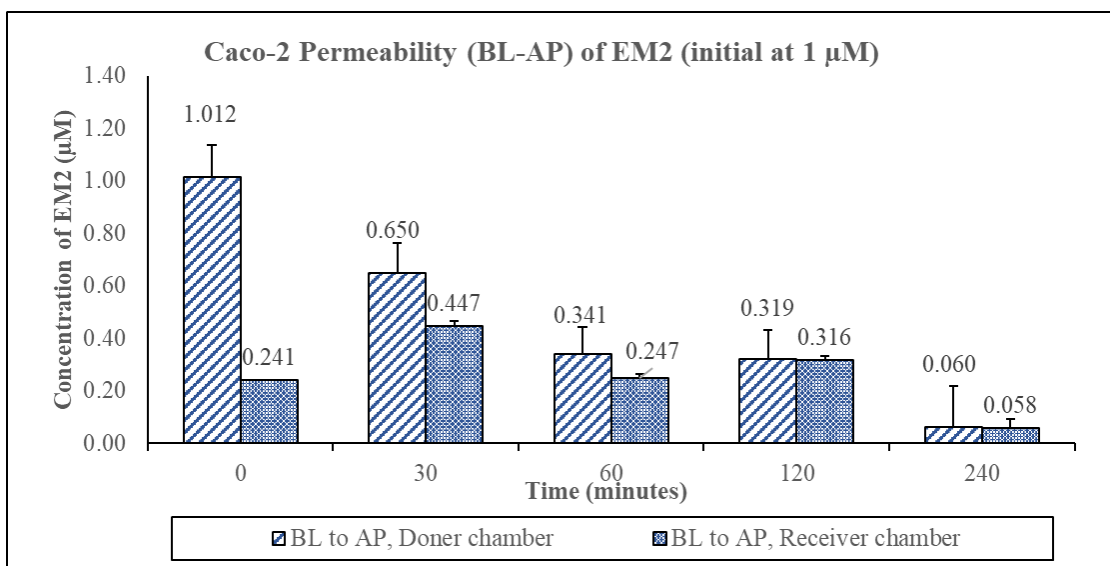
Figure 17 Bidirectional transport of EM2 (initial concentration at 1 µM). EM2 1 µM was added into donor chamber (BL) of Caco2 cell monolayers

Note: Samples were taken from both doner and receiver chambers at different time points (30, 60, 120 and 240 min) with replaced back by same concentration and volume and measured with HPLC. Results are expressed as concentration of EM2 dose (n = 3). Statistical analysis was done using one way ANOVA (Turkey post hoc test). Not significantly different from concentration of EM2 at 0 minute.
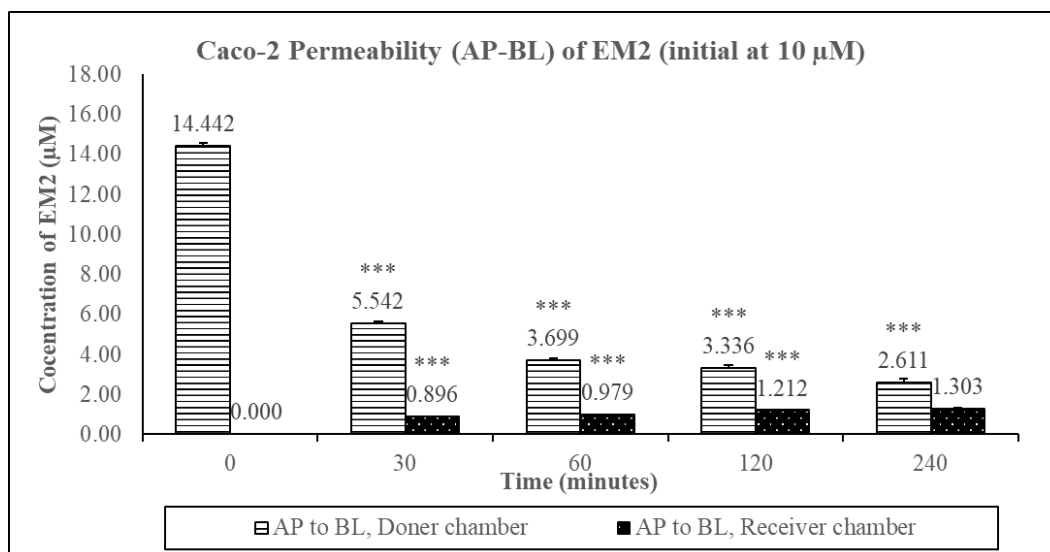
Figure 18 Bidirectional transport of EM2 (initial concentration at 10 μM). EM2 10 μM was added into donor chamber (AP) of Caco2 cell monolayers

Note: Samples were taken from both doner and receiver chambers at different time points (30, 60, 120 and 240 min) with replaced back by same concentration and volume and measured with HPLC. Results are expressed as concentration of EM2 dose (n = 3). Statistical analysis was done using one way ANOVA (Turkey post hoc test). Significantly different from concentration of EM2 at 0 minute. (*** = p-value < 0.001)
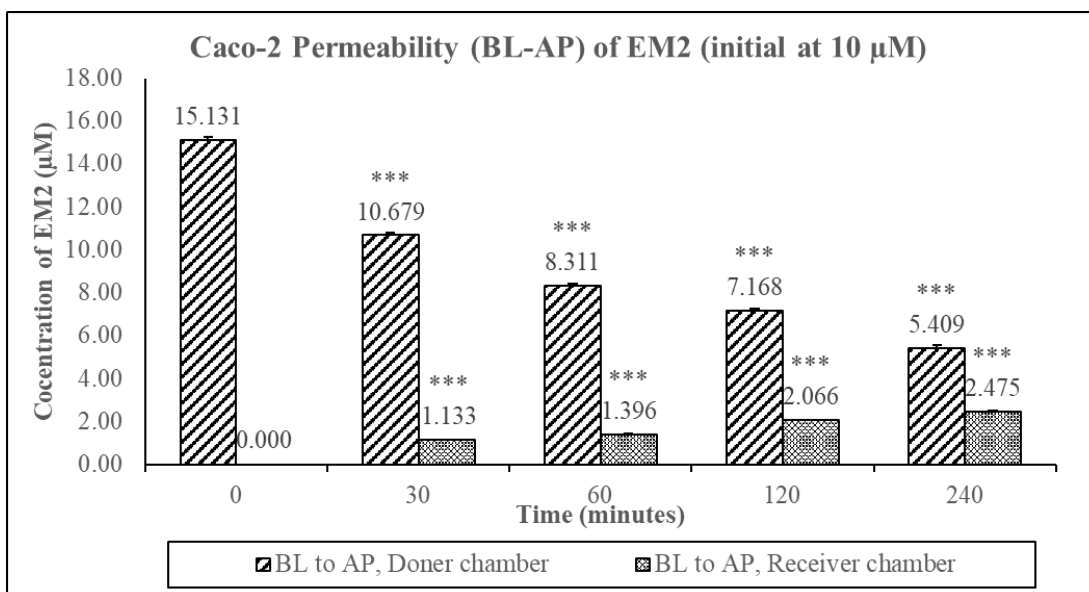
Figure 19 Bidirectional transport of EM2 (initial concentration at 10 μM). EM2 10 μM was added into donor chamber (BL) of Caco2 cell monolayers

Note: Samples were taken from both doner and receiver chambers at different time points (30, 60, 120 and 240 min) with replaced back by same concentration and volume and measured with HPLC. Results are expressed as concentration of EM2 dose (n = 3). Statistical analysis was done using one way ANOVA (Turkey post hoc test). Significantly different from concentration of EM2 at 0 minute. (*** = p-value < 0.001)
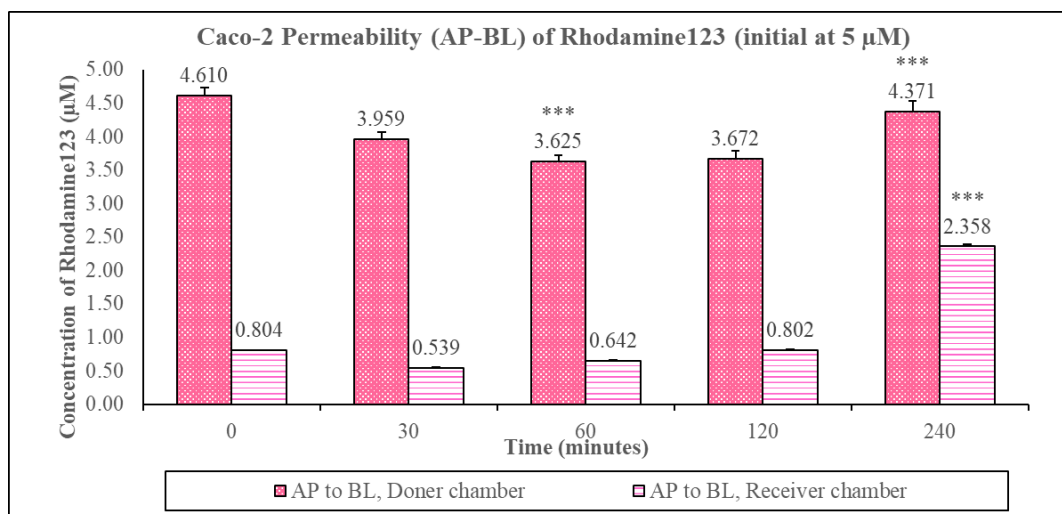
Figure 20 Bidirectional transport of EM2 (initial concentration at 10 µM).
Rhodamine123 5 µM was added into donor chamber (AP) of Caco2 cell
monolayers

Note: Samples were taken from both doner and receiver chambers at different time points (30, 60, 120 and 240 min) with replaced back by same concentration and volume and measured with microplate reader (fluorescence). Results are expressed as concentration of Rhodamine123 dose (n = 3). Statistical analysis was done using one way ANOVA (Turkey post hoc test). Significantly different from concentration of R123 at 0 minute. (*** = p-value < 0.001)
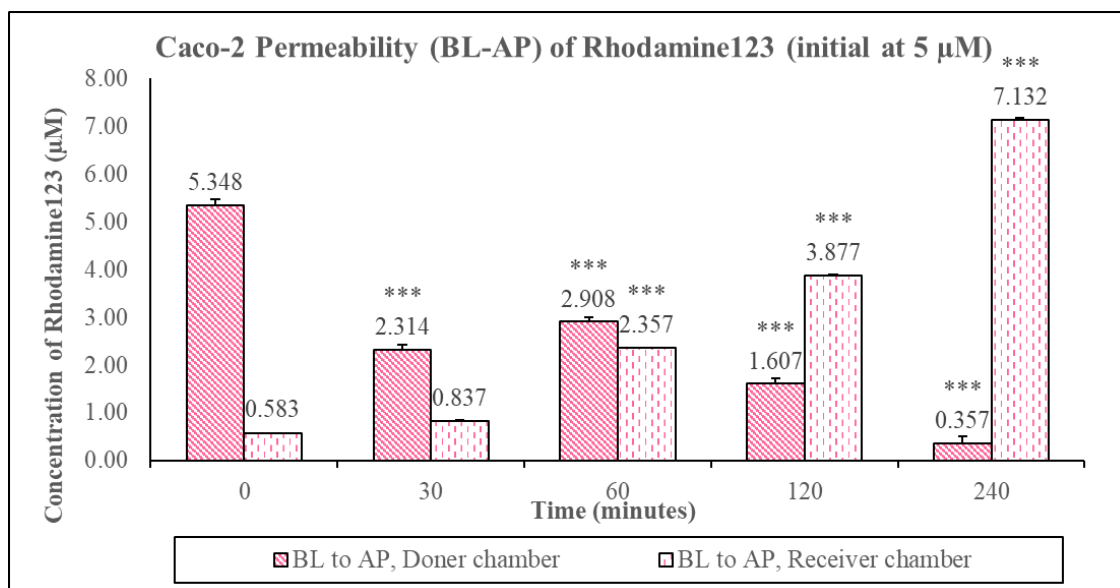
Figure 21 Bidirectional transport of EM2 (initial concentration at 10 µM).
Rhodamine123 5 µM was added into donor chamber (BL) of Caco2 cell
monolayers

Note: Samples were taken from both doner and receiver chambers at different time points (30, 60, 120 and 240 min) with replaced back by same concentration and volume and measured with microplate reader (fluorescence). Results are expressed as concentration of Rhodamine123 dose (n = 3). Statistical analysis was done using one way ANOVA (Turkey post hoc test). Significantly different from concentration of R123 at 0 minute. (*** = p-value < 0.001)

Transepithelial transport across Caco-2 cell monolayers

Table 5 Time dependence of samples in absorptive and secretory directions across Caco-2 monolayers

Name	Time (min)	Absorptive transport, $P_{app(AP-BL)}$, (cm/s)(10^{-4})	Secretory transport, $P_{app(BL-AP)}$, (cm/s)(10^{-4})	Uptake ratio, $[P_{app(AP-BL)}/P_{app(BL-AP)}]$	Efflux ratio, $[P_{app(BL-AP)}/P_{app(AP-BL)}]$
EM2 **(1 μM)**	30	6.48 ± 0.14	1.71 ± 0.08	3.80 ± 0.09	0.26 ± 0.01
	60	3.45 ± 0.17	0.92 ± 0.04	3.77 ± 0.18	0.27 ± 0.01
	120	1.82 ± 0.07	0.55 ± 0.10	3.19 ± 0.48	0.32 ± 0.04
	240	0.90 ± 0.03	0.30 ± 0.01	2.99 ± 0.23	0.34 ± 0.03
EM2 **(10 μM)**	30	1.20 ± 0.04	0.26 ± 0.01	4.57 ± 0.25	0.22 ± 0.01
	60	0.98 ± 0.04	0.21 ± 0.02	4.76 ± 0.56	0.21 ± 0.03
	120	0.68 ± 0.02	0.18 ± 0.02	3.83 ± 0.57	0.26 ± 0.04
	240	0.46 ± 0.03	0.14 ± 0.01	3.29 ± 0.38	0.31 ± 0.01
Rhoda-mine123 **(5 μM)**	30	1.01 ± 0.17	0.90 ± 0.02	1.13 ± 0.19	0.90 ± 0.15
	60	0.66 ± 0.01	1.00 ± 0.03	0.66 ± 0.01	1.53 ± 0.02
	120	0.41 ± 0.02	1.66 ± 0.55	0.27 ± 0.11	4.08 ± 1.33
	240	0.50 ± 0.02	6.20 ± 0.69	0.08 ± 0.01	12.39 ± 1.70
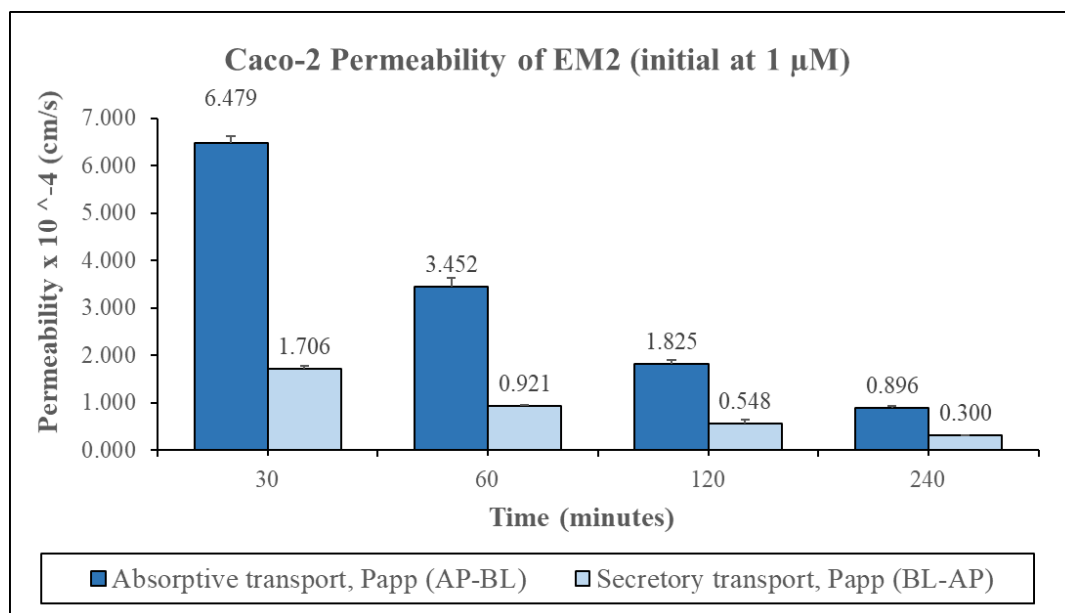
Figure 22 Time dependence of Sample EM2 at initial concentration 1 μM in absorptive and secretory directions across Caco-2 monolayers. Sample EM2 Papp at each transport direction was measured in triplicate. Data are shown as mean±SD
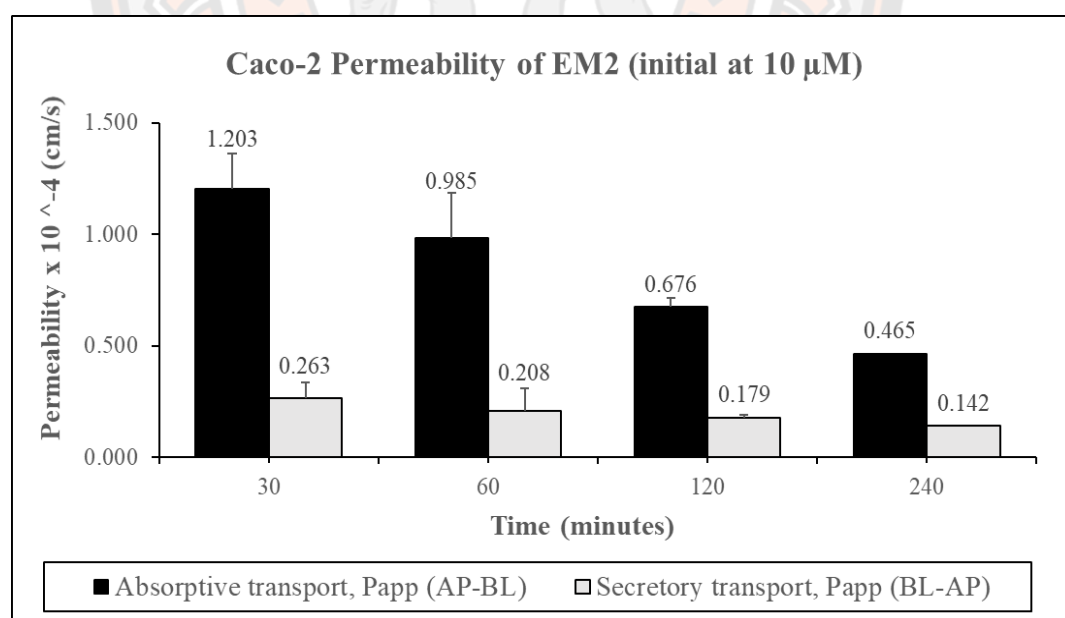
Figure 23 Time dependence of Sample EM-1 at initial concentration 10 μM in absorptive and secretory directions across Caco-2 monolayers. Sample EM-2 Papp at each transport direction was measured in triplicate. Data are shown as mean±SD

Figure 24 Time dependence of Sample EM-1 at initial concentration 10 μM in absorptive and secretory directions across Caco-2 monolayers. Sample EM-2 Papp at each transport direction was measured in triplicate. Data are shown as mean±SD
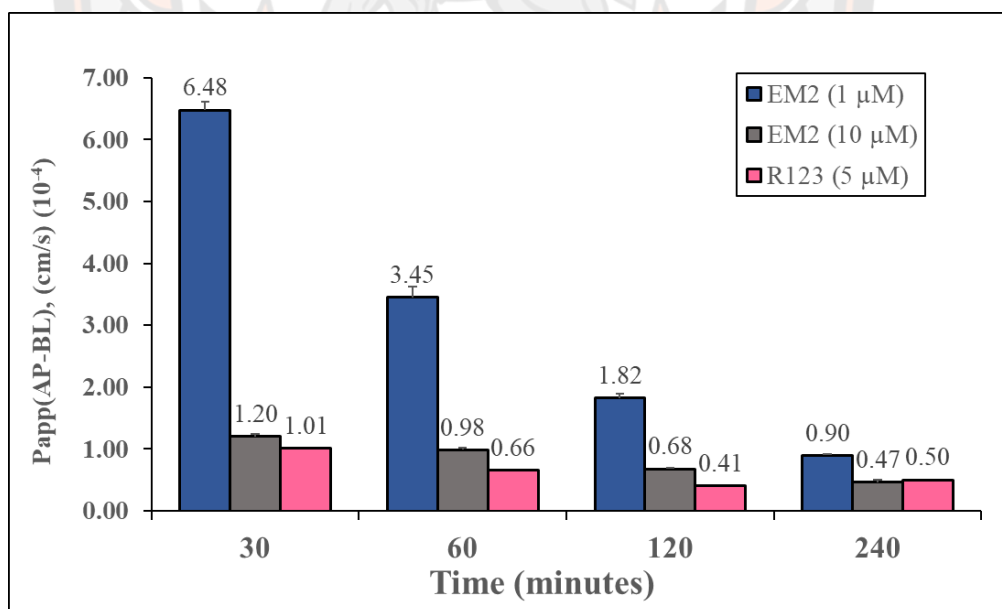
Figure 25 The conclusions of time dependence of Sample EM2 at initial concentrations 1 and 10 μM compare with Rhodamine123 (5 μM) in absorptive direction (AP-BL) across Caco-2 monolayers. Papp at each transport direction was measured in triplicate. Data are shown as mean±SD
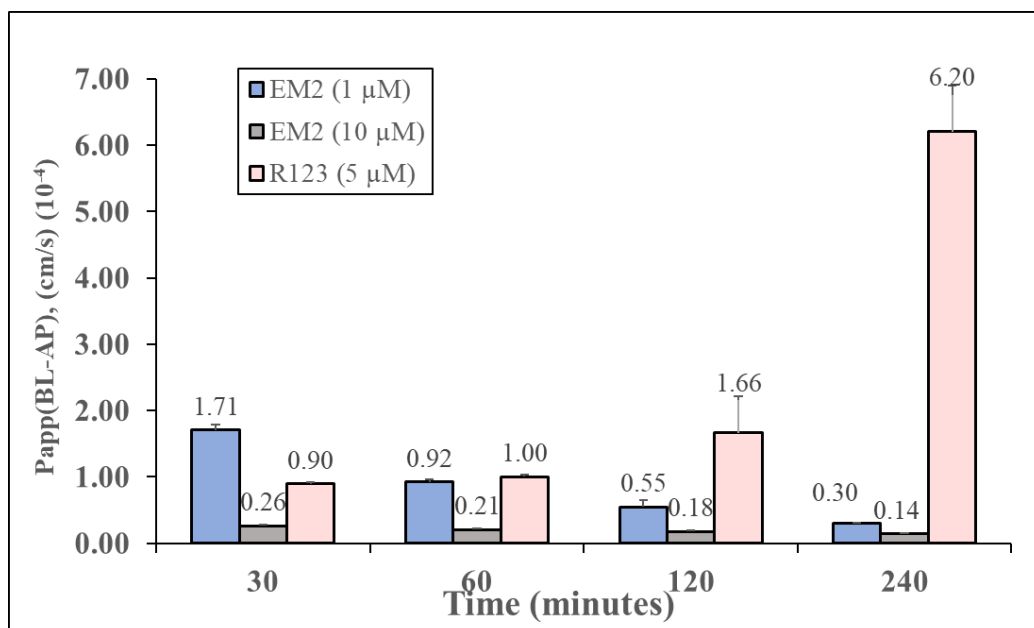
Figure 26 The conclusions of time dependence of Sample EM2 at initial concentrations 1 and 10 μM compare with Rhodamine123 (5 μM) in secretory direction (BL-AP) across Caco-2 monolayers. Papp at each transport direction was measured inlicate. Data are shown as mean±SD

The absorptive and secretory transport profiles of EM2 across cell monolayers in vitro, bi-directional transport of EM2 across Caco-2 cell monolayer at a different concentration (1 and 10 μM) and different time points (0~120 minutes) showed a consistent trend, the transport accumulation of EM2 increased with time. The absorptive permeability or $P_{app, (AP-BL)}$ values of EM2 1 and 10 μM were ranged 3.48~0.90 and 1.20~0.46 $\times 10^{-4}$ cm/s, respectively (for R123 were ranged 1.01~0.50 $\times 10^{-4}$ cm/s), the secretory permeability or $P_{app, (BL-AP)}$ values were 1.17~0.30 and 0.26~0.14 $\times 10^{-4}$ cm/s, respectively (for R123 were ranged 0.90~6.20 $\times 10^{-4}$ cm/s).
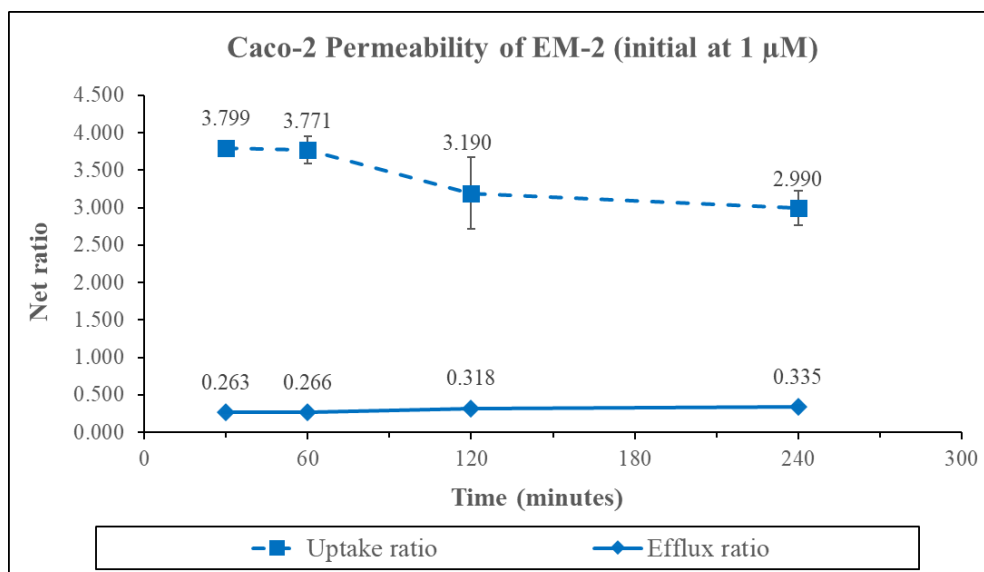
Figure 27 Net efflux and uptake ratio in time dependence of sample EM2 at initial concentration 1 μM, in absorptive and secretory directions across Caco-2 monolayers
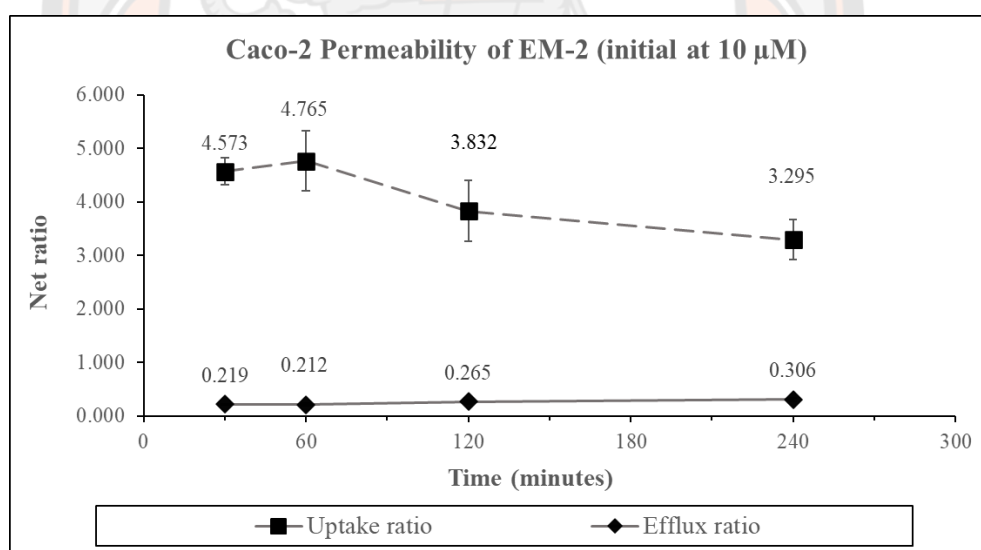
Figure 28 Net efflux and uptake ratio in time dependence of sample EM2 at initial concentration 10 μM, in absorptive and secretory directions across Caco-2 monolayers
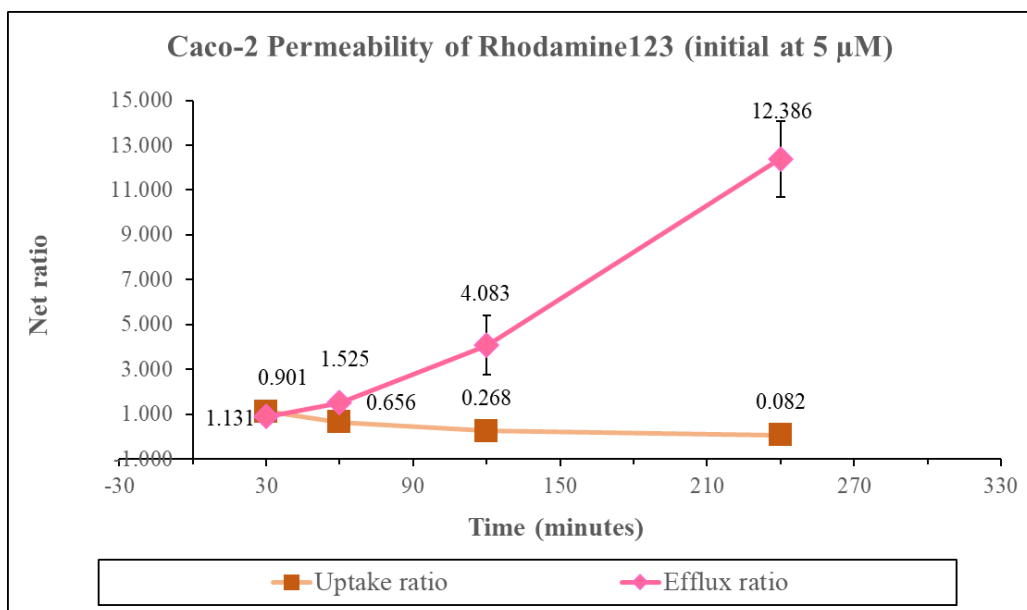
Figure 29 Net efflux and uptake ratio in time dependence of Rhodamine123 at initial concentration 5 µM, in absorptive and secretory directions across Caco-2 monolayers
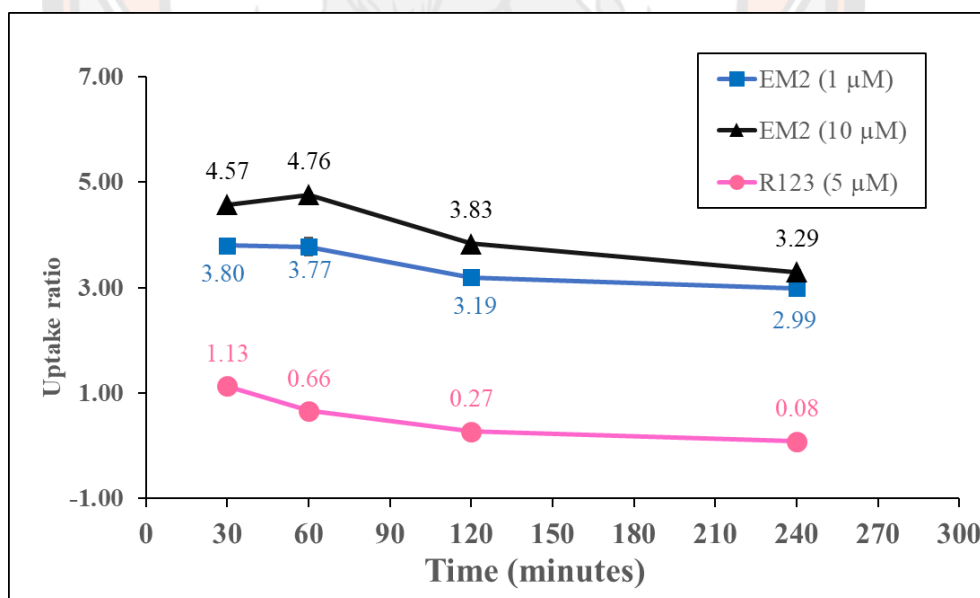
Figure 30 The conclusion of net uptake ratio in time dependence of sample EM2 at initial concentrations 1 and 10 µM and Rhodamine123 (5 µM) in absorptive and secretory directions across Caco-2 monolayers
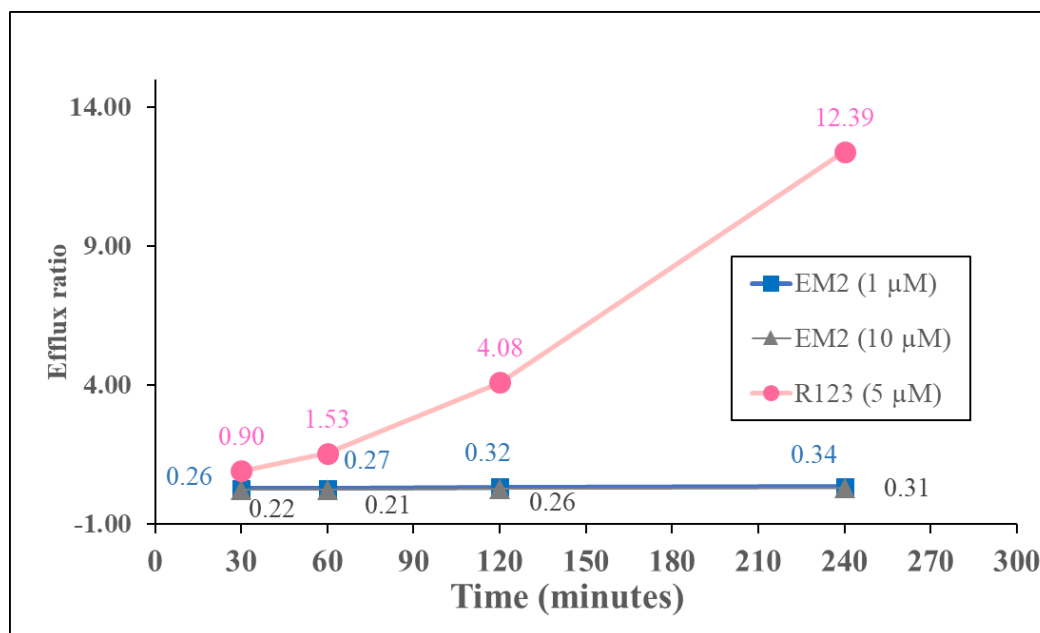
Figure 31 Net efflux ratio in time dependence of sample EM2 at initial concentrations 1 and 10 µM and Rhodamine123 (5 µM) in absorptive and secretory directions across Caco-2 monolayers

The uptake ratio values of EM2 were ranged 3.80~2.99 for 1 µM initial concentration and for 10 µM initial concentration were ranged 4.57~3.29 (for R123 were ranged 1.13~0.08). Rhodamine123, a specific substrate of P-gp was used to measure its transport across Caco-2 cell monolayer was mediated by P-gp (Aller SG et al., 2009). The data indicated that the efflux ratio of Rhodamine123 were induced in time dependent. The efflux ratio of EM2 were ranged 0.26~0.34 (initial 1 µM) and 0.22~0.31 (initial 10 µM). Rhodamine 123 were determined the efflux ratio were ranged 0.92~13.39, increasingly. As the body immune efflux of the exogenous materials is a key factor for the low oral drug bioavailability (Ma B et al., 2012), which mean that EM2 had high permeability.

4.2 Metabolic stability in vitro hepatocytes and microsomes.

4.2.1 Hep G2 stability
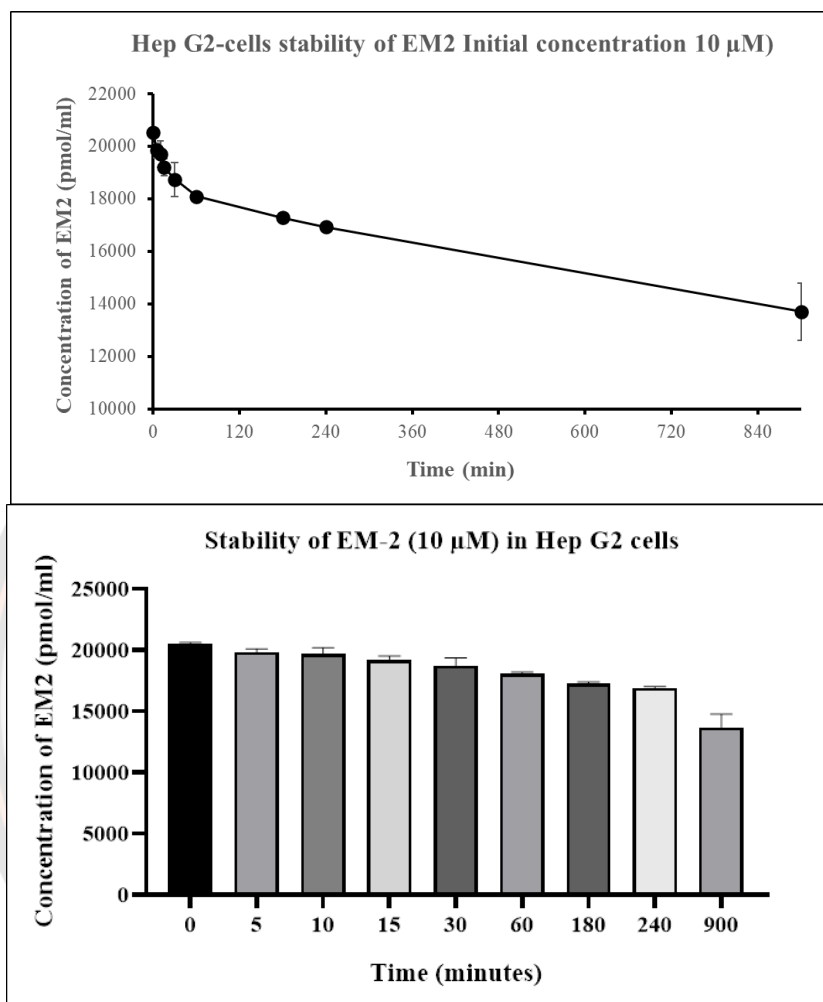
Figure 32 Metabolic study in time dependence of sample EM2 at initial concentration 10 μM in Hep G2 cells (n=3)

Table 6 Pharmacokinetic parameters from Metabolic study in time dependence of sample EM2 at initial concentration 10 μM in Hep G2 cells

Parameters	Units	Values
Initial Concentration	pmol/ml	20621.67 ± 91.14
ke	min^-1	1.75 ± 0.33 $(\cdot 10^{-4})$
t1/2	min	4.04 ± 0.69 $(\cdot 10^{3})$
$AUC_{(t0-t120)}$	pmol*min/ml	14.39 ± 0.37 $(\cdot 10^{6})$
$AUC_{(t900-infi)}$	pmol*min/ml	80.69 ± 19.29 $(\cdot 10^{6})$
AUC_{total}	pmol*min/ml	95.08 ± 19.66 $(\cdot 10^{6})$
Cl_{int}	$\mu l/min/10^{6}$ cells	0.22 ± 0.05
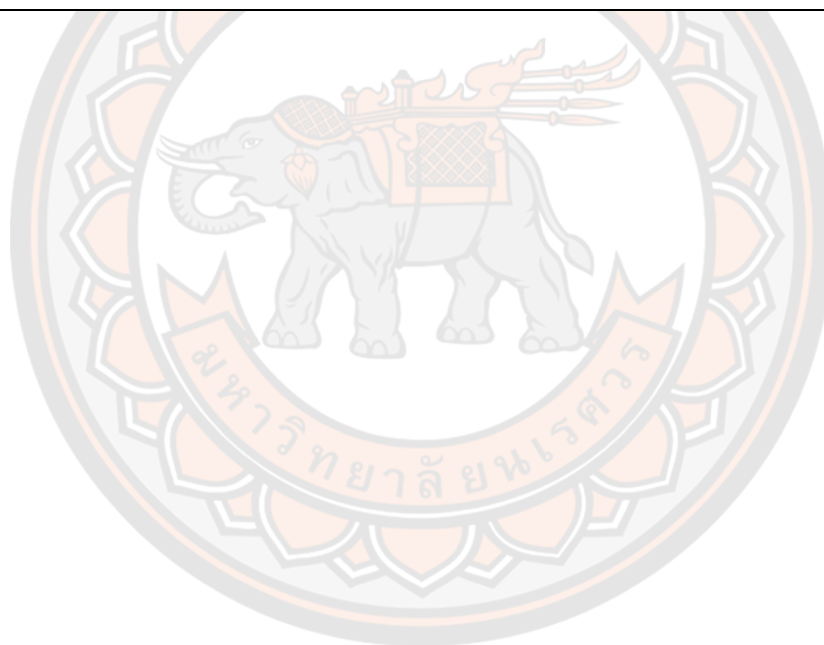
4.2.2 Hepatocytes stability

Hepatocyte stability assay is the method with measurement of in vitro intrinsic clearance using hepatocyte cells.
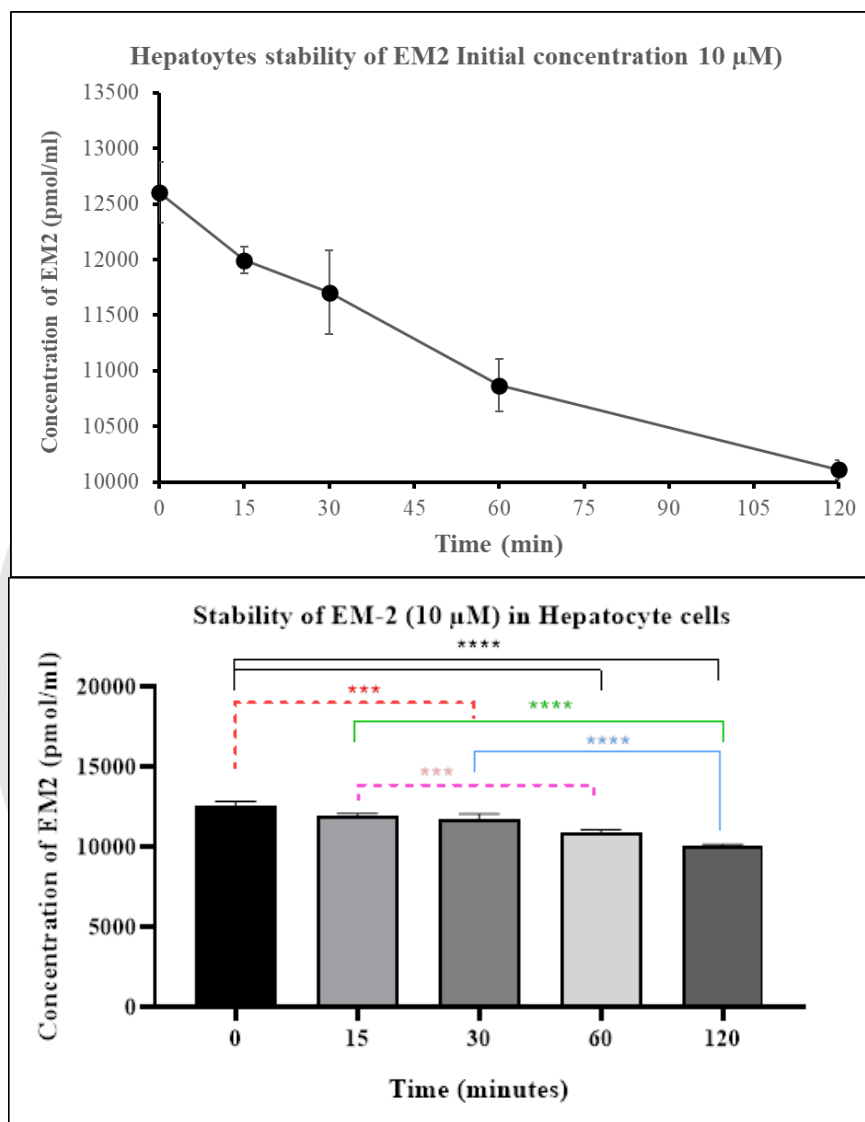
Figure 33 Metabolic study in time dependence of sample EM2 at initial concentration 10 µM in human hepatocyte cells (n=3)

Table 7 Pharmacokinetic parameters from Metabolic study in time dependence of sample EM2 at initial concentration 10 µM in human hepatocyte cells

Parameters	Units	Values
Initial Concentration	pmol/ml	12.60 ± 0.27 ($\cdot 10^{-3}$)
ke	min^-1	7.61 ± 0.25 ($\cdot 10^{-4}$)
t1/2	min	911.21 ± 30.82
$AUC_{(t0-t120)}$	pmol*min/ml	1.33 ± 0.02 ($\cdot 10^{6}$)
$AUC_{(t900-infi)}$	pmol*min/ml	13.29 ± 0.51 ($\cdot 10^{6}$)
AUC_{total}	pmol*min/ml	14.26 ± 0.53 ($\cdot 10^{6}$)
Cl_{int}	$\mu l/min/10^{6}$ cells	0.86 ± 0.04

4.2.3 Microsomal Stability

Microsomal stability assay is the method with measurement of in vitro intrinsic clearance using microsomes. The liver is the most important site of drug metabolism in the body.
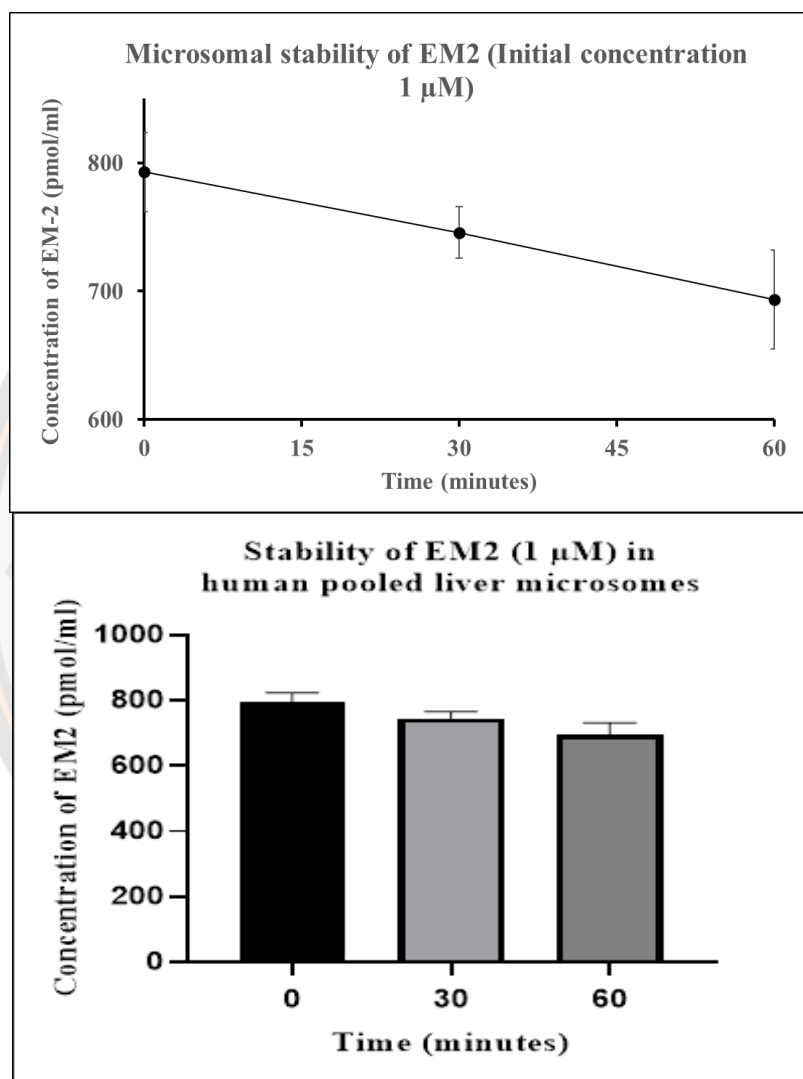
Figure 34 Metabolic study in time dependence of sample EM2 at initial concentration 1 µM in human pooled liver microsomes (n=3)
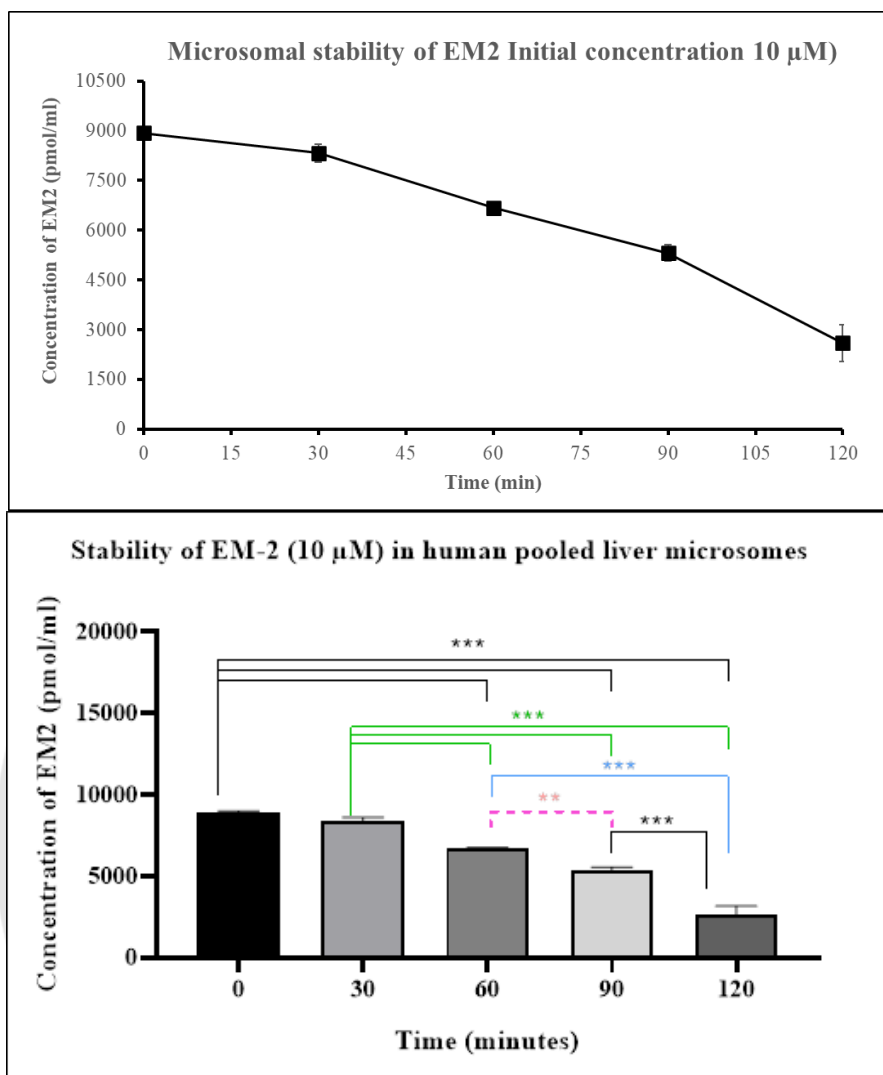
Figure 35 Metabolic study in time dependence of sample EM2 at initial concentration 10 µM in human pooled liver microsomes (n=3)

Table 8 Pharmacokinetic parameters from Metabolic study in time dependence of sample EM2 at initial concentration 10 μM in human pooled liver microsomes

Parameters	Units	EM2 (1 μM)	EM2 (10 μM)
Initial Concentration	pmol/ml	0.79±0.03 (·10-3)	8.94±0.07 (·10-3)
ke	min^-1	1.11±0.10 (·10-3)	4.30±0.00 (·10-3)
t1/2	min	659.94±7.265	162.71±18.94
$AUC_{(t0-t120)}$	pmol*min/ml	4.47±0.06 0(·104)	70.08±7.93 (·104)
$AUC_{(t900-infi)}$	pmol*min/ml	66.22±9.04(·104)	61.99±19.73 (·104)
AUC_{total}	pmol*min/ml	70.69±9.09(·104)	132.07±26.53 (·104)
Cl_{int}	μl/min/10^6 cells	1.13±0.11	6.95±1.37
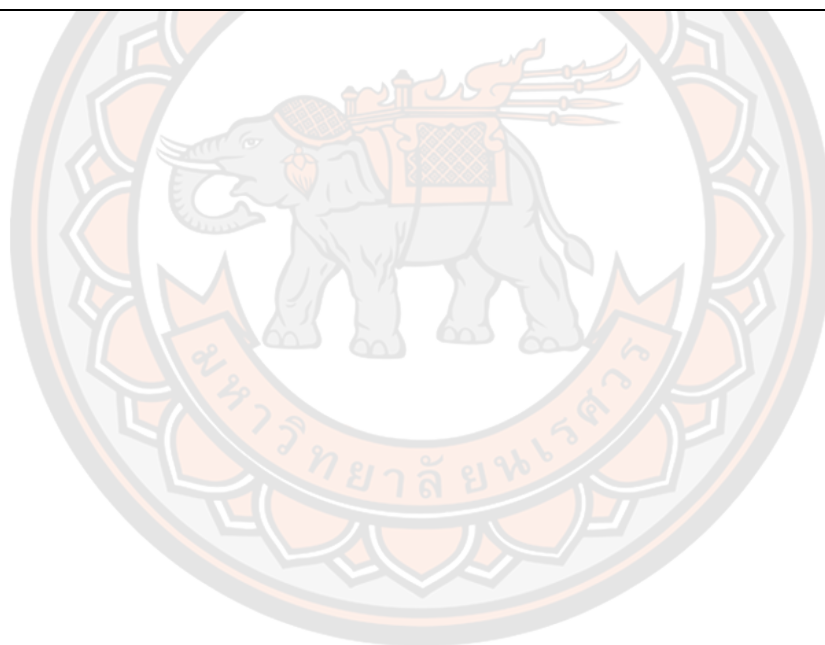
4.2.4 Phenotyping
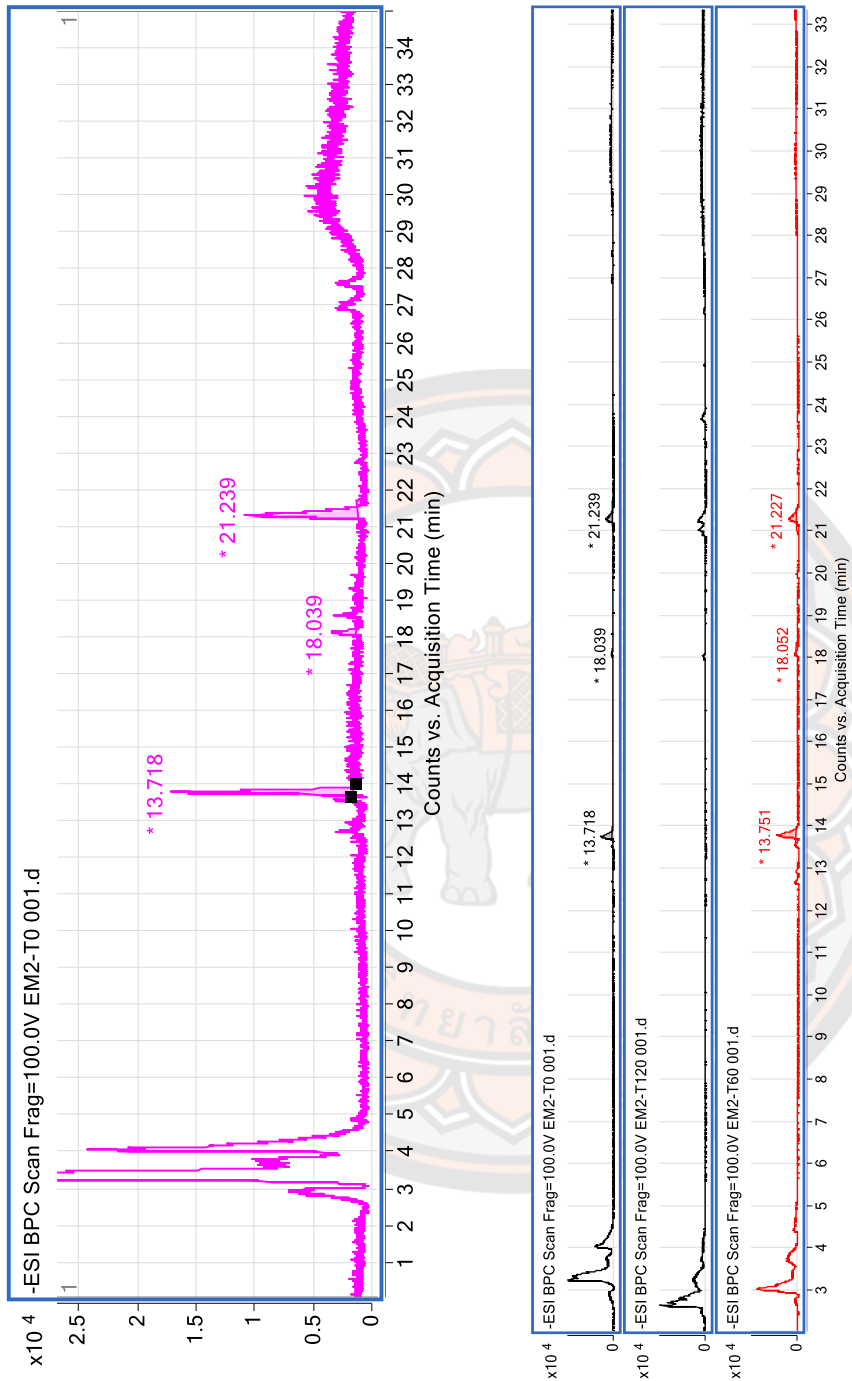
EM-2 incubation at 0 minute
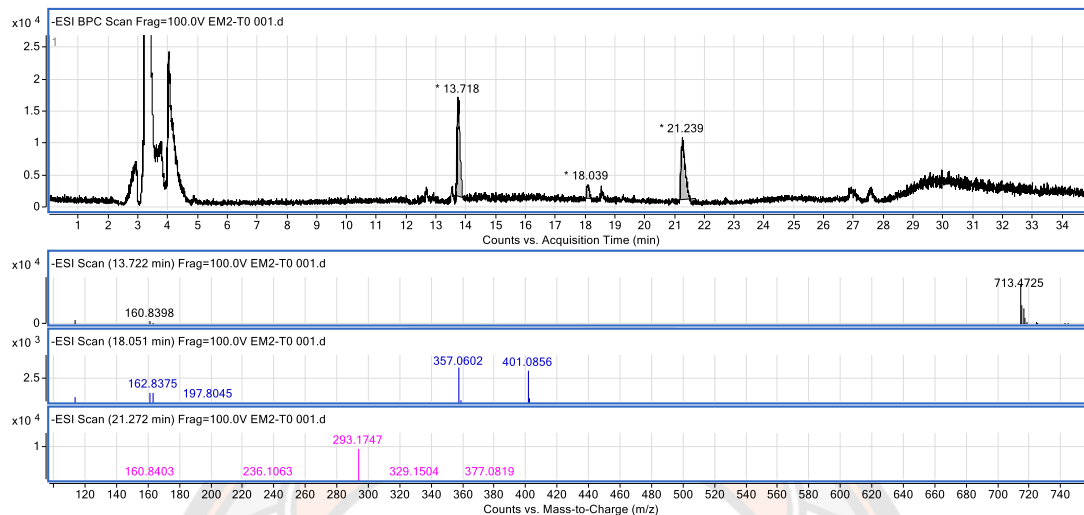
EM-2 incubation at 60 minutes
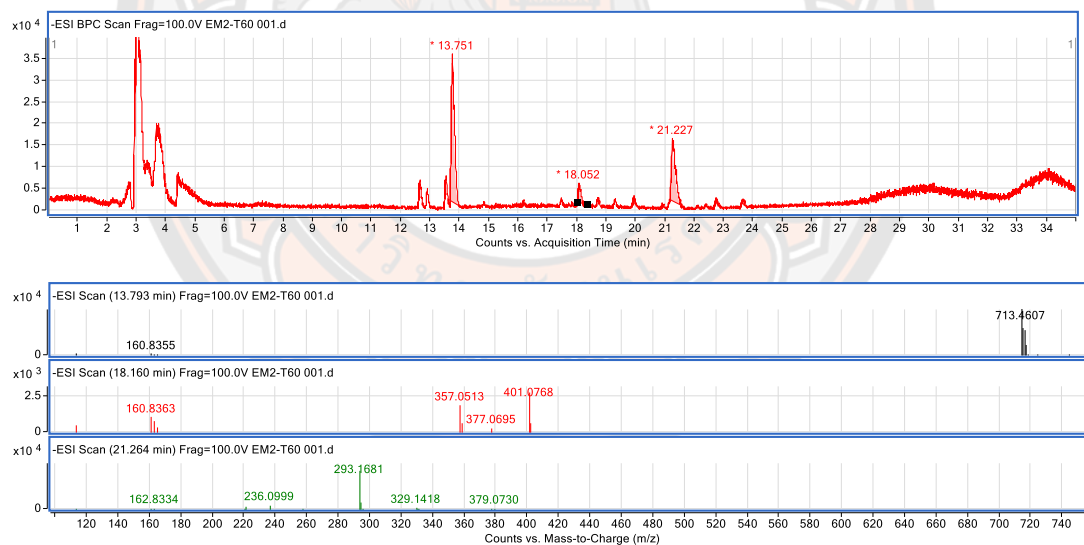
EM-2 incubation at 120 minutes
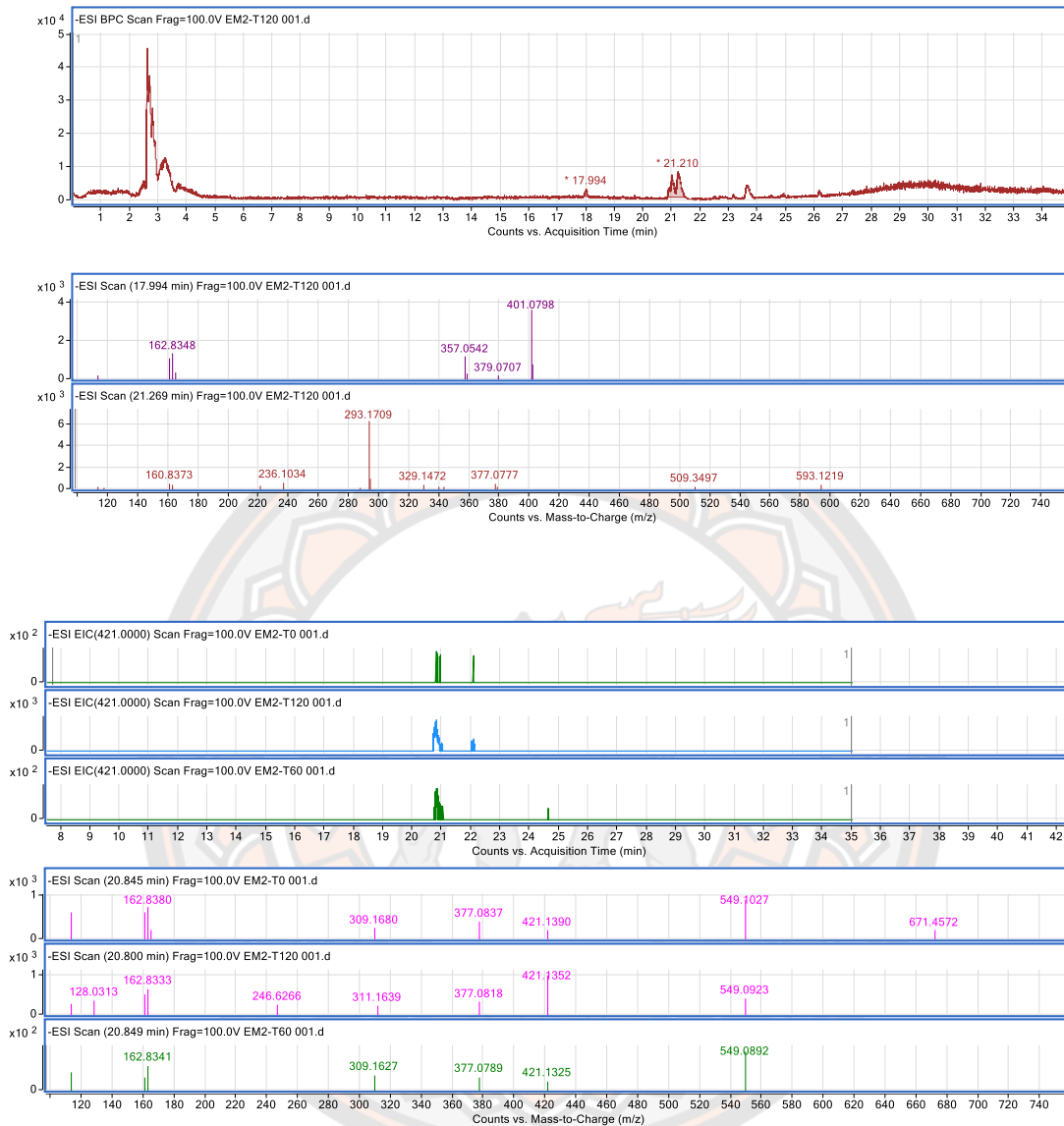
4.3 Plasma/Buffer concentration ratio (n=6)

This study was designed to determine the percent bound of the sample compound concentrations in whole blood or plasma or buffer chamber after reach equilibrium. The Single-Use RED Plate with Inserts (Thermo Scientific, cutoffs 8 K MWCO, Number; 90006) compose of 48 equilibrium dialysis membrane and dispersible high-density polyethylene was used in the study. EM2 was designed and widely validated for plasma protein binding. Calculate the percentage of the test compound bound as follows:

$$\% \text{ Free} = (\text{Concentration buffer chamber}/\text{Concentration plasma chamber}) \times 100\%$$

$$\% \text{ Bound} = 100\% - \% \text{ Free}$$

Table 9 Plasma to buffer concentration ratio of EM2

Parameters	EM2 (1 μM)	EM-2 (10 μM)
Plasma/Buffer	25.69 ± 0.98	102.18 ± 4.81
%Free	3.90 ± 0.15	0.98 ± 0.05
%Bound	96.10 ± 0.15	99.02 0.05

CHAPTER V

CONCLUSIONS

Eulophia macrobulbon belongs to Orchidaceae family, commonly known as Orchids. It has been used in Thai traditional medicine, especially as an aphrodisiac. The main bioactive compound of *E. macrobulbon* is EM2. There are reports on its chemical composition and pharmaceutical activity but reports about its cytotoxicity and pharmacokinetic parameters are rare. The objectives of this study are to gain new knowledge in the process of structural changes and pharmacokinetic values of EM2 by in vitro methods to predict the pharmacokinetics of EM2 for further safety data for humans. Also, to screen for cytotoxicity of EM2 using Hep G2 cells and Caco-2 cells. The cytotoxicity of EM2 in Hep G2 cells and Caco-2 cells were evaluated by MTT assay. The results showed that EM2 was toxic to 50% of Hep G2 cells at a concentration (IC_{50}) of 30.08 ± 0.62 micromolar compared with the control (the concentration of dimethyl sulfoxide (DMSO) was 0.01%). For the cytotoxicity of EM2 in Caco-2 cells, the result of IC_{50} was 41.64 ± 1.60 micromolar compared with the control. This, the concentrations of EM2 at 1 and 10 µM were chosen and use for further experiment to determine its effectives.

Caco-2 monolayers in 12 trans-well insert plate was collected to use in permeability testing of EM2 compound. The TEER values were checked to confirm monolayers formation between apical chamber (AP) and basolateral chamber (BL). The Papp values shows th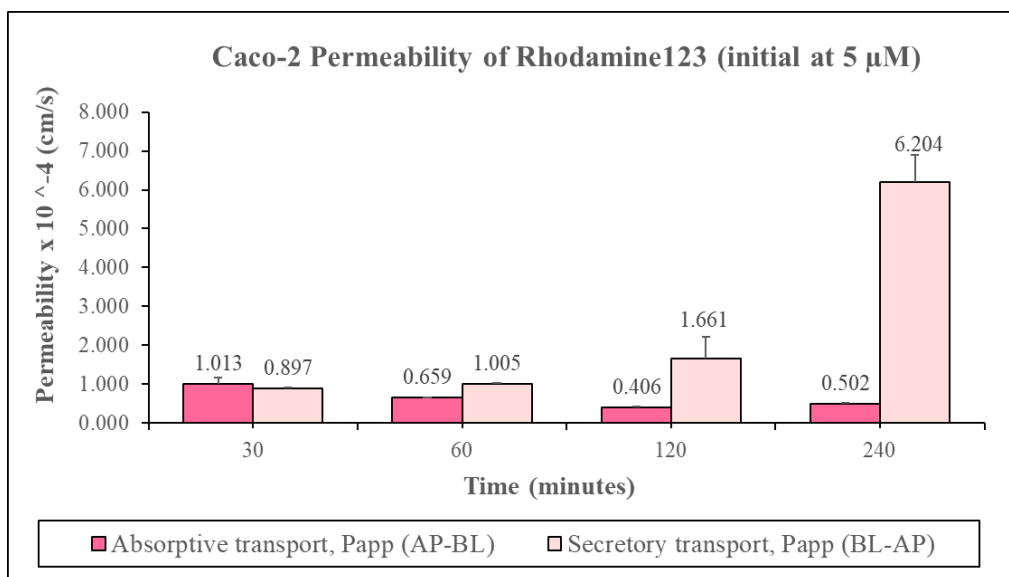e time dependence of sample EM2 at initial concentration 1 µM and 10 µM in absorptive and secretory directions across Caco-2 monolayers. The Papp values of EM2 results have shown that absorptive transport (AP-BL) from 30 to 120 minutes has decreased which means that sample EM2 at start concentration 1 µM and 10 µM has the high permeability through the Caco-2 monolayers compared to caffeine and rhodamine123. The absorptive permeability or $P_{app, (AP-BL)}$ values of EM2 at initial concentrations of 1 and 10 µM were ranged 3.48~0.90 and 1.20~0.46 $\times 10^{-4}$ cm/s, respectively (R123 was ranged 1.01~0.50 $\times 10^{-4}$ cm/s and caffeine was ranged 2.25~1.38 $\times 10^{-4}$ cm/s), the secretory permeability or $P_{app, (BL-AP)}$ values were 1.17~0.30 and 0.26~0.14 $\times 10^{-4}$ cm/s, respectively (R123 was ranged 0.90~6.20 $\times 10^{-4}$ cm/s and

caffeine was ranged 2.31~0.57 $\times 10^{-4}$ cm/s). EM2 was used to determines the concentration of the drug in dialysis buffer compared to plasma to provides an indication of drug binding protein. The results of EM2 at initial concentration of 1 and 10 µM were obtained %bound with protein in plasma close to 100%. Metabolic study in time dependence of EM2 at initial concentration 10 µM in pooled human liver microsomes, human hepatocytes and Hep G2 cells were half-life ($t_{1/2}$) at 2.71, 15.23 and 67.41 hours, respectively. The conventional clearance (CL) obtained from the comparison of hepatocytes applied to the total number of human hepatocytes were 7.56, 7.12 and 1.75 liters per hour, respectively. However, EM2 also be selected for investigation CYP-phenotyping. The results from exhibited that there were at least 4 metabolites showing in LC-MS chromatogram.

REFERENCES

[1] Temkitthawona, P., Changwichita, K., Khoranaa, N., Viyochb, J., Suwanboriruxc, K. (2017). Phenanthrenes from *Eulophia macrobulbon* as Novel Phosphodiesterase-5 Inhibitors. Natural Product Communications, 12(1), 79-82.

[2] Wisutthathum, S., Demougeot, C., Totoson, P., Adthapanyawanich, K., Ingkaninan, K., Temkitthawon, P., Chootip, K. (2018). *Eulophia macrobulbon* extract relaxes rat isolated pulmonary artery and protects against monocrotaline-induced pulmonary arterial hypertension. Phytomedicine, 15, 157-165.

[3] Changwichit, K., Thernier, C. G., Temkitthawon, P., Khorana, N., Ingkaninan, K. (2018). Quantitative analysis of a phenanthrene from Eulophia species by TLC-image analysis method. Journal of Science and Technology, 40(6), 1324-1328.

[4] Forest (Beta) [Internet]. สำนักงานคณะกรรมการวิจัยแห่งชาติ; ©2017 [updated 2017; cited 2020 February 1]. *Eulophia macrobulbon*-an orchid with significant anti-inflammatory and antioxidant effect and anticancerogenic potential exerted by its root extract.; [about 3 screens]. Available from: https://madlab.cpe.ku.ac.th/ThailandResearch/?itemID=71118

[5] Acharya, K. P., Wood, J. J., Berwian, R., Sharma, A. (2010). *Spiranthes spiralis* (Orchidaceae), A new record for the Nepal Himalaya. Harvard Papers in Botany, (15), 71–72.

[6] Schustera, R., Zeindla, L., Holzerb, W., Khumpirapangc, N., Okonogic, S. (2017). *Eulophia macrobulbon* – an orchid with significant anti-inflammatory and antioxidant effect and anticancerogenic potential exerted by its root extract. Phytomedicine, 24, 157-165.

[7] Orchidcambodia.com [Internet]. *Eulophia macrobulbon*; ©2014 [updated 2014; cited 2020 February 1]. *Eulophia macrobulbon* (Parish & Rchb.f.) Hook.f; [about 2 screens]. Available from: https://www.orchidcambodia.com/eulophia-macrobulbon.html

[8] Kong, J. M., Goh, N. K., Chia, L. S., Chia, T. F. (2003). Recent advances in traditional plant drugs and orchids. Acta Pharmacologica Sinica, 24, 7–21.

[9] Kovács, A., Vasas, A., Hohmann, J. (2008). Natural phenanthrenes and their biological activity. Phytochemistry, 69, 1084–1110.

[10] Singh, S., Singh, A. K., Kumar, S., Kumar, M., Pandey, P. K., Singh, M. C. (2012). Medicinal properties and uses of orchids: a concise review. Elixir International Journal (Applied Botany), 52, 11627–11634.

[11] Tuchinda, P., Udchachon, J., Khumtayeeporn, K., Taylor, W. C. (1989). Benzylated phenanthrenes from *Eulophia nuda*. Phytochemistry, 28, 2463-2466.

[12] Maridass, M., Hussain, M., Raju, G. (2008). Phytochemical survey of orchids in the Tirunelveli hills of South India. Ethnobotanical Leaflets, 705–712.

[13] Patil, M. C., Mahajan, R. T. (2013). Ethnobotanical potential of *Eulophia* species for their possible biological activity. International Journal of Pharmaceutical Sciences Review and Research, 21, 297–307.

[14] Narkhede, A. N., Kasote, D. M., Kuvalekar, A. A., Harsulkar, A. M., Jagtap, S. D. (2016). Amarkand: a comprehensive review on its ethnopharmacology, nutritional aspects, and taxonomy. Journal of Intercultural Ethnopharmacology, 5, 198–204.

[15] Dawande, V., Gurav, R. (2017). Total phenolics, flavonoids content and antioxidant activities of some *Eulophia* species. Journal of Medicinal Plants Research, 5, 106–111.

[16] Behera, D., Rath, C. C., Mohapatra, U. (2013). Medicinal orchids in India and their conservation: a review. Floriculture and Ornamental Biotechnology, 7, 53–59.

[17] Bulpitt, C. J. (2005). The uses and misuses of orchids in medicine. International Journal of Medicine, 98, 625–631.

[18] Pant, B. (2013). Medicinal orchids and their uses: tissue culture a potential alternative for conservation. African Journal of Plant Science, 7, 448–467.

[19] Suresh, P. K., Appian, S., Pushpangadan, P. (2000). Aphrodisiac activity of *Vanda tessellates* (Roxb.) Hook. ex Don extract in male mice. Indian Journal of Pharmacology, 32, 300–304.

[20] Hernández-Romero, Y., Acevedo, L., Ángeles, D. L., Sánchez, M., Shier, W. T., Abbas, H. K., Mata, R. (2005). Phytotoxic activity of bibenzyl derivatives from the orchid *Epidendrum rigidum*. Journal of Agricultural and Food Chemistry, 53, 6276–6280.

[21] Luo, J. P., Wawrosch, C., Kopp, B., Dendrobium, C. Z. Tang, S. J. (2007). Cheng: micropropagation and anticataract activity. Planta Medica, 73, 618.

[22] Datla, P., Kalluri, M. D., Basha, K., Bellary, A., Kshirsagar, R., Kanekar, Y. (2010). 9,10-dihydro-2,5dimethoxyphenanthrene-1,7diol, from *Eulophia ochreata*, inhibits inflammatory signaling mediated by Toll-like receptors. British Journal of Pharmacology and Chemotherapy, 160, 1158–1170.

[23] Chinsamy, M., Finnie, J. F. Anti-inflammatory, antioxidant, anti-cholinesterase activity and mutagenicity of South African medicinal orchids. South African.

[24] Shriram, V., Kumar, V., Kishor, P. B., Suryawanshi, S. B., Upadhyay, A. K., Bhat, M. K. (2010). Cytotoxic activity of 9,10-dihydro-2,5-dimethoxyphenanthrene-1,7-diol from *Eulophia nuda* against human cancer cells. Journal of Ethnopharmacology, 128, 251–253.

[25] Tatiya, A. U., Puranik, P. M., Surana, S. J., Patil, Y. S., Mutha, R. E. (2013). Evaluation of hypolipidemic, antidiabetic and antioxidant activity of *Eulophia herbacea* tubers. Bangladesh Journal of Pharmacology, 8, 269–275.

[26] PubChem [Internet]. Compound summary; ©2017 [updated 2020 January 22; cited 2020 February 1]. Phenanthrene; [about 2 screens]. Available from: https://pubchem.ncbi.nlm.nih.gov/compound/Phenanthrene

[27] ChemicalBook [Internet]. CAS DataBase List; ©2017 [updated 2017; cited 2020 February 1]. Phenanthrene; [about 2 screens]. Available from: https://www.chemicalbook.com/ChemicalProductProperty_EN_cb8854465.html

[28] Monographs on the Evaluation of the Carcinogenic Risk of Chemicals to Humans. Geneva: World Health Organization. International Agency for Research on Cancer. 2005; 92-773.

[29] Solbakken, J. E. (1986). The disposition of the xenobiotics phenanthrene and octochlorosytrene in spiny lobsters *Panulirus argus* after intergastric

administrations. Bulletin of Environmental Contamination and Toxicology, 37, 747-751.

[30] Palmork, K. H., Solbakken, J. E. (1982). Disposition of (9-14C) phenanthrene in a subtropical marine teleost (*Haemulon sciurus*). Bulletin of Environmental Contamination and Toxicology, 28(3), 285-289.

[31] Simmon, V. F., Rosenkranz, H. S., Zeiger, E., Poirier, L. A. (1979). Mutagenic activity of chemical carcinogens and related compounds in the intraperitoneal host-mediated assay. Journal of the National Cancer Institute, 62, 911-918.

[32] Nousiainen, U., Torronen, R., Hanninen, O. (1984). Differential induction of various carboxylesterases by certain polycyclic aromatic hydrocarbons in the rat. Toxicology, 32, 243-251.

[33] Tuchinda, P., Udchachon, J., Khumtaveeporn, K., Taylor, W. C., Engelhardt, L. M., White, A. H. (1988). Phenanthrenes of *Eulophia nuda*. Phytochemistry, 27, 3267-3271.

[34] Fan, C., Wang, W., Wang, Y., Qin, G., Zhao, W. (2001). Chemical constituents from *Dendrobium densiflorum*. Phytochemistry, 57, 1255-1258.

[35] Zhang, G. N., Zhong, L. Y., Bligh, S. A., Guo, Y. L., Zhang, C. F., Zhang, M., Wang, Z. T., Xu, L.S. (2005). Bi-bicyclic and bi-tricyclic compounds from *Dendrobium thyrsiflorum*. Phytochemistry, 66, 1113-1120.

[36] Hatzimouratidis, K., Amar, E., Eardley, I., Giuliano, F., Hatzichristou, D., Montorsi, F., Vardi, Y., Wespes, E. (2010). Guidelines on male sexual dysfunction: erectile dysfunction and premature ejaculation. European Urology, 57, 804-814.

[37] Diaz, V. A., Close, J. D. (2010). Male sexual dysfunction. Primary Care: Clinics in Office Practice, 37, 473-489.

[38] Corbin, J. D., Beasley, A., Blount, M. A., Francis, S. H. (2005). High lung PDE5: A strong basis for treating pulmonary hypertension with PDE5 inhibitors. Biochemical and Biophysical Research Communications, 334(3), 930–938.

[39] Wisutthathum, S., Chootip, K., Martin, H., Ingkaninan, K., Temkitthawon, P. T. (2018). Vasorelaxant and Hypotensive Effects of an Ethanolic Extract of

Eulophia macrobulbon and Its Main Compound 1-(4'-Hydroxybenzyl) -4,8-Dimethoxyphenanthrene-2,7-Diol. Frontiers in Pharmacology, 9, 484.

[40] Preedapirom, W., Changwichit, K., Srisawang, P., Ingkaninan, K., Taepavarapruk, P. (2018). Aphrodisiac activity of *Eulophia macrobulbon* extract on erectile dysfunction in male aged rats. Hindawi; BioMed Research International, 6217029, 1-8.

[41] Preedapirom, W., Changwichit, K., Tangchang, W., Ingkaninan, K., Taepawarapruk, P. (2019). A toxicological safety assessment of a standardized extract of *Eulophia macrobulbon* in rodents. Naresuan University Journal: Sciences and Technology, 27(1), 98-109.

[42] OECD GUIDELINE FOR TESTING OF CHEMICALS: 420. Acute Oral Toxicity–Fixed Dose Procedure (2001). Retrieved from: https://ntp.niehs.nih.gov/iccvam/suppdocs/feddocs/oecd/oecd_gl420.pdf

[43] OECD GUIDELINE FOR TESTING OF CHEMICALS: 452. Chronic toxicity studies (2018). Retrieved from: https://www.oecd-ilibrary.org/docserver/9789264071209-en.pdf?expires=1588968516&id=id&accname=guest&checksum=EB32C0EF6E60608FC06F82220ABCA8F0

[44] Sompod, A., Rujivipat, S., Apichatwatana, N., Ingkaninan, K. (2019). Penetration study of topical formulation containing *Eulophia macrobulbon* extract. The 35th International Annual Meeting in Pharmaceutical Sciences & CU-MPU International Collaborative Research Conference, Available online at http://www.pharm.chula.ac.th/am2019/

[45] Jansakul, C., Yorsin, S., Naphatthalung, J., Tachanaparugse, K., Changwichit, K., Chootip, K., Ingkaninan, K. (2019). Relaxant mechanism of *Eulophia macrobulbon* ethanolic extract and 1-(4′-hydroxybenzyl)-4,8-dimethoxyphenanthrene-2,7-diol on human corpus cavernosum. Functional Foods in Health and Disease, 9(5), 328-340.

[46] Tolosa, L., Donato, M. T., Gómez-Lechón, M. J. (2015). Cytotoxicity Assessment by Means of the MTT Assay. Protocols in In Vitro Hepatocyte Research, 1250, 333-348.

[47] Vistica, D. T., Skehan, P., Scudiero, D., Monks, A., Pittman, A., Boyd, M. R. (1991). Tetrazolium-based assays for cellular viability: a critical examination of selected parameters affecting formazan production. Cancer Research, 51, 2515–2520.

[48] Maehara, Y., Kusumoto, T., Kusumoto, H., Anai, H., Sugimachi, K. (1986). Sodium Succinate Enhances the Colorimetric Reaction of the in vitro Chemosensitivity Test: MTT Assay. European Journal of Cancer and Clinical Oncology, 23, 273–276.

[49] Slater, T. F., Sawyer, B., Sträuli, U. (1963). Studies on succinate-tetrazolium reductase systems: III. Points of coupling of four different tetrazolium salts III. Points of coupling of four different tetrazolium salts. Biochimica et Biophysica Acta, 77, 383-393.

[50] Berridge, M. V., Herst, P. M., Tan, A. S. (2005). Tetrazolium dyes as tools in cell biology: new insights into their cellular reduction. Biotechnology Annual Review, 11, 127–52.

[51] Berridge, M. V., Tan, A. S. (1993). Characterization of the cellular reduction of 3-(4,5-dimethylthiazol-2-yl)-2,5-diphenyltetrazolium bromide (MTT): subcellular localization, substrate dependence, and involvement of mitochondrial electron transport in MTT reduction. Archives of Biochemistry and Biophysics, 303(2), 474–82.

[52] Stockert, J. C., Blázquez-Castro, A., Cañete, M., Horobin, R. W., Villanueva, A. (2012). MTT assay for cell viability: Intracellular localization of the formazan product is in lipid droplets. Acta Histochemica. 114(8), 785–796.

[53] Stockert, J. C., Horobin, R. W., Colombo, L. L., Blázquez-Castro, A. (2018). Tetrazolium salts and formazan products in Cell Biology: Viability assessment, fluorescence imaging, and labeling perspectives. Acta Histochemica, 120(3), 159–167.

[54] Mosmann, T. (1983). Rapid Colorimetric Assay for Cellular Growth and Survival: Application to Proliferation and Cytotoxicity Assays. Journal of Immunological Methods, 65, 55–63.

[55] MERCK [Internet]. Protocol Guide; ©2020 [updated 2020; cited 2020 March 21]. MTT Assay for Cell Viability and Proliferation; [about 3 screens].

Available from: https://www.sigmaaldrich.com/technical-documents/protocols/biology/roche/cell-proliferation-kit-i-mtt.html

[56] Singhvi, G., Sonavane, S., Gupta, A., Gampa, G., Goyal, M. (2013). Design of a Modified Kinetic Solubility Determination Method at Laboratory Level for Early Drug Discovery. Asian Journal of Chemistry, 25(1), 237-239.

[57] Chaturvedi, P. R., Decker, C. J., Odinecs, A. (2001). Prediction of pharmacokinetic properties using experimental approaches during early drug discovery. Current opinion in chemical biology, 5(4), 452-463.

[58] Ballard, P., Brassil, P., Bui, K. H., Dolgos, H., Petersson, C., Tunek, A., Webborn, P. J. (2012). The right compound in the right assay at the right time: an integrated discovery DMPK strategy. Drug metabolism reviews, 44(3), 224-252.

[59] Gomez-Lechon, M. J., Ponsoda, X., Castell, J. V. (2000). In vitro toxicity testing. In: Doyle A, Griffiths JB (eds) Cell and tissue culture for medical research. Wiley, Chinchester, 402–419.

[60] CORNING; Transwell® Permeable Supports. (2007). Including Snapwell[TM] and Netwell[TM] Inserts. NY 14831-001

[61] Yu, S., Li, S., Yang, H., Lee, F., Wu, J. T., Qian, M. G. (2005). A novel liquid chromatography/tandem mass spectrometry-based depletion method for measuring red blood cell partitioning of pharmaceutical compounds in drug discovery. Rapid Communications in Mass Spectrometry, 19, 250-254.

[62] Skehan, P., Storeng, R., Scudiero, D. (1990). New colorimetric cytotoxicity assay for anticancer-drug screening. Journal of the National Cancer Institute, 82, 1107–1112.

[63] Niles, A. L., Moravec, R. A., Riss, T. L. (2008). Update on in vitro cytotoxicity assays for drug development. Expert Opinion on Drug Discovery, 3, 655–669.

[64] Stoddart, M. J. (2011). Cell viability assays: introduction. Methods in Molecular Biology, 740, 1–6.

[65] Kowapradit, J., Opanasopit, P., Ngawhirunpat, T., Apirakaramwong, A., Rojanarata, T. (2010). *In vitro* Permeability Enhancement in Intestinal Epithelial Cells (Caco-2) Monolayer of Water-Soluble Quaternary

Ammonium Chitosan Derivatives. Pharmaceutical Science and Technology, 11(2), 497-508.

[66] Liang, E., Chessic, K., Yazdanian, M. (1999). Evaluation of an Accelerated Caco-2 Cell Permeability Model. Journal of Pharmaceutical Sciences, 89(3), 336-345.

[67] Kanaan, M., Daali, Y., Dayer, P., Desmeules, J. (2009). Uptake/Efflux Transport of Tramadol Enantiomers and O-Desmethyl-Tranmadol: Focus on P-Glycoprotein. Basic & Clinical Pharmacology & Toxicology, 105, 199-206.

APPENDIX

Caco-2 Permeability
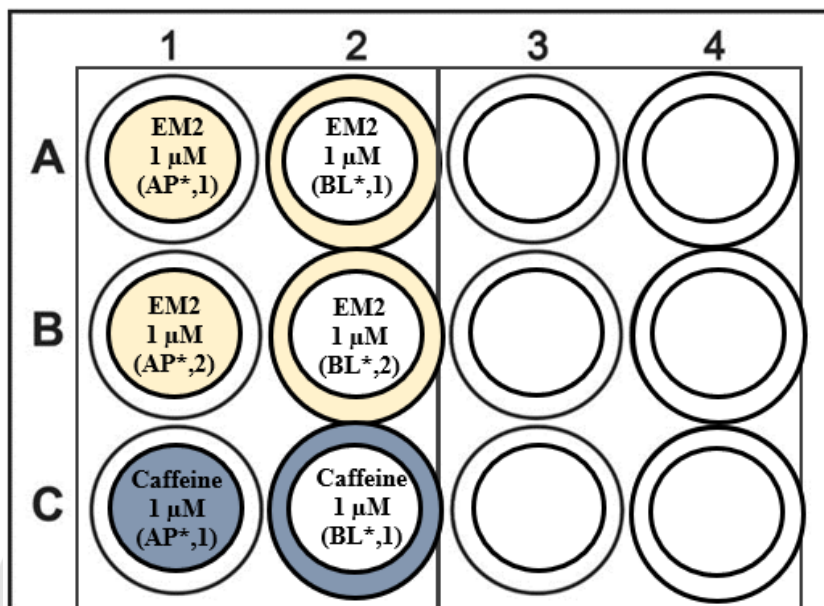
Figure 36 Sample position on 12-Transwell inserts for

Caco-2 permeability test (Time 1)
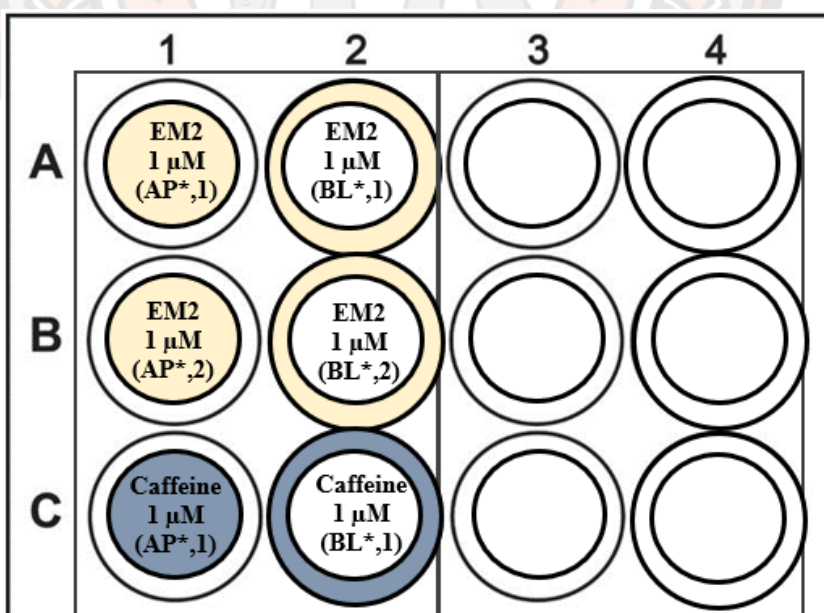
Figure 37 Sample position on 12-Transwell inserts for

Caco-2 permeability test (Time 2)
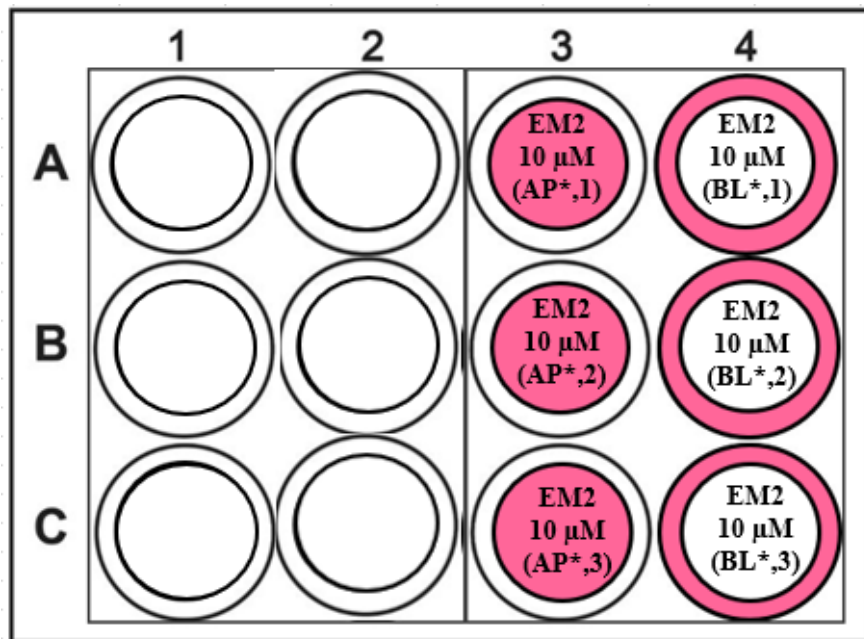
**Figure 38 Sample position on 12-Transwell inserts for
Caco-2 permeability test (Time 3)**
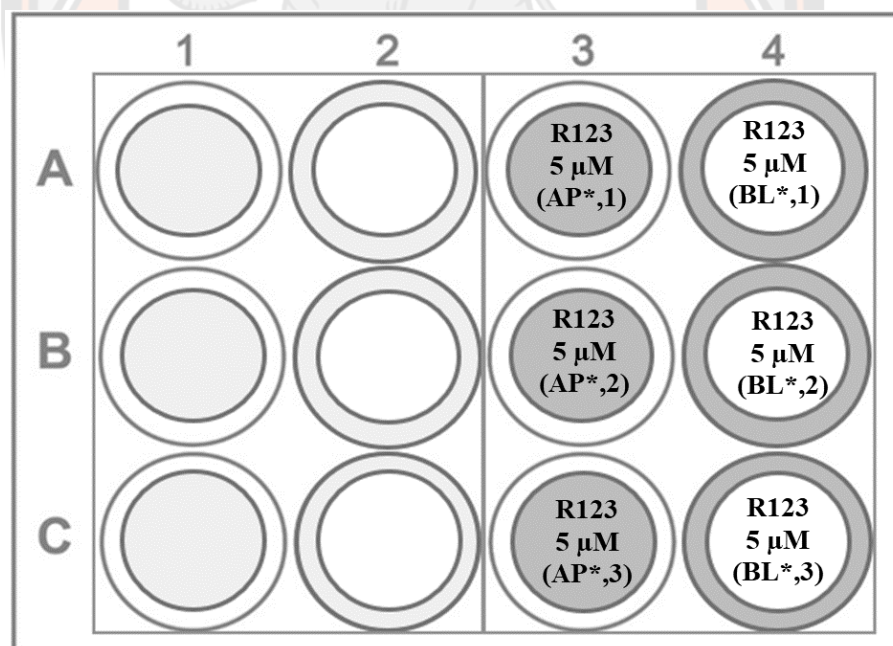
**Figure 39 Sample position on 12-Transwell inserts for
Caco-2 permeability test (Time 4)**

Table 10 The TEER values of each insert of sample EM2 (initial 1 μM)

Doner compartment		TEER values		
		Before replacing by HBSS-HEPES buffer	**After replacing by HBSS-HEPES buffer**	**After incubation in HBSS-HEPES buffer for 2/4 hrs.***
EM2 (1	1	347	345	340
μM)	2	352	342	341
*AP	3	352	345	343
chamber	AVG	350.33	344.00	341.33
(Time 1)	SD	2.89	1.73	1.53
EM2 (1	1	336	328	330
μM)	2	334	333	334
*AP	3	340	333	330
chamber	AVG	336.67	331.33	331.33
(Time 2)	SD	3.06	2.89	2.31
EM2 (1	1	586	401	374
μM)	2	585	399	374
*AP	3	586	399	374
chamber	AVG	585.67	399.67	374.00
(Time 3)	SD	0.58	1.15	0.00
EM2 (1	1	567	379	352
μM)	2	560	379	352
*AP	3	560	372	351
chamber	AVG	562.33	376.67	351.67
(Time 4)	SD	4.04	4.04	0.58

Doner compartment		TEER values		
		Before replacing by HBSS-HEPES buffer	**After replacing by HBSS-HEPES buffer**	**After incubation in HBSS-HEPES buffer for 2/4 hrs.***
EM2 (1	1	364	364	358
µM)	2	334	366	358
*BL	3	340	364	361
chamber	AVG	346.00	364.67	359.00
(Time 1)	SD	15.87	1.15	1.73
EM2 (1	1	358	356	357
µM)	2	356	355	354
*BL	3	355	355	352
chamber	AVG	356.33	355.33	354.33
(Time 2)	SD	1.53	0.58	2.52
EM2 (1	1	555	381	356
µM)	2	554	385	356
*BL	3	548	385	356
chamber	AVG	552.33	383.67	356.00
(Time 3)	SD	3.79	2.31	0.00
EM2 (1	1	541	376	351
µM)	2	544	376	351
*BL	3	549	376	353
chamber	AVG	544.67	376.00	351.67
(Time 4)	SD	4.04	0.00	1.15

Table 11 The TEER values of each insert of sample EM2 (initial 1 μM)

Doner compartment		TEER values		
		Before replacing by HBSS-HEPES buffer	After replacing by HBSS-HEPES buffer	After incubation in HBSS-HEPES buffer for 4 hrs.
EM2 (10 μM) *AP chamber (Time 1)	1	955	623	428
	2	958	620	429
	3	958	620	428
	AVG	957.00	621.00	428.33
	SD	1.73	1.73	0.58
EM2 (10 μM) *AP chamber (Time 2)	1	978	684	495
	2	978	687	496
	3	977	687	496
	AVG	977.67	686.00	495.67
	SD	0.58	1.73	0.58
EM2 (10 μM) *AP chamber (Time 3)	1	960	616	465
	2	963	616	465
	3	963	616	463
	AVG	962.00	616.00	464.33
	SD	1.73	0.00	1.15
EM2 (10 μM) *BL chamber (Time 1)	1	968	672	408
	2	968	674	408
	3	965	671	404
	AVG	967.00	672.33	406.67
	SD	1.73	1.53	2.31

Doner compartment		TEER values		
		Before replacing by HBSS-HEPES buffer	**After replacing by HBSS-HEPES buffer**	**After incubation in HBSS-HEPES buffer for 4 hrs.**
EM2 (10 µM) *BL chamber (Time 2)	1	976	640	387
	2	978	641	389
	3	978	641	386
	AVG	977.33	640.67	387.33
	SD	1.15	0.58	1.53
EM2 (10 µM) *BL chamber (Time 3)	1	1006	724	435
	2	1005	725	436
	3	1005	725	436
	AVG	1005.33	724.67	435.67
	SD	0.58	0.58	0.58

Table 12 Standard curve of EM2 (1 µM, Time 1) in Caco-2 permeability test; HPLC results

Name	Conc. (µM)	Retention time (min)	Peak area	Peak high
Standard EM2 at 0.1 µM	0.1	9.573	2374	176
Standard EM2 at 0.2 µM	0.2	9.612	2671	210
Standard EM2 at 0.5 µM	0.5	9.592	25981	1268
Standard EM2 at 1.0 µM	1	9.586	42108	2435
Standard EM2 at 2.5 µM	2.5	9.586	90637	5773
Standard EM2 at 5.0 µM	5	9.633	264641	18514
Standard EM2 at 7.5 µM	7.5	9.624	332432	19364
Standard EM2 at 10.0 µM	10	9.593	439117	28091
Standard EM2 at 15.0 µM	15	9.594	676094	44607
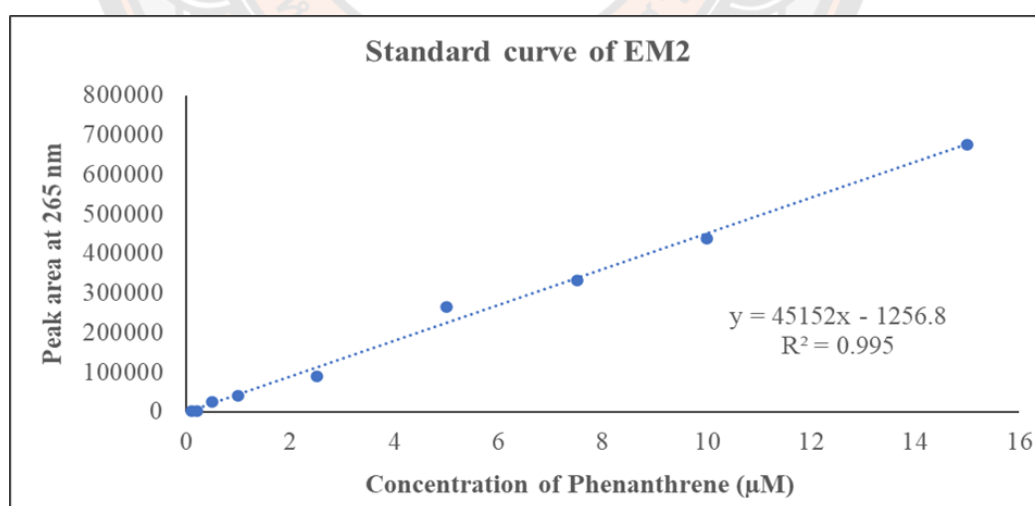
Figure 40 Standard curve of EM2 (1 µM, Time 1) in Caco-2 permeability test

Table 13 Sample concentration measurement of EM2 (initial 1 μM, Time 1) in Caco-2 permeability test; HPLC results (n=2)

Name	Retention time (min)	Peak high	Peak area	x (μM)	Concen-tration (μM)
EM2 1 μM (AP*t0, 1)	10.745	1620	38672	0.884	1.769
EM2 1 μM (AP t0, 1)	10.735	81	729	0.044	0.088
EM2 1 μM (AP*t0, 2)	10.747	238	4661	0.131	0.262
EM2 1 μM (AP t0, 2)	10.783	28	312	0.035	0.069
EM2 1 μM (BL*t0, 1)	10.754	439	28116	0.651	1.301
EM2 1 μM (BL t0, 1)	10.875	1	329	0.035	0.070
EM2 1 μM (BL*t0, 2)	10.774	146	2365	0.080	0.160
EM2 1 μM (BL t0, 2)	10.728	43	479	0.038	0.077
EM2 1 μM (AP*t60, 1)	10.719	23	220	0.033	0.065
EM2 1 μM (AP t60, 1)	10.69	12	181	0.032	0.064
EM2 1 μM (AP*t60, 2)	10.668	31	353	0.036	0.071
EM2 1 μM (AP t60, 2)	10.719	12	141	0.031	0.062
EM2 1 μM (BL*t60, 1)	10.715	39	584	0.041	0.082
EM2 1 μM (BL t60, 1)	10.814	9	139	0.031	0.062
EM2 1 μM (BL*t60, 2)	10.723	35	505	0.039	0.078
EM2 1 μM (BL t60, 2)	10.875	0	103	0.030	0.060
EM2 1 μM (AP*t120, 1)	10.792	0	94	0.030	0.060
EM2 1 μM (AP t120, 1)	10.712	5	23	0.028	0.057
EM2 1 μM (AP*t120, 2)	10.731	9	130	0.031	0.061
EM2 1 μM (AP t120, 2)	10.501	5	66	0.029	0.059
EM2 1 μM (BL*t120, 1)	10.736	26	421	0.037	0.074
EM2 1 μM (BL t120, 1)	10.749	2	19	0.028	0.057
EM2 1 μM (BL*t120, 2)	10.67	23	507	0.039	0.078
EM2 1 μM (BL t120, 2)	10.696	6	37	0.029	0.057

Name	Retention time (min)	Peak high	Peak area	x (µM)	Concen-tration (µM)
EM2 1 µM (AP*t240, 1)	10.698	9	86	0.030	0.059
EM2 1 µM (AP t240, 1)	10.68	4	65	0.029	0.059
EM2 1 µM (AP*t240, 2)	10.708	16	109	0.030	0.060
EM2 1 µM (AP t240, 2)	10.692	3	31	0.029	0.057
EM2 1 µM (BL*t240, 1)	10.651	14	165	0.031	0.063
EM2 1 µM (BL t240, 1)	10.62	7	75	0.029	0.059
EM2 1 µM (BL*t240, 2)	10.694	8	37	0.029	0.057
EM2 1 µM (BL t240, 2)	10.661	3	38	0.029	0.057

Table 14 Standard curve of EM2 (1 µM, Time 2) in Caco-2 permeability test; HPLC results

Name	Conc. (µM)	Retention time (min)	Peak area	Peak high
Standard EM2 at 0.1 µM	0.1	10.219	2196	117
Standard EM2 at 0.2 µM	0.2	10.213	3367	172
Standard EM2 at 0.5 µM	0.5	10.213	9475	486
Standard EM2 at 1.0 µM	1	10.221	39473	2074
Standard EM2 at 2.5 µM	2.5	10.203	50547	2360
Standard EM2 at 5.0 µM	5	10.246	165825	7760
Standard EM2 at 7.5 µM	7.5	10.255	247799	11244
Standard EM2 at 10.0 µM	10	10.296	321751	14563
Standard EM2 at 15.0 µM	15	10.21	502068	24560
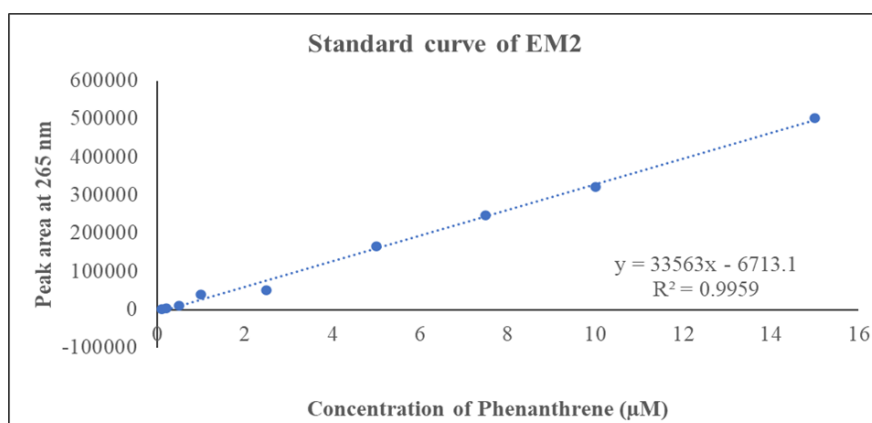
Figure 41 Standard curve of EM2 (1 µM, Time 2) in Caco-2 permeability test

Table 15 Sample concentration measurement of EM2 (initial 1 µM, Time 2) in Caco-2 permeability test; HPLC results (n=2)

Name	Retention time (min)	Peak high	Peak area	x (µM)	Concentration (µM)
EM2 1 µM (AP*t0, 1)	10.39	719	14605	0.64	1.270
EM2 1 µM (AP t0, 1)	10.238	7	135	0.20	0.408
EM2 1 µM (AP*t0, 2)	10.319	796	14972	0.65	1.292
EM2 1 µM (AP t0, 2)	10.222	8	100	0.20	0.406
EM2 1 µM (BL*t0, 1)	10.319	766	14972	0.65	1.292
EM2 1 µM (BL t0, 1)	10.142	6	174	0.21	0.410
EM2 1 µM (BL*t0, 2)	10.299	793	15031	0.65	1.296
EM2 1 µM (BL t0, 2)	10.143	1	122	0.20	0.407
EM2 1 µM (AP*t30, 1)	10.256	65	1117	0.23	0.467
EM2 1 µM (AP t30, 1)	10.083	9	207	0.21	0.412
EM2 1 µM (AP*t30, 2)	10.274	65	1333	0.24	0.479
EM2 1 µM (AP t30, 2)	10.058	10	189	0.21	0.411
EM2 1 µM (BL*t30, 1)	10.277	233	3984	0.32	0.637
EM2 1 µM (BL t30, 1)	10.017	32	879	0.23	0.452
EM2 1 µM (BL*t30, 2)	10.274	258	4402	0.33	0.662
EM2 1 µM (BL t30, 2)	10.008	23	692	0.22	0.441

Name	Retention time (min)	Peak high	Peak area	x (μM)	Concen-tration (μM)
EM2 1 µM (AP*t60, 1)	10.266	92	1473	0.24	0.488
EM2 1 µM (AP t60, 1)	10.008	23	782	0.22	0.447
EM2 1 µM (AP*t60, 2)	10.208	55	1064	0.23	0.463
EM2 1 µM (AP t60, 2)	10.051	24	706	0.22	0.442
EM2 1 µM (BL*t60, 1)	10.263	213	3703	0.31	0.621
EM2 1 µM (BL t60, 1)	10.226	37	589	0.22	0.435
EM2 1 µM (BL*t60, 2)	10.284	183	3080	0.29	0.584
EM2 1 µM (BL t60, 2)	10.266	45	539	0.22	0.432
EM2 1 µM (AP*t120, 1)	10.246	61	1057	0.23	0.463
EM2 1 µM (AP t120, 1)	10.224	57	1038	0.23	0.462
EM2 1 µM (AP*t120, 2)	10.206	49	808	0.22	0.448
EM2 1 µM (AP t120, 2)	10.211	61	999	0.23	0.460
EM2 1 µM (BL*t120, 1)	10.23	153	2705	0.28	0.561
EM2 1 µM (BL t120, 1)	10.287	197	3352	0.30	0.600
EM2 1 µM (BL*t120, 2)	10.274	163	2746	0.28	0.564
EM2 1 µM (BL t120, 2)	10.292	144	2517	0.28	0.550

Table 16 Sample concentration measurement of EM2 (initial 10 μM) in Caco-2 permeability test; HPLC results (n=3)

Name	Retention time (min)	Peak high	Peak area	x (μM)	Concen-tration (μM)
EM2 10 µM (AP*t0, 1)	7.502	9972	132694	7.17	14.330
EM2 10 µM (AP*t0, 2)	7.503	9917	133569	7.21	14.419
EM2 10 µM (AP*t0, 3)	7.502	9946	135106	7.29	14.576
EM2 10 µM (AP t0, 1)	N/A	N/A	N/A	N/A	N/A
EM2 10 µM (AP t0, 2)	N/A	N/A	N/A	N/A	N/A
EM2 10 µM (AP t0, 3)	N/A	N/A	N/A	N/A	N/A

Name	Retention time (min)	Peak high	Peak area	x (µM)	Concentration (µM)
EM2 10 µM (BL*t0, 1)	7.508	10194	139626	7.52	15.036
EM2 10 µM (BL*t0, 2)	7.513	10044	141635	7.62	15.241
EM2 10 µM (BL*t0, 3)	7.513	10655	140394	7.56	15.115
EM2 10 µM (BL t0, 1)	N/A	N/A	N/A	N/A	N/A
EM2 10 µM (BL t0, 2)	N/A	N/A	N/A	N/A	N/A
EM2 10 µM (BL t0, 3)	N/A	N/A	N/A	N/A	N/A
EM2 10 µM (AP*t30, 1)	7.506	3658	45176	2.71	5.414
EM2 10 µM (AP*t30, 2)	7.498	3565	46895	2.79	5.589
EM2 10 µM (AP*t30, 3)	7.494	3623	47204	2.81	5.621
EM2 10 µM (AP t30, 1)	7.476	72	951	0.45	0.909
EM2 10 µM (AP t30, 2)	7.484	51	617	0.44	0.875
EM2 10 µM (AP t30, 3)	7.48	79	889	0.45	0.903
EM2 10 µM (BL*t30, 1)	7.485	7819	99357	5.47	10.934
EM2 10 µM (BL*t30, 2)	7.48	7994	99649	5.48	10.964
EM2 10 µM (BL*t30, 3)	7.478	7271	91559	5.07	10.140
EM2 10 µM (BL t30, 1)	7.478	271	3276	0.57	1.146
EM2 10 µM (BL t30, 2)	7.475	252	3021	0.56	1.120
EM2 10 µM (BL t30, 3)	7.479	260	3143	0.57	1.132
EM2 10 µM (AP*t60, 1)	7.493	2267	28740	1.87	3.740
EM2 10 µM (AP*t60, 2)	7.486	2312	29066	1.89	3.773
EM2 10 µM (AP*t60, 3)	7.484	2144	27222	1.79	3.585
EM2 10 µM (AP t60, 1)	7.488	120	1511	0.48	0.966
EM2 10 µM (AP t60, 2)	7.488	112	1595	0.49	0.975
EM2 10 µM (AP t60, 3)	7.482	151	1795	0.50	0.995
EM2 10 µM (BL*t60, 1)	7.483	6246	74752	4.21	8.427
EM2 10 µM (BL*t60, 2)	7.485	6418	73353	4.14	8.285
EM2 10 µM (BL*t60, 3)	7.485	5816	72718	4.11	8.220

Name	Retention time (min)	Peak high	Peak area	x (µM)	Concentration (µM)
EM2 10 µM (BL t60, 1)	7.485	668	7444	0.79	1.570
EM2 10 µM (BL t60, 2)	7.487	370	4933	0.66	1.315
EM2 10 µM (BL t60, 3)	7.484	375	4816	0.65	1.303
EM2 10 µM (AP*t120, 1)	7.49	2054	25420	1.70	3.402
EM2 10 µM (AP*t120, 2)	7.492	2054	25371	1.70	3.397
EM2 10 µM (AP*t120, 3)	7.49	1858	23524	1.60	3.209
EM2 10 µM (AP t120, 1)	7.491	302	3809	0.60	1.200
EM2 10 µM (AP t120, 2)	7.496	276	4117	0.62	1.231
EM2 10 µM (AP t120, 3)	7.497	267	3852	0.60	1.205
EM2 10 µM (BL*t120, 1)	7.495	4972	62655	3.60	7.195
EM2 10 µM (BL*t120, 2)	7.49	5108	62415	3.59	7.171
EM2 10 µM (BL*t120, 3)	7.484	4871	62112	3.57	7.140
EM2 10 µM (BL t120, 1)	7.476	888	12262	1.03	2.061
EM2 10 µM (BL t120, 2)	7.467	1383	14927	1.17	2.333
EM2 10 µM (BL t120, 3)	7.462	704	9729	0.90	1.803
EM2 10 µM (AP*t240, 1)	7.45	1497	18303	1.34	2.677
EM2 10 µM (AP*t240, 2)	7.45	1569	18763	1.36	2.724
EM2 10 µM (AP*t240, 3)	7.451	1242	15897	1.22	2.432
EM2 10 µM (AP t240, 1)	7.451	423	5143	0.67	1.336
EM2 10 µM (AP t240, 2)	7.451	365	4495	0.64	1.270
EM2 10 µM (AP t240, 3)	7.448	409	4820	0.65	1.303
EM2 10 µM (BL*t240, 1)	7.451	3585	45424	2.72	5.440
EM2 10 µM (BL*t240, 2)	7.452	3681	45997	2.75	5.498
EM2 10 µM (BL*t240, 3)	7.45	3457	43963	2.65	5.291
EM2 10 µM (BL t240, 1)	7.464	1421	17155	1.28	2.560
EM2 10 µM (BL t240, 2)	7.484	1386	17309	1.29	2.575
EM2 10 µM (BL t240, 3)	7.507	934	14496	1.14	2.289

Table 17 Concentration of samples EM2 (initial 1 µM) in absorptive and secretory directions across Caco-2 monolayers (n=4)

Name, analysis compartment	Time (min)	Concentration (µM)				AVG	SD
		1	2	3	4		
	0	1.769	0.262	1.270	1.292	1.148	0.634
EM2 (1 µM),	30	-	-	0.467	0.479	0.473	0.009
AP to BL,	60	0.065	0.071	0.488	0.463	0.272	0.235
Doner chamber; AP	120	0.060	0.061	0.463	0.448	0.258	0.228
	240	0.059	0.060	-	-	0.060	0.001
	0	0.088	0.069	0.408	0.406	0.243	0.190
EM2 (1 µM),	30	-	-	0.412	0.411	0.412	0.001
AP to BL,	60	0.064	0.062	0.447	0.442	0.254	0.220
Receiver chamber; BL	120	0.057	0.059	0.462	0.460	0.259	0.233
	240	0.059	0.057	-	-	0.058	0.001
	0	1.301	0.160	1.292	1.296	1.012	0.568
EM2 (1 µM),	30	-	-	0.637	0.662	0.650	0.018
BL to AP,	60	0.082	0.078	0.621	0.584	0.341	0.302
Doner chamber; BL	120	0.074	0.078	0.561	0.564	0.319	0.281
	240	0.063	0.057	-	-	0.060	0.004
	0	0.070	0.077	0.410	0.407	0.241	0.194
EM2 (1 µM),	30	-	-	0.452	0.441	0.447	0.008
BL to AP,	60	0.062	0.060	0.435	0.432	0.247	0.215
Receiver chamber; AP	120	0.057	0.057	0.600	0.550	0.316	0.300
	240	0.059	0.057	-	-	0.058	0.001

Table 18 Concentration of samples EM2 (initial 10 µM) in absorptive and secretory directions across Caco-2 monolayers (n=3)

Name, analysis compartment	Time (min)	Concentration (µM)			AVG	SD
		1	2	3		
	0	14.330	14.419	14.576	14.442	0.124
EM2 (10 µM),	30	5.414	5.589	5.621	5.542	0.111
AP to BL,	60	3.740	3.773	3.585	3.699	0.100
Doner chamber; AP	120	3.402	3.397	3.209	3.336	0.110
	240	2.677	2.724	2.432	2.611	0.157
	0	0.000	0.000	0.000	0.000	0.000
EM2 (10 µM),	30	0.909	0.875	0.903	0.896	0.018
AP to BL,	60	0.966	0.975	0.995	0.979	0.015
Receiver chamber; BL	120	1.200	1.231	1.205	1.212	0.017
	240	1.336	1.270	1.303	1.303	0.033
	0	15.036	15.241	15.115	15.131	0.103
EM2 (10 µM),	30	10.934	10.964	10.140	10.679	0.467
BL to AP,	60	8.427	8.285	8.220	8.311	0.106
Doner chamber; BL	120	7.195	7.171	7.140	7.168	0.028
	240	5.440	5.498	5.291	5.409	0.107
	0	0.000	0.000	0.000	0.000	0.000
EM2 (10 µM),	30	1.146	1.120	1.132	1.133	0.013
BL to AP,	60	1.570	1.315	1.303	1.396	0.151
Receiver chamber; AP	120	2.061	2.333	1.803	2.066	0.265
	240	2.560	2.575	2.289	2.475	0.161

Table 19 Time dependence of sample EM2 (initial 1 μM) in absorptive and secretory directions across Caco-2 monolayers (n=4)

		EM2 (initial 1 μM)					
Name	**Time (min)**	**1**	**2**	**3**	**4**	**AVG**	**SD**
Absorptive	30	6.576	6.383	-	-	6.479	0.137
transport,	60	3.406	3.549	3.622	3.230	3.452	0.173
$P_{app(AP-BL)}$,	120	1.856	1.907	1.762	1.774	1.825	0.069
(cm/s)(10^{-4})	240	-	-	0.916	0.877	0.896	0.027
Secretory	30	1.760	1.652	-	-	1.706	0.076
transport,	60	0.869	0.940	0.957	0.918	0.921	0.038
$P_{app(BL-AP)}$,	120	0.663	0.471	0.455	0.605	0.548	0.102
(cm/s)(10^{-4})	240	-	-	0.290	0.310	0.300	0.014
Efflux ratio,	30	3.736	3.863	-	-	3.799	0.090
[$P_{app(AP-BL)}$/	60	3.918	3.865	3.784	3.518	3.771	0.178
$P_{app(BL-AP)}$]	120	2.800	3.153	3.875	2.933	3.190	0.479
	240	-	-	3.153	2.826	2.990	0.231
Uptake ratio,	30	0.268	0.259	-	-	0.263	0.006
[$P_{app(BL-AP)}$/	60	0.255	0.259	0.264	0.284	0.266	0.013
$P_{app(AP-BL)}$]	120	0.357	0.317	0.258	0.341	0.318	0.043
	240	-	-	0.317	0.354	0.335	0.026

Table 20 Time dependence of sample EM2 (initial 10 µM) in absorptive and secretory directions across Caco-2 monolayers (n=3)

	Time (min)	1	2	3	AVG	SD
EM2 (initial 10 µM)						
Absorptive transport, $P_{app(AP-BL)}$, (cm/s)(10^{-4})	30	1.249	1.165	1.195	1.203	0.043
	60	0.961	0.961	1.032	0.985	0.041
	120	0.656	0.674	0.698	0.676	0.021
	240	0.464	0.434	0.498	0.465	0.032
Secretory transport, $P_{app(BL-AP)}$, (cm/s)(10^{-4})	30	0.260	0.253	0.277	0.263	0.012
	60	0.231	0.197	0.197	0.208	0.020
	120	0.178	0.202	0.157	0.179	0.023
	240	0.146	0.145	0.134	0.142	0.007
Efflux ratio, [$P_{app(AP-BL)}$/ $P_{app(BL-AP)}$]	30	4.806	4.598	4.314	4.573	0.247
	60	4.158	4.883	5.253	4.765	0.557
	120	3.694	3.343	4.459	3.832	0.571
	240	3.182	2.986	3.716	3.295	0.378
Uptake ratio, [$P_{app(BL-AP)}$/ $P_{app(AP-BL)}$]	30	0.208	0.218	0.232	0.219	0.012
	60	0.240	0.205	0.190	0.212	0.026
	120	0.271	0.299	0.224	0.265	0.038
	240	0.314	0.335	0.269	0.306	0.034

Hep G2 stability

Table 21 Standard curve of EM2 in Hep G2 stability test; HPLC results

Name	Conc. (µM)	Retention time (min)	Peak area	Peak high
Standard EM2 at 0.01 µM	0.01	9.336	719	23
Standard EM2 at 0.1 µM	0.1	9.38	1710	74
Standard EM2 at 0.5 µM	0.5	9.384	18254	621
Standard EM2 at 1.0 µM	1	9.367	33198	1122
Standard EM2 at 2.5 µM	2.5	9.364	89911	2919
Standard EM2 at 5.0 µM	5	9.346	183082	6125
Standard EM2 at 10.0 µM	10	9.344	375811	12461

Standard curve of EM2

$y = 37621x - 2322$
$R^2 = 0.9997$
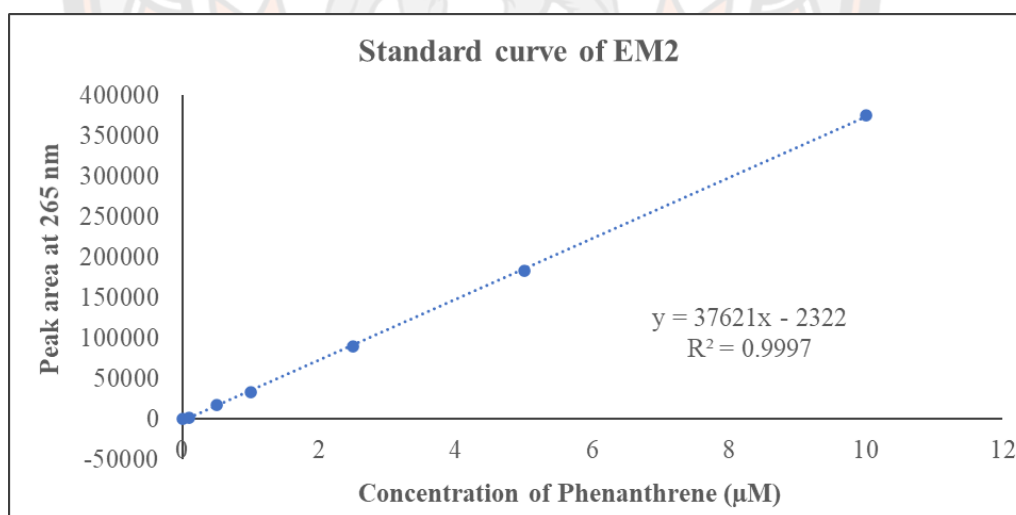
Figure 42 Standard curve of EM2 in Hep G2 stability test; HPLC results

Table 22 Sample concentration measurement of EM2 (initial 10 μM) in Hep G2 stability test; HPLC results (n=3)

Name	Retention time (min)	Peak high	Peak area	x (μM)	Concen-tration (μM)
EM2 10 μM (t0, 1)	9.208	16092	382210	8.15	16.308
EM2 10 μM (t0, 2)	9.271	15398	384435	8.20	16.402
EM2 10 μM (t0, 3)	9.724	16620	385582	8.23	16.450
EM2 10 μM (t5, 1)	9.267	14971	371207	7.92	15.843
EM2 10 μM (t5, 2)	9.259	15668	376024	8.02	16.047
EM2 10 μM (t5, 3)	9.252	15563	365665	7.80	15.609
EM2 10 μM (t10, 1)	9.25	14382	362156	7.73	15.461
EM2 10 μM (t10, 2)	9.238	15545	378946	8.08	16.170
EM2 10 μM (t10, 3)	9.238	15500	363945	7.77	15.537
EM2 10 μM (t15, 1)	9.239	14102	352449	7.53	15.052
EM2 10 μM (t15, 2)	2.245	14248	364419	7.78	15.557
EM2 10 μM (t15, 3)	9.241	14468	359688	7.68	15.357
EM2 10 μM (t30, 1)	9.246	14177	336432	7.19	14.376
EM2 10 μM (t30, 2)	9.24	14800	359485	7.67	15.349
EM2 10 μM (t30, 3)	9.246	14756	354617	7.57	15.143
EM2 10 μM (t60, 1)	9.249	14101	335465	7.17	14.335
EM2 10 μM (t60, 2)	9.255	13438	339896	7.26	14.522
EM2 10 μM (t60, 3)	9.25	13984	338649	7.23	14.469
EM2 10 μM (t180, 1)	9.522	10153	320297	6.85	13.695
EM2 10 μM (t180, 2)	9.36	10950	323031	6.90	13.810
EM2 10 μM (t180, 3)	9.325	10891	324853	6.94	13.887
EM2 10 μM (t240, 1)	9.396	11541	318131	6.80	13.603
EM2 10 μM (t240, 2)	9.326	11680	315747	6.75	13.503
EM2 10 μM (t240, 3)	9.32	11984	314466	6.72	13.448
EM2 10 μM (t900, 1)	9.328	9376	263854	5.66	11.312
EM2 10 μM (t900, 2)	9.311	9468	270376	5.79	11.588
EM2 10 μM (t900, 3)	9.346	7708	232165	4.99	9.975

Table 23 Pharmacokinetic parameters of EM2 (initial 10 µM) in Hep G2 stability test; (n=3)

Parameters	Linear regression	Initial Concentration, pmol/ml	Ke, min^-1	t$_{1/2}$, min
Time 1	y = -0.0001557x + 4.2797	20442.412	0.0001557	4450.867
Time 2	y = -0.0001563x + 4.2901	20560.697	0.0001563	4433.781
Time 3	y = -0.0002133x + 4.2884	20621.674	0.0002133	3248.945
AVG	-	20541.595	0.0001751	4044.531
SD	-	91.145	0.0000331	689.051

Parameters	AUC$_{(t0-t120)}$, pmol*min/ml	AUC$_{(t900-infi)}$, pmol*min/ml	AUC$_{total}$, pmol*min/ml	Cl$_{int}$, µl/min/10^6 cells
Time 1	14534006.805	90882432.411	105416439.215	0.194
Time 2	14673524.361	92751861.628	107425385.989	0.191
Time 3	13967476.808	58442337.139	72409813.947	0.285
AVG	14391669.325	80692210.392	95083879.717	0.223
SD	373926.136	19291613.107	19661991.524	0.053

Hepatocyte stability

Table 24 Standard curve of EM2 in hepatocyte stability test; HPLC results

Name	Conc. (µM)	Retention time (min)	Peak area	Peak high
Standard EM2 at 0.01 µM	0.01	9.336	719	23
Standard EM2 at 0.1 µM	0.1	9.38	1710	74
Standard EM2 at 0.5 µM	0.5	9.384	18254	621
Standard EM2 at 1.0 µM	1.0	9.367	33198	1122
Standard EM2 at 2.5 µM	2.5	9.364	89911	2919
Standard EM2 at 5.0 µM	5.0	9.346	183082	6125
Standard EM2 at 10.0 µM	10	9.344	375811	12461
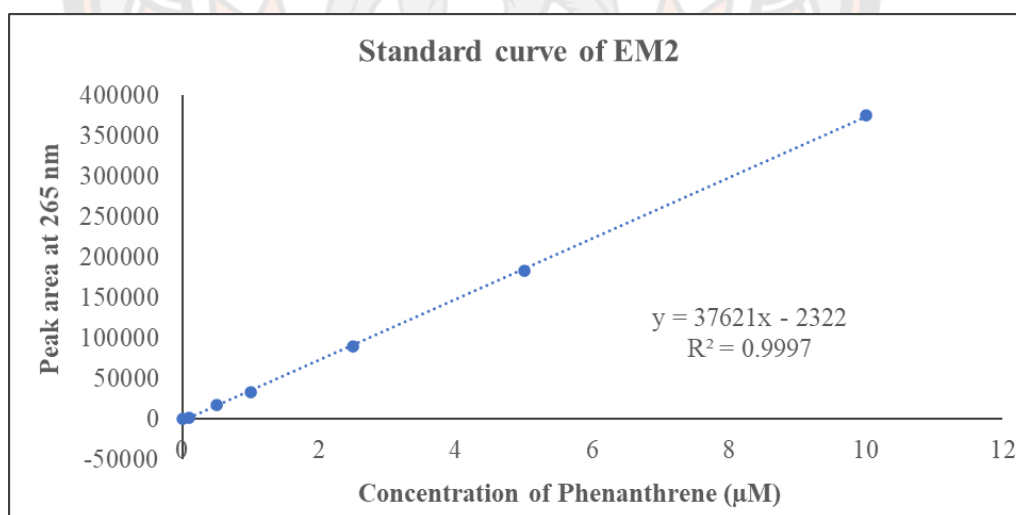
Figure 43 Standard curve of EM2 in hepatocyte stability test; HPLC results

Table 25 Sample concentration measurement of EM2 (initial 10 µM) in hepatocyte stability test; HPLC results (n=3)

Name	Retention time (min)	Peak area	x (µM)	Concen-tration (µM)
EM2 10 µM (t0, 1)	9.494	229947	6173.92	12347.84
EM2 10 µM (t0, 2)	9.412	234128	6285.05	12570.11
EM2 10 µM (t0, 3)	9.419	240126	6444.49	12888.97
EM2 10 µM (t15, 1)	9.426	221925	5960.69	11921.37
EM2 10 µM (t15, 2)	9.421	222119	5965.84	11931.69
EM2 10 µM (t15, 3)	9.443	225867	6065.47	12130.94
EM2 10 µM (t30, 1)	9.445	215266	5783.68	11567.37
EM2 10 µM (t30, 2)	9.455	225944	6067.52	12135.03
EM2 10 µM (t30, 3)	9.46	212411	5707.80	11415.59
EM2 10 µM (t60, 1)	9.46	198362	5334.36	10668.72
EM2 10 µM (t60, 2)	9.425	207061	5565.59	11131.18
EM2 10 µM (t60, 3)	9.477	200907	5402.01	10804.02
EM2 10 µM (t120, 1)	9.478	186062	5007.42	10014.83
EM2 10 µM (t120, 2)	9.486	189191	5090.59	10181.18
EM2 10 µM (t120, 3)	9.493	188224	5064.88	10129.77

Table 26 Pharmacokinetic parameters of EM2 (initial 10 µM) in hepatocyte stability test; (n=3)

Parameters	Linear regression	Initial Concentration, pmol/ml	Ke, min^-1	t$_{1/2}$, min
Time 1	y = -0.0007667X + 4.087	12347.838	0.0007667	903.8737446
Time 2	y = -0.0007333X + 4.097	12570.107	0.0007333	945.0429565
Time 3	y= -0.0007833X + 4.093	12888.972	0.0007833	884.7184987
AVG	-	20541.595	0.0001751	911.2117333
SD	-	91.145	0.0000331	30.82441583

Parameters	AUC$_{(t0-t120)}$, pmol*min/ml	AUC$_{(t900-infi)}$, pmol*min/ml	AUC$_{total}$, pmol*min/ml	Cl$_{int}$, µl/min/10^6 cells
Time 1	1312232.663	13062256.608	14374489.271	0.859
Time 2	1352627.522	13884052.103	15236679.625	0.825
Time 3	1325556.072	12932168.963	14257725.035	0.904
AVG	1330138.752	13292825.892	14622964.644	0.863
SD	20583.656	516131.789	534689.658	0.040

Microsomal stability

Table 27 Standard curve of EM2 in microsomal stability test; HPLC results

Name	Conc. (μM)	Retention time (min)	Peak area	Peak high
Standard EM2 at 0.1 μM	0.1	10.917	4441	264
Standard EM2 at 0.2 μM	0.2	10.908	9222	547
Standard EM2 at 0.5 μM	0.5	10.903	22952	1354
Standard EM2 at 1.0 μM	1	10.892	41486	2413
Standard EM2 at 2.5 μM	2	10.887	84520	4908
Standard EM2 at 5.0 μM	5	10.882	223623	12410
Standard EM2 at 10.0 μM	10	10.876	436642	24268

Standard curve of EM2
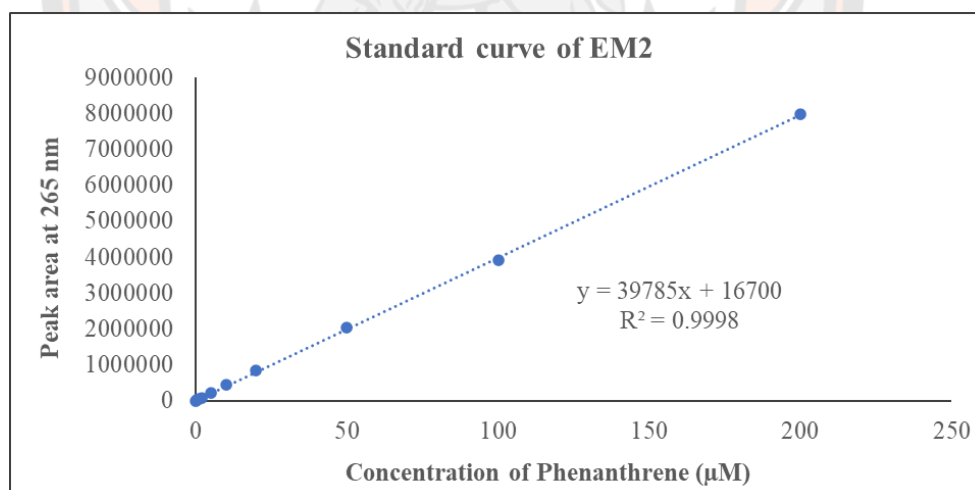
$y = 39785x + 16700$
$R^2 = 0.9998$

Figure 44 Standard curve of EM2 in microsomal stability test; HPLC results

Table 28 Sample concentration measurement of EM2 (initial 10 μM) in microsomal stability test; HPLC results (n=3)

Name	Retention time (min)	Peak high	Peak area	x (μM)	Concentration (μM)
EM2 10 μM (t0, 1)	10.576	909	196075	4.51	9.017
EM2 10 μM (t0, 2)	10.474	943	194363	4.47	8.931
EM2 10 μM (t0, 3)	10.441	989	193256	4.44	8.876
EM2 10 μM (t30, 1)	10.434	650	188710	4.32	8.647
EM2 10 μM (t30, 2)	10.369	916	179977	4.10	8.208
EM2 10 μM (t30, 3)	10.3	1039	178822	4.07	8.150
EM2 10 μM (t60, 1)	10.326	860	148482	3.31	6.625
EM2 10 μM (t60, 2)	10.342	973	149514	3.34	6.677
EM2 10 μM (t60, 3)	10.275	885	150784	3.37	6.740
EM2 10 μM (t90, 1)	10.667	831	117730	2.54	5.079
EM2 10 μM (t90, 2)	10.232	908	122193	2.65	5.303
EM2 10 μM (t90, 3)	10.674	925	127249	2.78	5.557
EM2 10 μM (t120, 1)	10.143	831	78325	1.55	3.098
EM2 10 μM (t120, 2)	10.099	908	70496	1.35	2.704
EM2 10 μM (t120, 3)	10.171	925	56244	0.99	1.988

Table 29 Pharmacokinetic parameters of EM2 (initial 10 µM) in microsomal stability test; (n=3)

Parameters	Linear regression	Initial Concentration, pmol/ml	Ke, min^-1	$t_{1/2}$, min
Time 1	Y = -0.003900*X + 4.018	9017.218	0.003900	177.692
Time 2	Y = -0.004100*X + 4.012	8931.155	0.004100	169.024
Time 3	Y = -0.004900*X + 4.040	8875.506	0.004900	141.429
AVG		8941.293	0.004300	162.715
SD	-	9017.218	0.003900	177.692

Parameters	$AUC_{(t0-t120)}$, pmol*min/ml	$AUC_{(t900-infi)}$, pmol*min/ml	AUC_{total}, pmol*min/ml	Cl_{int}, µl/min/10^6 cells
Time 1	792241.297	794333.646	1586574.943	5.683
Time 2	660098.404	659594.099	1319692.503	6.768
Time 3	650190.524	405690.792	1055881.316	8.406
AVG	700843.408	619872.846	1320716.254	6.952
SD	79307.768	197342.723	265348.295	1.371

BIOGRAPHY

Name-Surname   Kittiya Kamonlakorn

Date of Birth

Address

Current Workplace   99, Moo 9, Faculty of Pharmaceutical Sciences, Naresuan
                            University, Tha-pho sub-district, Muang district,
                            Phitsanulok convince, 65000

Current Position   Research Assistant in Pharmaceutical Chemistry and
                            Natural Products, Faculty of Pharmaceutical Sciences,
                            Naresuan University

Education Background   2019, B.S., Cosmetic Sciences, Faculty of Pharmaceutical
                            Sciences, Naresuan University

Publication   1. International Journal of Research Publications

               1.1 Kamonlakorn K, Supon C, Riankrasin A, Pekthong D, Parhira S. Quantitative phytochemicals determination of the extracts from the flowers of Alstonia scholaris and their anti-lipoxygenase activities. Key Engineering Materials. 2020; 859: 94-99. (Scopus) 2020 Aug 2018.

               1.2 Winitchaikul T, Sawong S, Surangkul D, Srikummool M, Somran J, Pekthong D, Kamonlakorn K, Nangngam P, Parhira S, Srisawang P. Calotropis gigantea stem bark extract induced apoptosis related to ROS and ATP production in colon cancer cells. Public Library of Science (PLOS) One. 2021; 16(8): e0254392. Available online at https://doi.org/10.1371/journal.pone.0254392

               2. International Conference Proceedings

               2.1 Kamonlakorn K, Parhira S. Qualitative and quantitative phytochemical analysis of the extracts from Dillenia indica L. AMPS 35th & CU-MPU International Collaborative Research Conference. 2019: 221-224. Available online at http://cu-amps2019.weebly.com/uploads/9/5/8/7/95877138/221-224_pn23_final.pdf

               3. National Conference Proceedings

               3.1 Kawiwong J, Injard A, Riankrasin A, Kamonlakorn K, Srisoithongsug P, Pekthong D, Parhira S. Chemical Constituents and Antioxidant Activity of the Alstonia scholaris Latex Extract. The 12th NPRU National Academic Conference. 2020: 53-60. Available online at http://dept.npru.ac.th/conference12/data/files/Full%20Paper%20NPRUConference2020.pdf

               3.2 Kamonlakorn K, Krueajan A, Pekthong D,

Parhira S. Quantitative Analysis of the Secondary Metabolites from Cerbera Odollam Fruit Extracts and Their Anti-albumin Denaturation Activities. The 12th NPRU National Academic Conference. 2020: 76-83. Available online at http://dept.npru.ac.th/conference12/data/files/Full%20Pape r%20NPRUConference2020.pdf

3.3 Kamonlakorn K, Parhira S, Srisawang P, Ingkaninan K, Pekthong D. Screening of Cytotoxicity and Hepato-stability of main bioactive constituent of Eulophia macrobulbon using Hep G2 Cells. PCRUSCI CONFERENCE 2022. 2022: 638-647. Available online at https://sci.pcru.ac.th/conference/

Awards 1. Certificate of "Academic Excellence" in recognition for outstanding academic performance in the 2017 year of the Cosmetics Sciences Programme at Faculty of Pharmaceutical Sciences, Naresuan University, Thailand

2. Certificate of "The Best Cosmetic Products" in recognition for 10th Herbal Cosmetic Fair in the 2018 year at Faculty of Pharmaceutical Sciences, Naresuan University, Thailand

3. Certificate of "The Popular Vote" in recognition for 10th Herbal Cosmetic Fair in the 2018 year at Faculty of Pharmaceutical Sciences, Naresuan University, Thailand

4. Certificate of "The 1st Runner up in Poster Presentation: Anti-albulmin Denaturation Activity of the Extracts from Dillenia indica Linn." in recognition for the Thesis Presentation in the 2018 year at Faculty of Pharmaceutical Sciences, Naresuan University, Thailand

5. Certificate of "The Best Innovation Project in Oral Presentation: Development of New Innovation Cosmetic Rinse-off Products and Leave-on Products from Jebsen & Jessen Ingredients (T) Ltd." in recognition for the Internship Research Presentation in the 2018 year at Naresuan University, Thailand